Turun yliopisto
University of Turku

CARDIAC IMAGING IN THE DIAGNOSIS
OF CORONARY ARTERY DISEASE:
THE VALUE OF QUANTITATIVE IMAGING OF
MYOCARDIAL PERFUSION AND
DEFORMATION

Valtteri Uusitalo

Turun yliopisto
University of Turku

CARDIAC IMAGING IN THE DIAGNOSIS OF CORONARY ARTERY DISEASE: THE VALUE OF QUANTITATIVE IMAGING OF MYOCARDIAL PERFUSION AND DEFORMATION

Valtteri Uusitalo

University of Turku

Faculty of Medicine
Department of Clinical Physiology and Nuclear Medicine
Doctoral Programme of Clinical Investigation
Turku PET Centre
Turku, Finland

Supervised by:

Professor Juhani Knuuti, MD, PhD
Turku PET Centre
University of Turku
Turku, Finland

Associate professor Antti Saraste, MD, PhD
Department of Cardiology and Turku PET Centre
University of Turku
Turku, Finland

Reviewed by:

Docent Antti Loimaala, MD, PhD
Clinical Physiology and Nuclear Medicine,
Helsinki University Central Hospital,
Helsinki, Finland

Professor Göran Bergström, MD, PhD
Ahlgrenska University Hospital,
Department of Molecular and Clinical Medicine,
Gothenburg, Sweden

Dissertation opponent:

Docent Juha Sinisalo, MD, PhD
Department of Cardiology,
Heart and Lung Center,
Helsinki University Central Hospital,
Helsinki, Finland

The originality of this thesis has been checked in accordance with the University of Turku quality assurance system using the Turnitin Originality Check service.

To my family and friends,

ABSTRACT

Valtteri Uusitalo

From Turku University, Faculty of Medicine, Department of Clinical Physiology and Nuclear Medicine, Doctoral Programme of Clinical Investigation, Turku PET Centre, Turku, Finland

Cardiac Imaging in the Diagnosis of Coronary Artery Disease: The Value of Quantitative Imaging of Myocardial Perfusion and Deformation

Atherosclerosis is a chronic and progressive disease of the vasculature. Increasing coronary atherosclerosis can lead to obstructive coronary artery disease (CAD) or myocardial infarction. Computed tomography angiography (CTA) allows noninvasive assessment of coronary anatomy and quantitation of atherosclerotic burden. Myocardial blood flow (MBF) can be accurately measured in absolute terms (mL/g/min) by positron emission tomography (PET) with $[^{15}O]$ H_2O as a radiotracer.

We studied the coronary microvascular dysfunction as a risk factor for future coronary calcification in healthy young men by measuring the coronary flow reserve (CFR) which is the ratio between resting and hyperemic MBF. Impaired vasodilator function was not linked with accelerated atherosclerosis 11 years later. Currently, there is a global interest in quantitative PET perfusion imaging. We established optimal thresholds of $[^{15}O]$ H_2O PET perfusion for diagnosis of CAD (hyperemic MBF of 2.3 mL/g/min and CFR of 2.5) in the first multicenter study of this type (Turku, Amsterdam and Uppsala).

In myocardial bridging a segment of the coronary artery travels inside the myocardium and can be seen as intramural course (CTA) or systolic compression (invasive coronary angiography). Myocardial bridging is frequently linked with proximal atherosclerotic plaques. We used quantitative $[^{15}O]$ H_2O PET perfusion to evaluate the hemodynamic effects of myocardial bridging. Myocardial bridging was not associated with decreased absolute MBF or increased atherosclerotic burden. Speckle tracking allows quantitative echocardiographic imaging of myocardial deformation. Speckle tracking during dobutamine stress echocardiography was feasible and comparable to subjective wall motion analysis in the diagnosis of CAD. In addition, it correctly risk stratified patients with multivessel disease and extensive ischemia.

Key Words: *coronary artery disease, positron emission tomography, computed tomography, myocardial bridging, stress echocardiography, speckle tracking*

TIIVISTELMÄ

Valtteri Uusitalo

Turun yliopisto, lääketieteellinen tiedekunta, kliininen fysiologia ja isotooppilääketiede, Turun yliopiston kliininen tutkijakoulu, Turun PET-keskus, Turku, Suomi.

Sydänkuvantaminen sepelvaltimotaudin diagnostiikassa: kvantitatiiviset kuvantamismenetelmät sydänlihaksen verenvirtauksen ja supistumisen arvioinnissa

Ateroskleroosi on krooninen ja etenevä verisuoniston sairaus. Oireettomuuden vuoksi sitä pidetään monesti subkliinisenä löydöksenä. Ateroskleroosi voi kuitenkin edetä verenvirtausta ahtauttavaksi sepelvaltimotaudiksi tai sydäninfarktiksi. Moderni sydänkuvantaminen on tuonut uusia mahdollisuuksia yksilöllisen sepelvaltimoanatomian ja fysiologian tutkimiseen kajoamattomasti. Sepelvaltimoiden tietokonetomografia (TT) angiografia mahdollistaa sepelvatimoiden anatomian kuvantamisen. Positroniemissiotomografiaa (PET) radioaktiivisesti leimatun veden avulla ($[^{15}O]$ H$_2$O) voidaan käyttää sydänlihaksen verenvirtauksen mittaamiseen (mL/g/min). Arvioimme tutkimuksessamme verisuonten laajenemiskyvyn vaikutusta ateroskleroosin syntyyn mittaamalla perfuusioreserviä, joka on verenvirtaus rasituksessa verrattuna lepoarvoon. Yllättäen alentunut perfuusioreservi ei ennustanut lisääntynyttä sepelvaltimoiden kalkkeutumista 11 vuoden seurannassa terveillä nuorilla miehillä. Kvantitatiivinen sydänlihaksen verenvirtauksen mittaaminen on herättänyt laaja-alaista kiinnostusta kardiologiassa. Arvioimme ensimmäisessä monikeskustutkimuksessa (Turku, Amsterdam ja Uppsala) PET-kuvantamisen tarkkuutta radioaktiivisesti leimatulla vedellä sepelvaltimotaudin diagnostiikassa. Tutkimuksessamme PET-kuvantamisen diagnostinen tarkkuus oli erinomainen ja optimaaliset raja-arvot ahtauttavalle sepelvaltimotaudille olivat rasituksessa sydänlihaksen verenvirtaus alle 2.3 mL/g/min ja perfuusioreservi alle 2.5. Sepelvaltimoiden lihassillat ovat anatominen variantti, jossa sepelvaltimon osa kulkee sydänlihaksen sisällä. Ne voidaan havaita TT:llä intramuraalisena sepelvaltimona tai kajoavalla sepelvaltimoiden angiografialla systolisena kompressiona. Arvioimme $[^{15}O]$ H$_2$O PET perfuusiolla lihassiltojen vaikutusta sydänlihaksen verenvirtaukseen. Lihassillat eivät olleet yhteydessä alentuneeseen verenvirtaukseen tai lisääntyneeseen ateroskleroosiin. Speckle tracking mahdollistaa kvantitatiivisen sydänlihaksen liikkeen ultraäänikuvantamisen. Sovelsimme speckle tracking- tekniikkaa rasitusultraäänikuvantamiseen dobutamiinirasituksen aikana. Se oli verrannollinen tavanomaisen silmämääräisen analyysin kanssa. Speckle trackingin avulla pystyttiin hyvällä tarkkuudella toteamaan vaikea monen suonen sepelvaltimotauti ja laaja-alainen sydänlihaksen hapenpuute.

Avainsanat: *sepelvaltimotauti, positroniemissiotomografia, tietokonetomografia, lihassillat, rasitusultra-ääni, speckle tracking*

ABBREVATIONS

CAD	Coronary artery disease
CCS	Coronary calcium score
CI	Confidence interval
CFR	Coronary flow reserve
CT	Computed tomography
CTA	Computed tomography angiography
DSE	Dobutamine stress echocardiography
ECG	Electrocardiogram
FFR	Fractional flow reserve
HDL	High-density lipoprotein
ICA	Invasive coronary angiography
IM	Intermediate artery
LAD	Left anterior descending artery
LCX	Left circumflex artery
LDL	Low-density lipoprotein
LM	Left main artery
MB	Myocardial bridge
MBF	Myocardial blood flow
MRI	Magnetic resonance imaging
PET	Positron emission tomography
PSI	Post-systolic strain index
RCA	Right coronary artery
ROC	Receiver-operator curve
SPECT	Single-photon emission computed tomography

LIST OF ORIGINAL PUBLICATIONS

This dissertation is based on the following original scientific publications, which are referred in the text by the corresponding Roman numerals (I-IV).

I   **Uusitalo V**, Saraste A, Kajander S, Luotolahti M, Wendelin-Saarenhovi M, Sundell J, Raitakari O, Knuuti J. The association between coronary flow reserve and development of coronary calcifications: a follow-up study for 11 years in healthy young men. Eur Heart J Cardiovasc Imaging. 2013;14:812-8.

II   **Uusitalo V**, Saraste A, Pietilä M, Kajander S, Bax JJ, Knuuti J. The Functional Effects of Intramural Course of Coronary Arteries and its Relation to Coronary Atherosclerosis. JACC Cardiovasc Imaging. 2015;8:697-704.

III   Danad I, **Uusitalo V**, Kero T, Saraste A, Raijmakers PG, Lammertsma AA, Heymans MW, Kajander SA, Pietilä M, James S, Sörensen J, Knaapen P, Knuuti J. Quantitative Assessment of Myocardial Perfusion in the Detection of Significant Coronary Artery Disease: Cutoff Values and Diagnostic Accuracy of Quantitative $[(15)O]H_2O$ PET Imaging. J Am Coll Cardiol. 2014;64:1464-75.

IV   **Uusitalo V**, Luotolahti M, Pietilä M, Wendelin-Saarenhovi M, Hartiala J, Saraste M, Knuuti J, Saraste A. Two-dimensional Speckle Tracking during Dobutamine Stress Echocardiography in the detection of Myocardial Ischemia in Patients with Suspected Coronary Artery Disease**.** JASE [*Accepted*]

1. INTRODUCTION

In the normal coronary artery, three separate layers can be histologically distinguished in the coronary artery wall. These layers are the inner intima, the intermediate media and the outer adventitia. The intima consists of a single layer of endothelial cells covering the lumen side and a few subendothelial smooth muscle cells. It is separated from the media by internal elastic lamina formed from collagen and elastin. In the normal coronary artery, the media is the thickest layer with multiple layers of smooth muscle cells. The outmost vascular layer, the adventitia, is composed of connective tissue, fibroblasts, nerves and small blood and lymphatic vessels. Atherosclerosis is a multifactorial chronic progressive disease of the vasculature characterized by pathological thickening of intimal layer. In Greek, *athere* means gruel (thin porridge) and *sklerosis* means hard. In the absence of clinical symptoms, nonobstructive atherosclerotic lesions are often considered subclinical. However, some of the lesions can progress into obstructive coronary artery disease (CAD) or acute myocardial infarction. Unlike nonobstructive atherosclerosis, obstructive CAD impairs myocardial blood flow (MBF) distal to coronary plaque resulting in an imbalance between myocardial oxygen supply and demand also known as myocardial ischemia. Stable CAD is a chronic disease with symptoms of chest pain during various levels of physical activity depending on its severity. In contrast to stable CAD, myocardial infarction is caused by sudden prolonged ischemia and results in irreversible myocardial injury (Thygesen et al. 2012). The rupture of an atherosclerotic plaque is the most common culprit in myocardial infarction. Multiple large clinical trials have also demonstrated increased mortality with clinically silent nonobstructive atherosclerosis (Min et al. 2011; Ostrom et al. 2008). It is now recognized that dangerous vulnerable coronary plaques prone to rupture are frequently nonobstructive (Ambrose et al. 1998; Narula 2008). Thus, nonobstructive atherosclerosis cannot be considered a truly benign phenomenon.

Common clinical risk factors of CAD are hypercholesterolemia, hypertension, diabetes, smoking, the male gender, a family history of premature vascular disease and obesity. Using these risk variables, clinical risk

assessment tools for the development of CAD such as the Framingham risk score and SCORE have been introduced (Montalescot et al. 2013). However, actual cardiac risk is frequently misclassified with the use of the current risk assessment tools based on conventional risk factors (Erbel et al. 2010; Hecht 2015). Fortunately, with the development of modern cardiac imaging coronary artery anatomy and physiology can be evaluated noninvasively. Anatomic imaging of coronary arteries enables individualized risk assessment based on the extent, location and morphology of atherosclerotic lesions. Previously the visualization of coronary anatomy has required invasive vascular access and coronary catheterization. With the use of computed tomography angiography (CTA), the anatomy of the coronary arteries can be studied with a great precision. The high negative predictive value of CTA in the exclusion of obstructive CAD is currently utilized in clinical cardiology. Multiple anatomic features of coronary plaques seen on CTA have also been correlated with the presence of vulnerable plaque prone to rupture (Maurovich-Horvat et al. 2014). However, the anatomic degree of coronary stenosis is a surprisingly poor predictor of the presence of myocardial ischemia (Shaw et al. 2008; Meijboom and Meijs et al. 2008). Accurate evaluation of the functional significance of coronary artery stenosis requires the assessment of coronary hemodynamics or cardiac physiology.

Positron emission tomography (PET) enables noninvasive imaging and quantification of myocardial blood flow (MBF) in absolute terms (mL/g/min). The diagnostic superiority of quantitative imaging of MBF compared to qualitative evaluation is well established (Saraste et al. 2012; Joutsiniemi et al. 2014). Absolute MBF excels in scenarios with balanced ischemia caused by multi-vessel CAD or global microvascular disease which can confound the subjective image assessment. Currently, PET perfusion with the use of $[^{15}O]$ H_2O can be considered the functional gold standard in the evaluation of MBF (Saraste et al. 2012). Another well-established functional imaging modality is stress echocardiography in which ischemia induced wall motion abnormalities are evaluated visually. Reaching the same level of diagnostic accuracy as previously published requires considerable expertise from echocardiographer. Quantification of wall motion with the use of speckle tracking is a promising technology to overcome the limitations of subjective image analysis (Marwick 2006). Recently, the combination of both anatomical and functional imaging modalities as hybrid

imaging have allowed comprehensive assessment of CAD. Hybrid imaging of CAD with the use of PET/CT has demonstrated incremental diagnostic value in the detection of obstructive CAD (Kajander et al. 2010). Moreover, the diagnosis of microvascular dysfunction requires anatomical imaging to demonstrate the absence of epicardial stenosis. This underlines the importance of both the anatomical and functional evaluation of CAD as they provide information on different aspects of coronary pathophysiology.

This thesis and studies I-IV focus on the combination of coronary artery anatomy and function to evaluate various aspects of CAD. In addition, the value of quantitative imaging of both anatomy and function with various cardiac imaging modalities is evaluated. Quantitative PET perfusion with the use of $[^{15}O]$ H_2O is utilized in all of the studies (I-IV). The main focus of this thesis is noninvasive cardiac imaging in the diagnosis of stable CAD.

2. REVIEW OF THE LITERATURE

2.1 Coronary Artery Disease

2.1.1 Coronary Artery Atherosclerosis

Atherosclerosis is characterized by vascular wall lipid accumulation, smooth muscle cell proliferation, inflammatory process, changes in hemostasis and progressive vascular calcification (Libby and Theroux 2005). These changes in coronary arteries typically begin in the 30's and progress depending on both hereditary and environmental factors (Strong et al. 1999). The clinical presentation of atherosclerotic disease depends on the anatomic location of the lesions. In addition to CAD, the spectrum of atherosclerotic vascular disease include transient ischemic attack, stroke, peripheral artery disease, renovascular disease and aortic aneurysms. The histological progression of atherosclerotic plaques is depicted in Table 1.

The initial culprit of the atherosclerotic process is low density lipoprotein (LDL) which accumulates in the intimal layer (Libby et al. 2000). It undergoes oxidation and other chemical modifications which result in a pro-inflammatory response and the induction of foam cell transformation of macrophages. The fatty streak caused by the transformation of lipid collecting macrophages into foam cells is the first visible presentation of atherosclerosis (Hilgendorf et al. 2015). The cytoplasm of the foam cells is filled with lipid droplets that cause the foamy outward appearance of the atherosclerotic vessel wall. Coronary bifurcations and curvatures are the most susceptible locations for the initiation of atherosclerosis due to the elevated shear stress which increases the permeability of the vessel wall for cholesterol rich macromolecules (Maurovich-Horvat et al. 2014). Intimal thickening activates endothelial adhesion molecules and leukocyte recruitment which in turn further increase plaque inflammation (Libby and Theroux 2005; Moore and Tabas 2011). The fatty streak can either progress into a mature coronary plaque or regress over time (Hanssen and Libby 2006). Atherosclerotic macrophages in particular are thought to promote the transformation of pathological intimal thickening into an actual fibroatheroma (Moore and Tabas 2011). As the fibroatheroma further matures, increasing calcification with the proliferation of smooth muscle cells and connective tissue matrix cause its protrusion to artery lumen. Vascular calcification is promoted by both the loss of inhibitors of mineralization and the induction of osteogenesis (Johnson et al. 2009). A more complicated lesion with vulnerable features may later form as a result of cell necrosis, mural thrombosis and plaque hemorrhage (Virmani et al. 2000). However, as the definition of atherosclerosis is anatomical, atherosclerotic changes do not necessarily result in functional abnormalities in MBF. Thus, nonobstructive atherosclerosis is often considered as subclinical. This does not mean that asymptomatic atherosclerosis can be considered a benign phenomenon. In multiple studies, extensive nonobstructive atherosclerosis is linked with worse cardiovascular prognosis than mild changes or completely normal coronaries (Min et al. 2011 and Ostrom et al. 2008).

Table 1. Histology and progression of atherosclerotic plaques

Stage	Presentation	Characteristic morphology
Type I	Xanthomata (fatty streak)	Intimal deposition of foam cells. No lipid core or fibrous cap. Non-atherosclerotic intimal lesion.
Development of progressive atherosclerotic lesion		
Type II	Pathological intimal thickening	Focal accumulation of lipids. Smooth muscle cell proliferation. Endothelial activation and recruitment of leukocytes.
Type III	Fibroatheroma	Development of the fibrous cap and necrotic lipid core
Type IV	Thin-cap fibroatheroma	Large necrotic core with thin fibrous cap. Relatively low number of smooth muscle cells. Intraplaque hemorrhage and high grade inflammation. High risk for myocardial infraction.
Type V	Disrupted plaque	Fibroatheroma with ruptured fibrous cap. Thrombus caused by hemostatic material communicating with blood. Can be occlusive or non-occlusive

Modified from Virmani et al. 2000.

2.1.2   Obstructive Coronary Artery Disease

As atherosclerotic changes become more severe MBF can be compromised by epicardial coronary stenosis causing an imbalance between the supply and demand of oxygen in the myocardium. This metabolic imbalance and obstruction of coronary blood flow is the key difference between subclinical atherosclerosis and CAD. As the number one cause of mortality in western countries prevention, accurate diagnosis and treatment of CAD is of great importance in clinical and experimental medicine (Lopez et al. 2001). Obstructive CAD can present as either stable chronic chest pain or more dramatically as acute myocardial infarction, heart failure or ventricular tachycardia (Kannel 1997; Mozaffarian et al. 2015). Unfortunately, also sudden cardiac death can be the first presentation of CAD (Virmani et al. 2000). Thus, early diagnosis

and correct risk stratification of CAD patients is imperative. In addition to epicardial stenosis, endothelial and microvascular function affect the coronary hemodynamics in CAD (Montalescot et al. 2013).

In clinical medicine the definition for obstructive CAD usually includes a significant atherosclerotic narrowing of the coronary arteries which cause symptomatic ischemia (Montalescot et al. 2013). However, myocardial ischemia can also be caused by other coronary etiologies such as microvascular dysfunction and vasospasm. These different etiologies of ischemia frequently overlap and can be all considered to belong in the spectrum of stable CAD (Montalescot et al. 2013). Further categorization of symptoms as stable or unstable is imperative in the management of chest pain. Stable CAD is typically characterized by short episodes of chest pain generally lasting less than 10 minutes during physical or emotional stress and are rapidly alleviated at rest or by anti-ischemic treatment with nitrates. Characteristic for acute coronary syndrome is prolonged, new or worsening chest pain. It can be further classified according to ECG and cardiac enzyme measurements (Thygesen et al 2012). In unstable angina pectoris there is no evidence of myocardial injury (Hamm et al. 2011). In contrast, myocardial infarction causes an elevation in cardiac biomarkers indicating myocardial cell death (Thygesen et al 2012).

2.1.3 Myocardial Ischemia

In myocardial ischemia there is an imbalance between the supply and demand of oxygen and metabolic substrates in myocardium. Unlike other vascular regions in the body, myocardial extraction of oxygen is near maximal during rest (about 75%) (Feigl 1983). This means that any increase in myocardial oxygen demand is primarily met by the increase of MBF. CAD impairs blood flow distal to the obstructive plaque and thus oxygen transportation becomes compromised. The greatest ischemic burden is in the subendocardial layer which is supplied by the more distal parts of the coronary tree. However, induction of myocardial ischemia by an atherosclerotic plaque requires the presence of surprisingly severe coronary stenosis (>50-70%) as small distal resistance vessels dilate to compensate for the diminished MBF (Klocke 1976; Klocke 1983; Gould and Lipscomb 1974; Muzik et al. 1998). Even then chest pain only appears in the presence of

increased myocardial oxygen consumption secondary to exercise or psychological stress. All factors affecting the supply or consumption of oxygen in the myocardium such as anemia, tachycardia or drop in blood pressure can precipitate the occurrence of ischemia. The impairment of resting MBF is seen only in a subtotal coronary artery obstruction (Klocke 1976; Klocke 1983; Gould and Lipscomb 1974; Detry 1996). Other minor factors affecting coronary flow resistance are the variable vascular compression caused by left ventricular pressure and myocardial contraction during the heart cycle (Feigl 1983; Klocke 1976). This effect is small compared to the importance of small resistance vessels. In addition to vascular resistance, upstream coronary artery stenoses, diffuse atherosclerosis, endothelial function and collateral circulation are important factors in determining MBF in CAD (Gould et al. 2000; Bartenstein et al. 1992; Abrams 1997).

Increasing myocardial ischemia initiates the characteristic ischemic cascade (Detry 1996). The first observable physiological effects after decrease in blood flow are biochemical changes of the myocardium followed by diastolic dysfunction, systolic dysfunction, elevated filling pressure and ECG changes. The final step of the ischemic cascade is the symptom of chest pain. However, ischemia caused by CAD can also present as a more atypical symptom such as dyspnea or decreased functional capacity and thus careful clinical evaluation is needed. In some cases myocardial ischemia can be asymptomatic (Schang and Pepine 1977). Clinically silent ischemia has also been associated with worse cardiovascular prognosis (Deedwania and Carbajal 1990). Recent studies suggest that patients with demonstrable ischemia due to epicardial CAD benefit the most from coronary revascularizations (Tonino et al. 2009; Shawn et al. 2008). This underlines the importance of functional imaging in guiding the treatment choices of CAD.

2.1.4 Risk Factors

The classic risk factors for CAD include high blood pressure, elevated low-density lipoprotein (LDL), diabetes mellitus, smoking, age, and family history of CAD (Castelli et al 1986; Kannel and McGee 1979; Myers et al. 1990; Wilson et al. 1998). Other hyperlipidemias such as hypertriglyseridemia and decreased

high-density lipoprotein have been also associated with CAD (Castelli et al 1986; Davignon and Cohn 1996). Lipoprotein A is a subclass of LDL that has been linked with the development of atherosclerosis (Tsimikas et al. 2010). In addition, obesity and sedentary lifestyle are independent predictors of CAD (Franco et al. 2005; Ingelsson et al. 2007). Elevated biomarkers of inflammation and the presence of an inflammatory disease such as rheumatoid arthritis are now recognized as a risk factor for the development of CAD (Danesh et al. 2004; Wolfe 2003). There are multiple genes associated with accelerated atherosclerosis. Previously, the most commonly studied polymorphic genes are involved in inflammation, lipid metabolism, hemostasis and fibrinolysis (Roberts 2015). Not all patients deemed as high risk by the traditional risk factors develop CAD. Similarly, some in the small risk population suffer from myocardial infarction. Clearly, novel biomarkers and diagnostic methods are required to complement the traditional risk scores to correctly reclassify patients according to their true cardiovascular risk.

2.1.5   Vulnerable Plaque

There are certain recognized high risk features of coronary plaques that make them more prone to rupture and cause myocardial infarction. Vulnerable coronary plaques tend to have a large necrotic lipid cores and thin inflamed fibrous caps (Finn et al. 2010). Two-thirds of acute coronary syndromes are caused by the rupture of the fibrous cap and the remaining one-third result from the erosion of the intimal surface (Narula et al. 2008). As the fibrous cap ruptures, the prothrombotic material inside is exposed to circulating blood and acute thrombosis results. In vulnerable plaques, active inflammation is usually present with macrophage infiltration and matrix metalloproteinases, which causes progressive matrix degeneration (Finn et al. 2010). Outward remodeling is a characteristic for vulnerable plaques as is the pausity of smooth muscle cells (Maurovich-Horvat et al 2014; Virmani et al 2003; Narula et al. 2008). The number of these high risk plaques is limited, and there are usually less than three in one individual (Virmani et al 2003; Narula et al. 2008). They are frequently located in the LAD and usually in the proximal coronary segment (Virmani et al. 2003; Narula et al. 2008). A proximal high risk plaque increases the possibility of lethal myocardial infarction as a larger myocardial area is affected. Vulnerable plaques are often large in volume and 75% of

them cause greater than 50% coronary artery stenosis (Narula et al. 2008). However, a significant number of myocardial infarctions are caused by non-obstructive coronary plaques that can be only detected by anatomical imaging modality (Ambrose et al. 1998; Narula et al. 2008).

2.1.6   Coronary Flow Reserve

Coronary flow reserve (CFR) is the ratio between MBF during stress and rest. It's a measure of the coronary arteries' ability to increase MBF during maximal exercise or pharmacological stress. Usually myocardial resting flow is between 0.7-1 mL/g/min and can increase 4-5 times during stress as distal resistance vessels open (Klocke 1976; Uusitalo et al. 2012). According to previous observations validated against fractional flow reserve (FFR), CFR can be considered abnormal when the ratio is less than 2.5 (Kajander et al. 2010). However, in other quantitative perfusion studies there is a high variance in the optimal CFR threshold which is probably caused by methodological differences between studies (Danad et al. 2013; Muzik et al. 1998). CFR gives information on both epicardial and microvascular function and in the absence of epicardial CAD, it can be used to evaluate microvascular dysfunction. The importance of microvascular integrity to has been increasingly recognized. Furthermore, pharmacologic treatment of microvascular angina may differ from the treatment of epicardial CAD (Montalescot et al. 2013). In addition, CFR confers prognostic value independent of the anatomic degree of CAD (Murthy et al. 2012; Taqueti et al. 2015).

2.1.6.1 Endothelial Dysfunction

The vascular endothelium contributes to the regulation of coronary vasomotor activity by both endothelium-derived relaxing and contracting factors. The main endothelium-dependent control of vascular smooth muscle tone is mediated through the production of vasodilator substances. In addition to the regulation of vascular tone, the endothelium is also physiologically active in the regulation of blood coagulation and the modulation of inflammatory response (Münzel et al. 2008). Thus, alterations in endothelial function have important role in the pathophysiology of atherosclerosis (Abrams 1997; Münzel et al. 2008). Dysfunctional

endothelium is characterized by the impaired release of vasodilative factors such as nitric oxide while release of vasoconstrictive factors are increased (Abrams 1997; Münzel et al. 2008). Endothelial function can be assessed by measuring vasodilation in coronary or brachial arteries after infusion of acetylcholine, by releasing manual pressure or by modulating blood pressure by cold pressor test (Zeiher et al. 1991; Münzel et al. 2008). Impairment of vasodilation due to endothelial dysfunction may cause decrease in MBF during stress and thus contribute to myocardial ischemia. The risk factors of endothelial dysfunction are similar to those of CAD including hypertension, diabetes, high cholesterol, smoking, positive family history, and age (Abrams 1997; Münzel et al. 2008).

2.1.6.1 Microvascular Dysfunction

Microvascular dysfunction is a result of the impaired vasodilative function of small distal resistance vessels. It can cause clinical symptoms of microvascular angina similar to obstructive CAD (Camici and Crea 2007: Parrinello et al. 2014). Microvascular dysfunction can be primary or related to heart diseases such as left ventricular hypertrophy, dilated cardiomyopathy or hypertrofic cardiomyopathy (Camici and Crea 2007). Iatrogenic causes of microvascular disease are radiation therapy and percutaneus coronary intervention (Camici and Crea 2007). Microvascular angina has been linked with more atypical clinical presentation and is frequently nonresponsive for nitrates (Lanza and Crea 2010; Montalescot et al. 2013). Similarly to epicardial disease, microvascular dysfunction can be stable or unstable (Lanza and Crea 2010). In a previous study, myocardial infarction without epicardial disease was associated with poor outcome, probably reflecting the lack of possible treatment interventions to microvasculature (Planer et al. 2014). Stable microvascular angina is linked with a more favorable prognosis (Kaski et al. 1995; Lamendola et al. 2010). However, 20-30% of patients may have progressively worsening symptoms (Cannon et al. 1990; Lanza 2007; Lanza and Crea 2010). Differentiation of CAD and microvascular disease is problematic without the use of both an anatomical and functional imaging modality.

2.1.7 Myocardial Bridging

Myocardial bridging is a common variant of coronary artery anatomy where a segment of coronary artery travels inside myocardium instead of the normal epicardial route (Alegria et al. 2005; Bruschke et al. 2013). In a segment with myocardial bridging, contracting myocardium results in the obstruction of coronary flow during systole and sharp increase of flow velocity when the bridging segment opens in diastole. After an initial sharp increase in flow velocity during diastole velocity decreases and plateaus (Ge et al. 1999; Schwarz et al. 1997). Interestingly, although the majority of MBF occurs during diastole, previous observations have demonstrated that coronary hemodynamics are affected beyond systolic coronary flow (Escaned et al. 2003; Ge et al. 1999; Schwarz et al. 1997). As the heart rate increases during exercise, diastole shortens in relation to systole and cardiac contractility in the covering myocardial band increases, which may induce myocardial ischemia. Previously, myocardial bridges have been associated with stable chest pain and reversible ischemia (Gawor et al. 2011; Alegria et al. 2005; Bruschke et al. 2013). In addition, atherosclerotic plaques tend to develop proximally in myocardial bridges while the coronary segments affected by bridging are spared (Kawawa et al. 2007; Konen et al. 2007). Currently, it is unclear whether myocardial bridging is associated with increased atherosclerotic burden or just the proximal location of plaques. In diagnostic medicine myocardial bridging is a frequent incidental finding as intramural course on CTA and systolic compression on ICA. In previous studies the prevalence of intramural coronary artery have been 5-58% on autopsies and 4-58% on CTA studies (Möhlenkamp et al. 2002; Wirianta et al. 2012; Bruschke et al. 2013). Only 21-46% of intramural courses are functionally active and cause systolic compression (Leschka et al. 2008; Kim et al. 2009; Kim et al. 2011). The prognosis of myocardial bridging is usually excellent (Kramer et al. 1982; Ural et al. 2009; Rubinshtein et al. 2013).

2.1.8   The Effect of Pretest Probability on the Selection of Diagnostic Test

Chest discomfort is a common symptom in clinical practice and can be caused by multiple different etiologies. Accurate anamnesis of both symptoms and risk factors of CAD are required to assess the possibility of cardiac etiology. Typical angina pectoris is defined as retrosternal pain that presents during physical or psychological stress and is alleviated by nitrates and rest within minutes. The retrosternal pain can typically radiate to the arms or neck. Atypical chest pain shares two and nonanginal chest pain only one or none of the features of typical angina pectoris (Montalescot et al. 2013). Using presentation, gender and age, patients can be categorized according to their pretest probability of CAD (Genders et al. 2011; Montalescot et al. 2013). This is of great importance since according to the Bayes' theorem pretest probability of the disease affects the accuracy of diagnostic testing (Diamond and Forrester 1979). However, before any diagnostic testing comorbidities and their prognosis needs to be pragmatically considered. If it is unlikely that revascularization is a reasonable option, further clinical testing should be kept to a minimum. Instead, a trial with anti-anginal medication could be performed (Montalescot et al. 2013). Exercise ECG is a good, inexpensive initial diagnostic test for evaluating a patient with stable chest pain as it also offers important prognostic information and guides the decision between pharmacological treatment and possible revascularization. However, ECG abnormalities such as left bundle branch block, paced rhythm and Wolf-Parkinson-White syndrome may distort the ST-segment analysis and cardiac imaging might be needed. Other known factors affecting exercise ECG interpretation are abnormal resting ECG, left ventricular hypertrophy, electrolyte imbalance, atrial fibrillation, female gender, conduction abnormalities and the use of digitalis (Morise and Diamond 1995; Androulakis et al. 2007; Montalescot et al. 2013). Furthermore, patients with conditions like arthrosis or peripheral vascular disease might be unable to exercise and thus require pharmacologic stress testing. Table 2 demonstrates the rationale of the pretest probability of CAD in clinical evaluation.

Table 2. Evaluation of the pretest probability of coronary artery disease.

Age (years)	Typical angina pectoris		Atypical angina		Non-anginal chest pain	
	Men	Women	Men	Women	Men	Women
30-39	59 %	28 %	29 %	10 %	18 %	5 %
40-49	69 %	37 %	38 %	14 %	25 %	8 %
50-59	77 %	47 %	49 %	20 %	34 %	12 %
60-69	84 %	58 %	59 %	28 %	44 %	17 %
70-79	89 %	68 %	69%	37 %	54 %	24 %
>80	83 %	76 %	78 %	47 %	65 %	32 %

Data are presented as percentages. Color indicates different pretest likelihoods (Gray < 15%, green 15-65%, yellow 66-85% and red > 85%, respectively). Modified from Genders et al. 2001.

2.1.8.1 Low Pretest Probability

Evaluating patients with low pretest probability of CAD (<15%) with exercise ECG can be problematic. Although a negative test result is a reassuring finding, the low likelihood of disease greatly increases the chance of a false positive test (Diamond and Forrester 1979; Genders et al. 2011). False positive findings are a frequent problem especially in women (Morise and Diamond 1995; Kwok et al. 1999). Because of a high rate of false positive findings, no diagnostic testing is recommended without a compelling reason if the pretest probability of CAD is below 15% (Montalescot et al. 2013). To complement the low pretest likelihood, a diagnostic test with good sensitivity for exclusion of obstructive CAD is required. CTA is widely used in the exclusion of CAD in the intermediate pretest risk population given its excellent sensitivity (Budoff et al. 2008; Meijboom et al 2008). Patients with low pretest probability of CAD also have less coronary calcification which improves the image quality and thus increases the diagnostic accuracy of CTA (Budoff et al. 2008; Chen et al. 2011). Even though problematic and not recommended, exercise ECG is frequently used in the low risk population as it is inexpensive, provides information about functional capacity and a negative test result may reassure patient (Miller et al. 2005).

2.1.8.2 Intermediate Pretest Probability

Patients with intermediate pretest probability (15-85%) are ideal candidates for further diagnostic evaluation of CAD (Diamond and Forrester 1979; Genders et al. 2011). Intermediate probability can be further divided into low- (15-65%) and high intermediate (66-85%) probability. Exercise ECG is an ideal initial test in the low intermediate probability group (Montalescot et al. 2013; Genders et al. 2011). Further diagnostic evaluation should be done as needed with the use of noninvasive cardiac imaging. With increasing pretest probability, the chance of incorrect exercise ECG results becomes higher than true positive results. Thus, exercise ECG is not recommended in patients with high intermediate pretest probability (Montalescot et al. 2013; Genders et al. 2011). Nevertheless, exercise ECG can still be used for risk stratification of patients while further noninvasive cardiac imaging with better diagnostic accuracy is used to establish the diagnosis. CTA without combined hybrid imaging should only be considered in the low intermediate pretest group since its greatest strength is in ruling out obstructive CAD (Budoff et al. 2008; Meijboom et al 2008). Other noninvasive cardiac stress testing modalities such as stress echocardiography, single-photon emission computed tomography (SPECT), PET and magnetic resonance imaging (MRI) should be used according to patient suitability, availability and local expertise (Montalescot et al. 2013).

2.1.8.3 High Pretest Probability

In the case of high pretest probability, the diagnosis of CAD is essentially clinical as the further testing has little to add in terms of diagnostic value. However, exercise ECG and cardiac imaging can still provide prognostic information (Montalescot et al. 2013). The next recommended imaging modality in patient management is invasive coronary angiography (ICA). Cardiac imaging of myocardial viability before or after ICA may be used to guide revascularization. Other noninvasive evaluation with cardiac imaging is not generally recommended as it only increases radiation and contrast agent dose without further adding to accuracy of the diagnosis (Fihm et al. 2012; Montalescot et al. 2013).

2.1.9   Clinical Risk Stratification

Risk assessment is always necessary to guide treatment choices in CAD. Factors associated with severe CAD include male gender, previous myocardial infarction, typical angina pectoris, old age, diabetes and the use of insulin (Pryor et al. 1993; Miller et al. 2005). Progressive severe angina unresponsive to treatment is a high risk feature (Califf et al. 1988; Fihm et al. 2012). The presence of peripheral atherosclerotic vascular disease and chronic kidney disease increase cardiovascular risk (Pryor et al. 1993; Di Angelantonio et al. 2010). Since exercise ECG is widely available and inexpensive, it is frequently used for further risk stratification. Moreover, low functional capacity remains one of the strongest predictors of cardiac adverse events (Myers et al. 2002; Gupta et al. 2011; Lauer 2011). Other high risk features on exercise ECG include ischemia or chest pain at low level of exercise, slow heart rate recovery, frequent ventricular ectopic beats and inadequate rise of blood pressure (Myers et al. 2002; Lauer 2007; Fihn et al. 2012; Montalescot et al. 2013). High risk patients benefit from further invasive assessment of coronary arteries while patients with normal exercise test or good functional capacity have a favorable prognosis (Miller et al. 2005; Lauer 2011; Montalescot et al. 2013). In the presence of left ventricular dysfunction patient should be referred to ICA for the assessment of possible ischemic cardiomyopathy as depressed left ventricular function is strongly associated with increased mortality (Emond et al. 1994; Daly et al. 2003). Interestingly, Daly et al. observed that only a minority of patients with left ventricular dysfunction had prior diagnosis of heart failure which underlines the importance of routine echocardiography in risk stratification (Daly et al. 2003). Furthermore, with echocardiography the presence of valvular heart disease or left ventricular thrombus can be evaluated for prediction of additional cardiac risk (Fihn et al. 2012). Left ventricular hypertrophy and increased chamber diameter independently predicts future cardiac events (Levy et al. 1990; Fihn et al. 2012).

2.2 Anatomical Imaging of Coronary Artery Disease

2.2.1 Computed Tomography Angiography (CTA)

2.2.1.1 Basics of CTA

Modern CTA imaging have been feasible since the arrival of multi-detector computed tomography technology. In 2005, a 64-row computed tomography (CT) device became available allowing 64 slices in one gantry rotation and image slices as thin as 0.5mm. Further development of CT technology has been rapid and 256- and 320-row machines have now been introduced. The basic concept of CTA is the reconstruction of image slices of the heart from multiple projections obtained by rotating X-ray source and detector around the patient. These slices are combined to form a three-dimensional dataset that can form unlimited reconstructed oblique slices with dedicated analysis software. In the reconstructed image of the heart anatomical structures can be differentiated by different attenuation values. An iodine based contrast agent is used to visualize the coronary artery lumen. Prospective ECG-triggering, sequential and high pitch scans, lower tube voltage and iterative reconstruction algorithms have decreased the radiation dose substantially (Roobottom et al. 2010). The average radiation dose of modern CTA is around 1-5 mSv. Limitations to consider in patient selection are the poor quality of the image in patients with elevated heart rate (> 70/min) and irregular rhythm. Beta-blockers can be used before the study to decrease the heart rate. Other exclusion criteria for a CTA study are pregnancy, iodine allergy and kidney disease.

2.2.1.2 Calcium Score

Coronary calcium score (CCS) is a measure of total atherosclerotic burden of coronary arteries obtained by non-contrast computed tomography. The possibility to detect coronary calcification by fluoroscopy was demonstrated in the late 1950s and the ability to predict cardiovascular risk was subsequently observed

(Blankenhorn and Stern 1959; Margolis et al. 1980). Electron beam computed tomography was commonly used for CCS but has now been replaced by modern multi-detector computed tomography. The most widely used method for calculating a calcium score is the Agatston CCS where the area of coronary calcifications are multiplied by different weight factors according to plaque's radiodensity (1 for 130-190 HU, 2 for 200-299 HU, 3 for 300-399 HU and 4 for $\geq$ 400 HU) (Alluri et al. 2014). A CCS of zero rules out significant CAD with good probability and is a strong predictor of good cardiovascular prognosis even in the presence of conventional CAD risk factors (Blaha et al. 2009; Sarwar et al. 2010). The risk for future cardiac events rises in a step-wise manner as CCS increases in both symptomatic and asymptomatic population (Detrano et al. 1996; Greenland et al. 2007; Detrano et al. 2008). The technique for obtaining CCS is simple with a low radiation dose and without the use of contrast agent. In addition, new radiation dose reduction techniques such as tube current optimization, overlapping thick image slices and prospective triggering can be used to decreases the radiation dose even further (Alluri et al. 2014). The average radiation dose for obtaining CCS is less than 1 mSv which is comparable to mammography. The clinical use of CCS in the screening of atherosclerosis and guiding treatment choices has long been debated. The strengths of CCS are its low radiation dose, low price and the possibility to use it as a gate keeper for further diagnostic testing. CCS could also be used to evaluate the suitability of patients for a CTA study as its image quality decreases in the presence of extensive calcification (Gutstein et al 2008; Arbab-Zadeh et al. 2012).

2.2.1.3 Diagnostic Value

The strength of CTA in the evaluation of CAD is its excellent negative predictive value of almost 100% (Budoff et al. 2008; Meijboom and Meijs et al. 2008). However, the relationship between stenosis severity and the presence of myocardial ischemia is complex. As an anatomical imaging modality CTA cannot accurately evaluate the presence of ischemia caused by intermediate plaques (30-70%) (Meijboom and van Mieghem et al. 2008). The strongest indication for CTA is currently the exclusion of obstructive coronary plaques in patients with low intermediate pretest probability of CAD (Taylor et al. 2010; Montalescot et al. 2013). Patients with high pretest probability of CAD have a high probability for intermediate lesions and

extensive calcification which lowers the accuracy (Taylor et al. 2010; Montalescot et al. 2013; Arbab-Zadeh et al. 2012). Furthermore, lower specificity frequently leads to subsequent imaging with functional imaging modality or invasive coronary angiography to evaluate the hemodynamic significance of the found coronary plaque. This results in an increased dose of contrast agent and radiation. The unique strength of CTA is the ability to visualize the coronary artery wall and to assess the coronary plaque morphology for properties of vulnerable plaque (De Graaf et al. 2013; Maurovich-Horvat et al. 2014). The characterization of coronary atherosclerosis by CTA has been well validated against intravascular imaging (Fischer et al. 2013).

Table 3. Sensitivity and specificity of different noninvasive cardiac imaging modalities

	Sensitivity (%)	Specificity (%)
Anatomical imaging modality:		
CTA	95-99	64-83
Magnetic resonance angiography*	87-88	56-70
Functional imaging: Exercise stress		
Exercise ECG	45-50	85-90
SPECT	73-92	63-87
Stress echocardiography	80-85	80-88
Functional imaging: Pharmacological stress		
SPECT	90-91	75-84
PET	81-97	74-91
Dobutamine stress echocardiography	79-83	82-86
Vasodilator stress echocardiography	72-79	92-95
Dobutamine stress MRI	79-88	81-91
MRI perfusion	67-94	61-85

CTA = computed tomography angiography; MRI = magnetic resonance imaging; PET = positron emission tomography; SPECT = Single-photon emission computed tomography. Modified from Montalescot et al. 2013. * from Fihn et al. 2012

Coronary artery anomalies and coronary bypass grafts can also be studied by CTA. However, coronary artery stents cause a blooming artefact similar to extensive calcification and high spatial resolution is needed for successful imaging. Currently there are no data to support CTA screening of asymptomatic individuals for CAD (Taylor et al. 2010). Although, screening for CAD in patients with strong family history for premature heart disease might be appropriate (Taylor et al. 2010). An overview of the diagnostic accuracy of different cardiac imaging modalities in the diagnosis of CAD are shown in Table 3.

2.2.1.4 Prognostic Value

CTA has great potential in clinical risk stratification of patients with either atherosclerosis or obstructive CAD since it can offer information about atherosclerotic burden, location, degree of obstruction and plaque composition. Interestingly, in a recent study coronary anatomy was an even better predictor of adverse events than the presence of ischemia in a myocardial perfusion study (Mancini et al. 2014). Multiple large clinical trials have demonstrated an association between the number of obstructive coronary vessels and cardiovascular prognosis (Ostrom et al. 2008; Min et al. 2011). Although the culprit lesion for myocardial infarction can be a nonobstructive plaque, the majority of culprit lesions are obstructive (Narula et al. 2008). However, extensive nonobstructive atherosclerosis is also associated with worse prognosis in both obstructive and nonobstructive disease (Bittencourt et al. 2014; Ostrom et al. 2008; Min et al. 2011). Elevated plaque burden might increase the possibility of the vulnerable plaques. More proximal coronary lesions are associated with worse prognosis, and based on previous observations, vulnerable plaques also tend to be located in the proximal coronary segments (Narula et al. 2008).

Unfortunately, the spatial resolution of the current CTA technology is insufficient for measuring the thickness of the fibrous cap of the coronary plaque. Fortunately, other markers for thin-cap fibroatheroma have been described and validated against intravascular ultrasound, optical coherence tomography and autopsy studies (Narula 2008; De Graaf et al. 2013; Maurovich-Horvat et al. 2014). The CTA characteristics

of vulnerable plaqsue in previous studies have been low-attenuation plaque (<30 HU), positive remodelling and spotty calcification (Narula 2008; Maurovich-Horvat et al. 2014). Especially the small spotty calcification phenotype has been associated with the presence of thin-cap fibroatheromas (van Velzen et al. 2011). As the amount of calcification increases, the chance of thin-cap fibroatheroma decrease (van Velzen et al. 2011). The finding of a hypoattenuation area surrounded by ring-like fibrous density attenuation in coronary plaque (napkin-ring sign) is frequently associated with the presence of thin-cap fibroatheroma and the risk of future cardiac events (Otsuka et al. 2013; Maurovich-Horvat et al. 2014). These high risk features of atherosclerotic plaque are additive in the prediction of acute coronary syndrome (Motoyama et al. 2009; Otsuka et al. 2013). Curiously, the features of plaque vulnerability are also associated with the presence of inducible ischemia (Shmilovich et al. 2011; Park et al. 2015).

2.2.2 Invasive Coronary Angiography

ICA is the gold standard of anatomical coronary artery imaging. A catheter is brought to the coronary artery by arterial access from a radial of the femoral artery. After a bolus of contrast agent X-ray images can be obtained from multiple different angles. The strengths of ICA are its excellent spatial resolution (0.2-0.5mm) and the ability to perform interventional procedures immediately after diagnostic angiography. Patients with high pretest probability of CAD or with high risk features should be primarily referred to ICA (Montalescot et al. 2013). A coronary artery stenosis degree greater than 70% is usually considered obstructive. However, there is a poor correlation between the anatomical degree of stenosis and its functional significance (Fischer et al. 2002; Park 2015). To complement this limitation, fractional flow reserve (FFR) with a pressure wire can be used to evaluate the pressure drop after atherosclerotic lesion. FFR is calculated by comparing the ratio of pressure after coronary lesion to the pressure in the coronary ostium during adenosine vasodilatation. Previous studies have demonstrated the superiority of ischemia guided revascularization by FFR (Tonino et al. 2009; Pijls et al. 2010). Unfortunately, standard ICA and FFR measurements do not offer information about microvascular integrity.

2.2.3   Magnetic Resonance Angiography

Magnetic resonance imaging (MRI) is based on the resonance of hydrogen atom nuclei to radiofrequency waves. When a strong magnetic field is applied, all hydrogen protons align instead of the normal random orientation. By radiofrequency excitation the alignment of nuclei can be disturbed. After excitation nuclei relaxation occurs and resulting received radiofrequency waves can be used to construct image. Using a gadolinium contrast agent MRI can be used for coronary angiography. Yet, in clinical cardiology CTA is more frequently used since it has superior sensitivity in the exclusion of obstructive CAD (Schuetz et al. 2010). Cardiac motion, complex three-dimensional anatomy and the small diameter of the coronary artery cause technical challenges for MRI technology (Pennell et al. 2004; Fihn et al. 2012). CTA is also faster and currently has better availability. However, the strength of MRI is that it is a radiation free imaging modality. Similarly to CTA, MRI can be used to visualize abnormalities in coronary anatomy. In addition, MRI is also the gold standard of the anatomical imaging of the myocardium. Furthermore, late gadolinium enhancement can be used to image cardiac fibrosis caused by a previous myocardial infarction which provides incremental prognostic information (Pennell et al. 2004; Catalano et al. 2012: Rachid et al. 2013).

2.3   Functional Imaging of Coronary Artery Disease

2.3.1   Exercise Stress vs. Pharmacological Stress

In stable CAD, an elevation of myocardial oxygen demand is needed for induction of physiological effects of ischemia. The heart muscle's metabolic demand increases during exercise. The oxygen demand can only be met by increasing the MBF. At lower levels of exercise higher cardiac output is achieved by elevation in both stroke volume and heart rate. At maximal stress cardiac output MBF may need to increase more than fourfold which is mainly dependent on heart rate (Christie et al. 1987; Laaksonen et al. 2007). Exercise stress is usually recommended whenever patient is able to exercise as functional capacity is a strong

prognostic indicator (Myers et al. 2002; Gupta et al. 2011; Lauer 2011). The level of exercise can be easily correlated with the patient's work capacity and daily symptom burden. Moreover, symptoms during exercise and the Duke exercise score help in risk stratification (Mark et al. 1991). The goal of exercise stress is usually to reach at least 85% of the age predicted maximal heart rate. However, a significant proportion of patients do not reach the target heart rate and pharmacological stress might be needed. In addition, patients with pulmonary disease, an orthopedic condition, obesity, frailty or peripheral vascular disease might be unable to exercise and need a pharmacological stressor. Some imaging modalities and protocols such as PET perfusion also favor pharmacological stress for technical reasons. Furthermore, patients with conditions like left bundle branch block or paced rhythm have uninterpretable stress ECG. Left bundle branch block may also cause heart rate dependent perfusion artefacts and thus vasodilator stress should be favored.

Vasodilator stress induces maximal coronary vasodilatation with a decreased peak MBF in areas with obstructive CAD compared to normal coronary artery segments. Adenosine is a heterocyclic purine compound produced in vascular endothelium. Adenosine 2A receptor stimulation induces vasodilatation of coronary arteries (Sato et al. 2005). Caffeine and theophylline are competitive inhibitors of adenosine receptor and may thus interfere with vasodilator stress (Henzlova et al 2006). Adenosine has a short half-life of less than two minutes and is completely cleared from the body within two minutes (Henzlova et al. 2006). Like adenosine, dipyridamole is a vasodilative substance. Its mechanism of coronary vasodilatation is indirect by preventing adenosine reuptake and deamination (Henzlova et al 2006). Regadenoson is a novel selective adenosine 2A receptor agonist which is given as an intravenous bolus at a fixed dose and has less side effects than adenosine stress (Jaroudi and Iskandrian 2009). As a limitation in patient selection, vasodilator stress may aggravate underlying asthma or bradycardia. Dobutamine is a synthetic catecholamine. Unlike adenosine or dipyridamole, an infusion of dobutamine results in strong B1- receptor depended elevation in heart rate and myocardial contractility (Elhendy et al. 2002; Henzlova et al. 2006). (Elhendy et al. 2002). Beta-blockers attenuate dobutamine stress significantly and should be withdrawn prior to testing. Side effects with dobutamine are common and include palpitations, chest pain, arrhythmia and hypotension (Elhendy et al. 2002).

2.3.1.1 Comparison of Pharmacological Stressors in Perfusion Imaging

Vasodilator stress works through decreased subendocardial blood flow secondary to inappropriate coronary vasodilation and coronary steal phenomenon. Adenosine, dipyridamole and regadenoson stress cause modest increase in heart rate (10-20 min^{-1}) and decrease in systolic and diastolic blood pressure (8-10 mmHg) (Cerqueira et al. 1994; Miller et al. 2009). Increase in heart rate with regadenoson is slightly higher compared to adenosine (Jaroudi and Iskandrian 2009). Adenosine is usually given as a 4-6 minute infusion (140 ug/Kg/min) and the isotope is injected 3 minutes after initiation of stress (Henzlova et al. 2006; Miller et al. 2009). For dipyridamole stress, an infusion of 0.56 mg/Kg over 4-minute period is generally used (Henzlova et al. 2006). The hemodynamic effect of dipyridamole is longer and the isotope is injected 3-5 minutes after the initiation of infusion. Regadenoson is given as a rapid injection (400 ug) followed by saline flush. The isotope is usually injected 10-20 seconds after the saline flush (Iskandrian et al. 2007). The diagnostic accuracy of perfusion imaging during vasodilator stress with adenosine, dipyridamole and regadenoson appears to be comparable (Kim et al. 2001; Iskandrian et al. 2007; Jaroudi and Iskandrian 2009).

In contrast to vasodilator stress, dobutamine acts through the increase in myocardial oxygen demand. Dobutamine is frequently used as a stressor for stress echocardiography and MRI. However, it is less frequently utilized for perfusion imaging. For PET and SPECT perfusion imaging, dobutamine can be given at a starting dose of 5 ug/Kg/min and increased in step-wise manner every three minutes to a maximum of 40 ug/Kg/min (Henzlova et al. 2006). If dobutamine infusion is insufficient in reaching the target heart rate, intravenous atropine can be administered as 0.5 mg to 1 mg increments (up to 2 mg) (Elhendy et al. 2002; Henzlova et al. 2006). Dobutamine generally increases the heart rate greatly with a modest increase in systolic blood pressure and with a decrease in diastolic blood pressure at a moderate dobutamine dose (around 20 ug/Kg/min) (Hays et al. 1993; Elhendy et al. 2002). Absolute MBF measured during dobutamine stress appears to differ from MBF measured during vasodilator stress (Tadamura et al. 2001; Jagathesan et al. 2006) Therefore, dobutamine stress for perfusion imaging should be reserved for patients with

contraindications for exercise and vasodilator stress.

2.3.2 Positron Emission Tomography (PET)

2.3.2.1 Basics of Cardiac PET

PET technology uses beta-plus decay of radioactively labeled tracers to produce images of the target organ. In the 1980's multiple studies demonstrated the feasibility of cardiac PET perfusion (Hack, et al 1980; Bergmann, et al 1984; Knabb, et al 1985). Usually the PET target molecule labeled with radiopharmaceutical is given as an intravenous bolus. The administered radiopharmaceutical has surplus of protons and thus nuclear imbalance. The proton converts to a neutron and a positron is emitted. The positron immediately annihilates with contact with an electron in the surrounding tissue. This results in two 511 kilo-electron volt gamma rays that travel in opposite directions in a 180 degree angle. Higher energy (511 vs. 140 keV for ^{99m}Tc) leads into less scatter and better spatial resolution compared to SPECT imaging which translates into a better image quality (Bateman et al. 2006; Yoshinaga et al. 2006). The PET scanner's detector ring around the patient detects these two opposite and simultaneous gamma rays and records them. A computer algorithm is used for subsequent reconstruction of a tomographic image from the raw PET data. Short-lived radionuclides of PET imaging can be labeled with a wide range of different molecules to study normal physiological or pathological processes. The strengths of PET technology in cardiology are good spatial resolution and the ability to quantitate MBF (Saraste et al. 2012). The radiation dose for PET perfusion is also significantly lower than for cardiac SPECT (Einstein 2008).

The feasibility of MBF quantification is determined by both the properties of imaging device and tracer characteristics. The device used defines the robustness and overall accuracy of the quantified signal. The most commonly used tracers for the quantitative imaging of MBF are ^{15}O water and ^{13}N-ammonia. For

absolute quantification of perfusion, mathematical tracer kinetic modelling is used. Different compartment models representing tissue volumes can be used depending on radiotracers' properties (Tamaki et al. 2010; Saraste et al. 2012). These compartment models include both biochemical (tracer and labelled metabolite) and physical factors (blood and intracellular fluid). During the dynamic acquisition the time-course of radioactive signal within the left ventricular cavity can be measured. Usually, correction for spill over and partial volume effect is included. Dedicated software can perform the kinetic modeling in the selected volumes to calculate regional blood flow values.

2.3.2.2 Perfusion Imaging with ^{15}O-Water

[15]O-labeld water is close to an ideal tracer for quantification of MBF and can be considered as the gold standard of myocardial perfusion imaging (Saraste et al. 2012). It is metabolically inert, not affected by the metabolic state of the myocardium and freely diffusible (Saraste et al. 2012). In addition, its extraction factor is not affected by the flow rate and thus mathematical extraction correction is not required at high flow values (Saraste et al. 2012). ^{15}O-water has a short half-life of 123 seconds and has to be produced by an on-site cyclotron which limits its spread to clinical use. On the other hand, the short half-life means that studies can be repeated in a fast sequence. It is administrated an intravenous bolus. ^{15}O-labeld water is well validated for quantitative imaging of absolute MBF (Iida, et al 1988). Recently, an MBF less than 2.5 mL/g/min was shown to be highly accurate in the diagnosis of CAD when compared to invasive coronary angiography and fractional flow reserve (Kajander et al. 2010). The radiation dose of rest-stress [15O] H_2O cardiac PET (around 1 mSv) is significantly lower than for SPECT perfusion imaging (Kajander et al. 2009).

2.3.2.3 Other Radiotracers of PET Perfusion imaging

Multiple other PET radiotracers can also be used to image and quantitate MBF. Since [82]Rubidium can be produced by a [82]Strontium reactor and does not require on-site cyclotron, it is the most widely used radiotracer in cardiac PET imaging (Yoshinaga et al. 2010). [82]Rubidium is a potassium analogue with a short

half-life of 76 seconds and similar kinetic properties with [201]Thallium (Yoshinaga et al. 2010). The short

half-life enables effective sequential rest-stress imaging. However, the limitations of [82]Rubidium perfusion

are its nonlinear extraction fraction and high positron range which affects the image quality. This makes its

application to the quantitative measurement of MBF challenging but with technological advancements

several previous studies have reported its feasibility and value in the diagnosis of CAD (Beanlands et al.

2007; Yoshinaga et al. 2010).

[13]N-ammonia has a half-life of 10 minutes and thus requires production by on-site cyclotron. It diffuses

freely through cell membranes and is retained in the myocardium (Krivokapich et al. 1982). The extraction

of ^{13}N-ammonia is not complete and mathematical correction is needed at higher myocardial flow rates

(Schindler 2015; Saraste et al. 2012). The strength of ^{13}N-ammonia is high retention of tracer in the

myocardium resulting in good image quality. Compared to other cardiac PET tracers, the longer half-life of

10 minutes requires a longer imaging protocol for rest-stress study. However, the longer half-life also

enables the use of exercise stress (Krivokapic et al. 1989; Aggarwal et al. 2015). Quantitative imaging of

MBF with ^{13}N-ammonia is well validated and comparable to that of ^{15}O-labeld water (Bol et al. 1993; Muzik

et al. 1993; Swada et al. 1995).

To overcome the requirement of an on-site cyclotron, fluorine-18 based radiotracers for PET perfusion have

been developed (Saraste et al. 2012; Schindler 2015). Fluorine-18 has a longer half-life of 110 minutes and

can be transported to other regional imaging facilities. F18-Flupiridatz binds to the mitochondrial complex I

with high affinity (Nekolla and Saraste 2011; Schindler et al. 2015). The safety and feasibility of [18]F-

flupiridaz have been established recently (Berman et al. 2013). In addition, Flupiridatz PET was superior to

SPECT imaging in the diagnosis of CAD (Berman et al. 2013). It has a good extraction rate to the

myocardium which is proportional to flow rate. (Schindler et al. 2015). This combined with good signal to

noise ratio suggests great potential in PET perfusion imaging. However, further validation studies for [18]F-

Flupiridaz are warranted.

2.3.2.4 PET Perfusion and Coronary Artery Disease

PET perfusion is an accurate modality for the diagnosis of obstructive CAD and it is superior to SPECT perfusion in both image quality and detection (Mc Ardle et al. 2012; Jaarsma et al. 2012; Montalescot et al. 2013). In previous diagnostic studies the sensitivity and specificity of PET perfusion for obstructive CAD have been 81-97% and 74-91%, respectively (Mc Ardle et al. 2012; Jaarsma et al. 2012; Montalescot et al. 2013). MBF distal to obstructive plaque is diminished in the corresponding myocardial area, which can be detected and quantified. Perfusion abnormalities occur early in the ischemic cascade which translates into a good sensitivity for PET perfusion technology. The quantitation of MBF has been shown to be more accurate than qualitative flow analysis in the diagnosis of CAD (Saraste et al. 2012; Joutsiniemi et al. 2014). Furthermore, the superior accuracy of hyperemic MBF compared to CFR has been shown, which has paved a way to stress-only imaging protocols (Kajander et al. 2010). Since MBF is a measure of both epicardial and microvascular function it can be used for the diagnosis of microvascular disease (Knuuti et al. 2009). Another strength of absolute MBF is the possibility to demonstrate balanced ischemia in a three vessel disease (Knuuti et al. 2009). With the conventional qualitative reading severe multivessel disease might be underestimated or missed. Currently, the cost of the PET technology and the availability of PET perfusion tracers limit its more wide-spread use in clinical practice.

2.3.2.5 Prognostic Value

The extent of myocardial ischemia reflects the myocardium at risk and is a strong incremental predictor of cardiovascular prognosis. Patients with greater than 10% of ischemic myocardium or ischemia at multiple vessel areas are at higher risk (Dorbala et al. 2013; Dorbala and Di Carli 2014). Conversely, lack of inducible ischemia is associated with lower cardiac risk (Dorbala 2013). The clinical value of ischemia guided revascularization has also been demonstrated (Tonino et al. 2009; Pijls et al. 2010). The presence of viable myocardium can be studied with use of glucose analogue FDG. The presence of mismatch between myocardial flow and metabolism helps to identify the presence and size of viable myocardium that could be salvaged with a subsequent coronary revascularization (Tillisch et al 1986; Bax and Wijns 1999). The size of

nonviable myocardium is also associated with cardiac risk (Bax and Wijns 1999). CFR is an important prognostic marker as it reflects both epicardial and microvascular health. Diminished CFR is related to a worse prognosis independent of the presence of epicardial CAD (Dorbala and Di Carli 2014; Taqueti et al. 2015). Compromised microvascular integrity is also associated with a poor prognosis after coronary revascularization (Taqueti et al. 2015).

2.3.3 Single-Photon Emission Computed Tomography

SPECT perfusion imaging has been widely used with a good clinical experience in the evaluation of stable chest pain. The availability and cost of SPECT scanners and radiopharmaceuticals are better compared to PET technology. Previously published results on the sensitivity and specificity of SPECT perfusion for the diagnosis of CAD ranges from 73-92% and 63-87%, respectively (Heijenbrok-Kal et al. 2007; Montalescot et al. 2013). To diagnose ischemia, relative MBF distribution at rest and during stress is qualitatively analyzed. With the use of rest images, the viability of ischemic myocardial areas can also be evaluated. ECG gating allows the imaging of left ventricular function and volumes. Regional assessment of myocardial contractility adds to diagnostic confidence (Abidov et al. 2013). The limitation of SPECT technology is the frequent underestimation of the extent of ischemic myocardium. Qualitative analysis of MBF might even misdiagnose balanced ischemia caused by three vessel CAD as normal flow (Heller et al. 2009; Knuuti et al. 2009). However, assessment of transient ischemic dilatation and increased lung up-take provide some benefit for the diagnosis of severe CAD. Compared to PET technology, attenuation artefacts are common clinical problem with cardiac SPECT (Heller et al. 2009). Perfusion defects in SPECT perfusion is a strong prognostic marker of cardiac events while the lack of ischemia is associated with a favorable prognosis (Iskander and Iskandrian 1998; Hachamovitch et al. 2003). Normal SPECT perfusion indicates a small annual risk of cardiac events less than 1% while abnormal scan increases the risk approximately 12-fold higher (Iskander and Iskandrian 1998).

The most common SPECT radiotracers are [99m]Technetium and [201]Thallium which both are reactor produced. [201]Thallium is a potassium analog and thus its myocardial uptake relies on Na/K transport. Since its transportation inside the myocardial cell is energy dependent, uptake can only occur in viable myocardium. [201]Thallium's long half-life of 73 hours allows subsequent redistribution imaging. [99m]Technetium is currently more used than [201]Thallium. The two main radiotracers of [99m]Technetium include Sestamibi and Tetrofosfim. These tracers cross the cell membrane passively and are bound to the negative charge of mitochondria. The higher energy of [99m]Technetium (140 keV) over [201]Thallium (69-80 keV) is more optimal for detection with standard collimated cameras and with less attenuation. Furthermore, technetium has a significantly shorter half-life of 6 hours which allows injection of a higher tracer dose safely. The limitation of both [201]Thallium and [99m]Technetium is their low extraction factor resulting in a plateau of tracer uptake during high myocardial flow rates.

2.3.4   Echocardiography

2.3.4.1   Basics of Stress Echocardiography

An ultrasound probe uses alternating current to a quartz crystal to emit ultrasound frequency radio waves. These waves are reflected back to the probe from different anatomic structures and used to build an ultrasound image. In stress echocardiography the diagnosis of CAD is based on the visual assessment of regional wall motion (Pellikka et al. 2007). Imaging is done during exercise or pharmacological stress. For pharmacologic stress dobutamine or a vasodilator can be used. In standard dobutamine protocol, the dose is increased step-wise until 40 ug/Kg/min is reached. If the heart rate is still not sufficiently elevated repeated doses of atropine can be given (Sicari et al. 2008). Echocardiographic images are recorded and can be subsequently studied offline. The limitation of stress echocardiography is that it requires considerable experience to reach the published level of accuracy. In some of the patients image quality is suboptimal and another imaging modality or the use of contrast echocardiography should be considered. The strengths of

stress echocardiography are that it is a radiation free and inexpensive technology compared to other cardiac imaging modalities. In addition to wall motion assessment, coronary flow velocity can be measured with the use of pulsed wave Doppler (Meimoun and Tribouilloy 2008). Furthermore, gas-filled microbubbles can be used to image myocardial perfusion (Seol and Lindner 2014).

2.3.4.2 *Deformation imaging*

In deformation imaging myocardial wall motion is quantitatively analyzed (Marwick 2006). Tissue Doppler uses the Doppler effect to measure myocardial motion relative to a transducer. In contrast, two-dimensional speckle tracking measures the motion of myocardial speckles relative to each other. Speckles can be thought of as the fingerprints of the myocardium and differ in each myocardial region. The limitation of tissue Doppler is that it is angle dependent (Mor-Avi et al. 2011). On the other hand, speckle tracking might be limited by its frame rate requirements at higher heart rates (Mor-Avi et al. 2011). Both techniques require good image quality for the accurate calculation of strain curves. With speckle tracking technology, longitudinal, circumferential and radial strain can be assessed and multiple different echocardiographic variables derived. The basic deformation variable strain is the percentage of myocardial shortening. The strain rate is strain divided by time (% / seconds) (Marwick 2006). Both strain and strain rate are decreased in the presence of obstructive CAD (Voigt et al. 2003; Mor-Avi et al. 2011). Post-systolic strain is another potential marker of ischemia (Voigt et al. 2003; Asanuma and Nakatani 2015). It is defined as the difference in peak strain and peak systolic strain. The post-systolic strain index (PSI) is a measure of post-systolic strain and defined as post-systolic strain divided by peak strain. In previous studies deformation imaging has been successfully applied to stress echocardiography (Voigt et al. 2003; Bjork Ingul et al. 2007). A potential advantage of deformation imaging is that it does not require the considerable experience of subjective wall motion analysis. There is also evidence that deformation imaging provides incremental prognostic information independent of ejection fraction (Bjork Ingul et al. 2007; Kalam et al. 2014).

2.3.4.3 Stress Echocardiography

In the diagnosis of CAD stress echocardiography has excellent specificity (80-88%) with slightly lower sensitivity (72-85%) as wall motion abnormalities come late in the ischemic cascade. Previously published results on accuracy are mainly from the time before echocardiographic contrast which may considerably affect the current diagnostic value (Plana et al. 2008). Exercise, vasodilator and dobutamine stress seem to confer similar diagnostic accuracy for CAD (Cohen et al. 1993; Loimaala et al. 1999; Picano et al. 2000). In wall motion analysis, new or increasing wall motion abnormality is considered as a positive test. Small CAD lesions, distal stenoses and single vessel disease do not always cause wall motion abnormality and may result in a false negative test (Geleijnse et al. 1997; Marwick 2003). Compared to pharmacological stress, exercise offers additional diagnostic and prognostic information about heart rate, blood pressure and ECG. However, if there is a known wall motion abnormality in rest echocardiogram, dobutamine stress should be considered as the viability of myocardium can be assessed (Sicari et al. 2008; Montalescot et al. 2013). With a low dose of dobutamine, the contraction of the viable myocardium improves and the nonviable myocardium stays unchanged (Sicari et al 2008).

2.3.4.4 Prognostic Value

The prognostic value of stress echocardiography is well established in previous studies and is incremental to clinical risk factors and exercise ECG (Chuah et al. 1998; McCully et al. 2002; Marwick et al. 2002). For prognostic evaluation the presence, location, severity, extent and timing of stress induced wall motion abnormalities should be assessed (Chuah et al. 1998; Sicari et al. 2008). A normal echocardiographic finding is associated with very low event rate (< 1% per year) (Marwick et al. 2002) while left ventricular dysfunction is a strong predictor of poor prognosis (Chuah et al. 1998; Sicari et al. 2008). The prognostic value of exercise and different pharmacological stressors seem to be comparable (Pingitore et al. 1999; Marwick et al. 2002). Furthermore, stress echocardiography provides similar prognostic information as cardiac SPECT imaging (Olmos et al. 1998). Stress echocardiography after myocardial infarction can help in the risk stratification of patients (Carlos et al. 1997). It also aids in the prediction of perioperative risk of

major vascular surgery (Poldermans et al. 1995).

2.3.5 Functional Magnetic Resonance Imaging

MRI can be used for the functional imaging of CAD with either the assessment of myocardial perfusion or wall motion. Currently, MRI perfusion is more commonly used than wall motion analysis. Perfusion MRI with gadolinium is comparable or even better than nuclear perfusion imaging in the diagnosis of obstructive CAD (Greenwood et al. 2012; Schwitter et al. 2012). Furthermore, MRI perfusion has shown good agreement with both qualitative and quantitative assessment of MBF compared to invasive FFR measurements (Lockie et al. 2011; Manka et al. 2015). Perfusion analysis can be done either visually or with the use of computer assistance to identify the areas of decreased MBF. An ischemic finding on MRI perfusion is associated with elevated cardiac risk while normal perfusion confers favorable prognosis (Jahnke et al. 2007; Macwar et al. 2013).

Using cine images, regional wall motion abnormalities can be assessed by MRI during dobutamine infusion (Wahl et al. 2004). The assessment of wall motion is similar to stress echocardiography but provides superior image quality. In addition, deformation of myocardium can be quantified similarly to speckle tracking technology (Korosoglou et al. 2009). Moreover, newer 3 Tesla MRI technology seems to increase diagnostic accuracy even further in the evaluation of ischemia (Cheng et al. 2007; Bernhardt et al. 2012). Dobutamine stress MRI is an attractive option for patients with a suboptimal acoustic window and contraindications for vasodilator stress. Normal stress MRI is associated with a small annual event rate (< 1%) while the presence of ischemia elevates cardiovascular risk significantly (Lipinski et al. 2013; Al Sayari et al. 2015).

2.3.6 Computed Tomography Perfusion Imaging

Recent advancements in CTA technology offer the new possibility of noninvasive imaging of MBF (Becker

and Becker 2013). Vasodilator stress such as adenosine or dipyridamole is used similarly to nuclear perfusion imaging. Perfusion is assessed by tracking the flow of an ionated contrast agent. Maximal enhancement difference between ischemic and nonischemic myocardium can only be seen for a brief duration and the imaging needs to be performed at this time window. Differences in myocardial regions can be quantitated as Hounsfield units but absolute MBF cannot be measured. The accuracy of CT perfusion in the diagnosis of obstructive CAD has been comparable to SPECT perfusion and has shown good sensitivity (75-100%) and specificity (74-99%) (Blankstein et al 2009; Rocha-Filho et al. 2010). In addition, a novel noninvasive assessment of FFR by CT perfusion has been developed using computational fluid dynamics (Deng et al. 2015). However, noninvasive FFR is still an experimental technique (Precious et al. 2015). Further studies before wide-spread use in the clinical cardiology are warranted for both CT perfusion and noninvasive FFR.

2.3.7   Fractional Flow Reserve vs. Coronary Flow Reserve

FFR is currently considered as the gold standard of the functional imaging of CAD (Pijls et al. 1996). Normally the epicardial coronary artery exerts an insignificant amount of resistance to MBF. Since pressure is fully maintained throughout the epicardial coronary artery, distal coronary pressure equals the central aortic pressure. In the case of obstructive CAD, pressure declines in the coronary artery lumen distal to a stenosis. This pressure drop can be invasively measured by an intracoronary pressure wire. The microvasculature is fully opened with adenosine to account for microvascular resistance. Then the FFR is calculated as the ratio between the central pressure in coronary orifice and the pressure distal to the coronary lesion. An FFR less than 0.75 or 0.8 is considered as ischemia causing. The clinical value of FFR quided revascularizations have been demonstrated (Tonino et al. 2009; Pijls et al. 2010). Unlike FFR, CFR is not a lesion specific measurement. CFR is composed from both epicardial coronary arteries and microvasculature. This explains the previously found only modest correlation between FFR and CFR (Johnson et al. 2012). In the presence of normal microvasculature and endothelial function, CFR and FFR are similar (Johnson et al. 2012). Since FFR and CFR reflect different aspects of coronary pathophysiology, the information they

provide should be viewed as complementary instead of conflicting (Johnson et al. 2012).

2.4   Hybrid Imaging

2.4.1   Basics of Hybrid Imaging

Hybrid imaging techniques combine the information provided by two different imaging modalities. The technology was at first used mostly in oncology in the late 1990's (Beyer et al. 2000). With the progress in modern CTA technology, the hybrid imaging approach became more attractive for the evaluation of CAD. The most common hybrid imaging modalities are SPECT/CT and PET/CT. In this combination the CTA image locates the coronary arteries and epicardial plaques. Perfusion imaging can be used to assess the presence of ischemia matching with coronary stenosis (Valenta et al. 2013). PET/MRI is another promising but currently rare hybrid imaging modality (Rischpler et al. 2015). It is possible to produce hybrid images by either a software of hardware based approach. The hardware based approach uses a PET/CT or SPECT/CT scanner that can obtain a CTA and nuclear perfusion image almost simultaneously. Since the patient's position is fixed, image fusion can be performed fully or semi-automatically. The strengths of this approach are a fast imaging protocol and the ability to use anatomical data in attenuation correction. In the software based approach, image data is obtained by separate devices at different time points and later fused manually. The main limitations of hybrid imaging are its higher cost and increased radiation dose. Fortunately, developments especially in CTA technology have decreased radiation doses substantially. Currently, the radiation dose for combination of CTA and rest-stress PET perfusion is usually less than 10 mSv (Kajander et al. 2009).

2.4.2 Diagnostic Value of PET/CT

The diagnostic strength of PET/CT is that anatomy (CTA) and physiology (PET) both complement each other's limitations. The strength of the CTA is the high negative predictive value in the exclusion of obstructive CAD (Budoff et al. 2008; Meijboom and Meijs et al. 2008). However, there is a poor correlation between coronary stenosis severity and the presence of myocardial ischemia (Shaw et al. 2008; Meijboom and Meijs et al. 2008) which limits the specificity of CTA technology in the diagnosis of CAD. With the hybrid imaging approach, PET perfusion can be used to further confirm or exclude the presence of ischemia. This combination of anatomical and functional imaging has been shown to add incremental value in the diagnosis of CAD (Kajander et al. 2010). Accurate identification of the culprit lesion and assessment of its anatomy is also possible with CTA. This is of great importance in the presence of complex coronary anatomy such as coronary artery bypass grafts or coronary anomalies and might help to guide revascularizations. Normal coronary arteries by CTA and decreased MBF by PET can point to a disease of distal coronary arteries which might be hard to visualize by CTA or the presence of microvascular dysfunction (Kaufmann & DiCarli 2009; Knuuti et al. 2009).

2.4.3 Prognostic Value of Hybrid Imaging

The size of the ischemic myocardial area is a well-established prognostic marker and also helps to guide revascularizations (Dorbala et al. 2013; Dorbala and Di Carli 2014). However, nuclear perfusion alone cannot evaluate the presence and extent of nonobstructive atherosclerosis. The prognostic strength of CTA is the ability to accurately evaluate atherosclerotic burden which is a well-known predictor of adverse events (Bittencourt et al. 2014; Ostrom et al. 2008; Min et al. 2011). Furthermore, CTA can assess plaque vulnerability and the location of coronary obstructions. It is logical that this combination of myocardial perfusion imaging and CTA would also yield complementary value in the prediction of cardiac events. In the presence of extensive atherosclerosis, CTA also helps to guide the initiation of preventive cardiovascular medication. Interestingly, in a recent SPECT/CT study, the worst prognosis was observed in patients with matching CTA stenosis and perfusion abnormality (Pazhenkottil et al. 2011). This suggests a potential

incremental prognostic value for hybrid imaging. The prognostic value of cardiac PET/CT and its ability to

guide treatment choices needs to be confirmed in future studies.

3.   AIMS OF THE STUDY

The purpose of the present study was to evaluate novel noninvasive and quantitative cardiac imaging modalities in the diagnosis and evaluation of coronary artery disease. We used quantitative positron emission tomography imaging to evaluate the effect of myocardial bridging to myocardial blood flow. The detailed objectives were as follows:

1. To study whether a reduced coronary flow reserve in healthy young men independently predicts the extent of future coronary artery calcification (Study I).

2. To evaluate the hemodynamic significance of myocardial bridging and its effect on coronary atherosclerosis (Study II).

3. To determine the accuracy of quantitative $[^{15}O]$ H_2O PET perfusion in the diagnosis of obstructive coronary artery disease in a multicenter setting and to establish the optimal threshold for absolute myocardial blood flow and coronary flow reserve in the detection of flow-limiting coronary artery stenosis (Study III).

4. To study the clinical value of quantitative two-dimensional speckle tracking technology applied to stress echocardiography in the diagnosis of obstructive CAD (Study IV).

4.   MATERIALS AND METHODS

4.1   Study Design

The study consists of four sub-studies (I-IV). Study I was conducted between years 1996-1997 for baseline PET perfusion and 2007-2008 for follow-up CCS. PET/CT imaging for Study II was carried out during 2007-2009. Imaging studies for Study IV was done during 2009-2012. Patients from Study II and IV were included in the Study III conducted in 2012-2013. The purpose of this thesis was to evaluate novel quantitative and noninvasive cardiac imaging modalities in the diagnosis and evaluation of CAD. We also evaluated the hemodynamic effect of myocardial bridging to MBF measured in absolute terms by $[^{15}O]$ H_2O PET perfusion (Study II).

The objective of the study I was to evaluate the longitudinal association between decreased CFR as measured by $[^{15}O]$ H_2O PET and the extent of coronary calcification by calcium score. Study I brings novel information about the relationship between the anatomical and functional features of coronary atherosclerosis. At the baseline of our study, absolute MBF at rest and during vasodilator stress was obtained. After median of 11 years CCS was measured by computed tomography. Study II investigates the effect of myocardial bridging to MBF as assessed by quantitative perfusion PET. Myocardial bridges were identified as both intramural coronary artery (CTA) and systolic compression (ICA). Furthermore, the relationship between atherosclerosis and myocardial bridging was studied. Study III evaluates the diagnostic value and optimal cutoff values for quantitative $[^{15}O]$ H_2O PET perfusion for the diagnosis of obstructive CAD. The study was conducted as a multicenter study and patients were enrolled in Turku, Amsterdam and Uppsala. Study IV investigates the diagnostic value of quantitative two-dimensional speckle tracking applied to stress echocardiography for the diagnosis of obstructive CAD. In addition, the value of speckle tracking in the detection of severe CAD was assessed.

4.2   Study Population

The total number of participants in all studies was 414. The characteristics of the patients in Studies I-IV are depicted in Table 4. For Study I individuals were enrolled from the healthy control group of two different PET perfusion studies (Laine et al. 1998; Raitakari et al. 2001). The initial study group consisted of 129 healthy, lean, non-smoking, normotensive and non-diabetic men of the age of less than 45 years. The average age was 36 ± 4 at baseline. After a median of 11 years of follow-up, 77 individuals underwent CCS measurement and formed the final study group. At the follow-up 52 subjects were lost. One individual had died of a non-cardiac cause and the others either could not be contacted (n=25) or refused to participate (n =26). The exclusion criteria for Study I were a body mass index greater than 27 kg/m^2, blood pressure higher than 150/90 mmHg, elevated serum fasting glucose (>6.0 mmol/L) or known atherosclerotic disease.

The study population of Study II consisted of 100 patients aged 63 ± 7 years. The patients were being evaluated for stable chest pain with an intermediate pretest likelihood of obstructive CAD. The exclusion criteria were previous acute coronary syndrome, atrial fibrillation, second- or third-degree atrioventricular block, heart failure (NYHA IV), iodine allergy, severe kidney failure, pregnancy and severe symptomatic asthma. Patients with a previously ICA proven CAD were excluded.

In Study III, three institutions participated in patient enrollment: Amsterdam's VU University Medical Center (n=163), Turku University Hospital (n=161) and Uppsala University Hospital (n=6). All patients were referred to ICA with a clinical indication. The patients were enrolled prospectively to undergo quantitative $[^{15}O] H_2O$ perfusion PET. The exclusion criteria were atrial fibrillation, second- or third-degree atrioventricular block, severe symptomatic asthma, pregnancy or a documented history of CAD (previous revascularization or myocardial infarction). There were no ECG signs of previous myocardial infarctions in any of the study participants. Echocardiography, when performed, showed normal left ventricular function without regional wall motion abnormalities. All myocardial coronary artery areas with intermediate stenosis

(30-90%) without FFR measurements were excluded from the study.

In study IV, 52 patients were prospectively recruited for the investigation of stable chest pain. All patients had an intermediate likelihood for significant CAD based on the clinical symptoms, gender, age and exercise ECG finding. The exclusion criteria for study IV were: age (<30 or >75 years), acute coronary syndrome, known diagnosis of CAD, ejection fraction < 35%, asthma, significant valvular disease, congenital heart disease, cardiomyopathy, uncontrolled severe hypertension, recent (<6 months) cerebral ischemic attack, active cancer, atrial fibrillation, atrioventricular block and pregnancy. One patient was excluded because of poor image quality and one because of known obstructive CAD. Thus, the final study group consisted of 50 individuals aged 63 ± 7 years.

Table 4. Patient characteristics in studies I-IV

Variable	Study I *	Study II	Study III	Study IV
Patients (males)	77 (100%)	100 (42%)	330 (58%)	50 (26%)
Age (years)	36 ± 4	63 ± 7	61 ± 9	63 ± 7
Hypercholesterolemia	0	52%	50%	62%
Hypertension	0	41%	46%	58%
Smoking history	0	16%	33%	16%
Diabetes	0	14%	14%	14%
Family history of CAD	-	11%	30%	14%

Data are presented as numbers and percentages. * At the baseline of the study.

4.3   Methods

4.3.1   Imaging Acquisition

4.3.1.1 CTA Imaging

The CCS scan of Study I was done with a 64-row PET/CT scanner (GE Discovery VCT, General Electric Medical Systems, Waukesha, WI, USA). The tube voltage was 120 kV, tube current 200 mA, rotation time 400 ms and collimation 16 × 2.5 mm. Data were acquired using a prospective ECG-triggering at 70% of the R–R interval. CTA imaging for Study II was also done with a 64-row PET/CT scanner (GE Discovery VCT, General Electric Medical Systems, Waukesha, WI, USA). The collimation was 64 x 0.625 mm, gantry rotation time was 350 ms, tube current was 600-750 mA, and voltage was 100-120 kV, depending on patient size. For CTA imaging in Study II patients received 800 ug of sublingual nitrate before the scan. Intravenous metoprolol 0-30 mg was also administered before the CTA scan to reach a target heart rate of 60 bpm. Iodinated contrast infusion (60-80 mL of 400 mg iodine/mL iomeprol at 4-4.5 mL/s) was followed by a saline flush. To reduce the radiation dose, prospectively triggered acquisition was applied whenever possible.

4.3.1.2 PET Imaging

All PET imaging in Studies I-IV were done after an overnight fast. Caffeine and alcohol were prohibited 12h before the PET study. Rest-stress perfusion PET was performed in all of the individual studies (I-IV). In Study I hyperemic MBF was measured during intravenous adenosine (n=42) or dipyridamole (n=35) stress. In Studies II-IV only intravenous adenosine was used for pharmacologic stress. For quantification of MBF ^{15}O-labeled water was used in all studies (I-IV). For the production of ^{15}O, a low energy deuteron accelerator Cyclone 3 was used (Ion Beam Application, Louvain-la-Neuve, Belgium). ^{15}O-labeled water was produced

using dialysis techniques in a continuously working water module. In all studies (I-IV) ^{15}O-labeled water (900-1100 MBq) was injected (Radiowater Generator, Hidex Oy, Finland) at rest as an intravenous bolus over 15s. A dynamic acquisition of the heart was performed (14x5 s, 3x10 s, 3x20 s, and 4x30 s), after which a vasodilator-induced stress scan was performed. Adenosine infusion was started 2 minutes before the scan and continued at the rate of 140 µg/Kg/min until the scan was completed. In patients imaged with dipyridamole, the flow was measured after 2 minutes of administrated intravenous dipyridamole (0.56 mg/Kg body weight over 4 min).

4.3.1.3 Stress Echocardiography

In Study I, an Acuson 128XP/10 or Sequoia 512 (Acuson, Inc., Mountain View, CA, USA) equipped with a 2.5/3.5 MHz phased arrayed transducer was used for echocardiography and bicycle exercise was used as a stressor. In study IV, images were obtained with a GE Vivid 7 and M4S transducer (GE Healthcare, Horten, Norway). The dobutamine stress echocardiography (DSE) in study IV was performed using a standard staged protocol (Sicari et al. 2008). Dobutamine was infused intravenously with a mechanical pump. The starting dose was 10 µg/Kg/min. The dose was increased every 3 minutes to 20, 30 and 40 µg/Kg/min. Intravenous atropine up to 2 mg was given if necessary to reach the target heart rate (85% of age-predicted maximal). Blood pressure and ECG were continuously monitored. The termination criteria of the test were achieving the target heart rate, development of new wall motion abnormalities, angina pectoris, severe ischemic ECG changes, systolic blood pressure above 240 mmHg, abnormal blood pressure reaction or significant arrhythmia. Beta blockers were withdrawn for two days and long acting nitrates from the morning of DSE. Standard two-dimensional grey scale images of three standard apical views (four chamber, two chamber and apical long axis), parasternal long axis and parasternal short axis views at the level of mitral valve, papillary muscles and apex were acquired at each dobutamine dose. A cine image of one representative cardiac cycle per stage and view was digitally stored for subsequent off-line analysis. In order to optimize the speckle tracking analyzes in study IV, the echocardiographic image was optimized for left ventricle individually. Analysis and frame rate was increased to achieve the target of 60 - 90 frames/second

without compromising image quality.

4.3.1.4 Invasive Coronary Angiography

ICA was used as the gold standard for obstructive CAD in studies II-IV and was performed according to the standard clinical protocol. In Study II, ICA was also used to visualize and quantitate systolic compression of myocardial bridges. All patients studied in Turku university hospital were studied with a Siemens Axiom Artis coronary angiography system (Siemens, Erlangen, Germany). The quantitative analysis of coronary angiograms (Quantcore, Siemens) for CAD and systolic compression was done by an experienced reader. Coronary branches were studied according to the seventeen standard segments model (Austen et al. 1975). For the measurement of FFR, a 0.014-inch sensor tipped guide wire was used. Intravenous adenosine was used for vasodilator stress. FFR was calculated as the ratio of average distal coronary pressure and average arterial pressure during adenosine induced hyperemia.

4.3.2   Cardiac Risk Factors and Laboratory tests

In all studies (I-IV), conventional CAD risk factors and medications were screened by interview and laboratory tests. Blood pressure was measured by the electronic oscillometric arm cuff method. All venous blood tests were taken after an overnight fast. Serum total cholesterol, HDL cholesterol and triglycerides were measured using standard enzymatic methods (Boehringer Mannheim GmbH) with an automated analyzer (Hitachi 704; Hitachi Ltd, Tokyo, Japan). LDL concentration was calculated using the Friedwald formula. Plasma glucose concentration was determined by the enzymatic hexokinase technique (Glucose reagent, Olympus). Serum creatinine concentration was measured using standard photometric methods (Olympus Diagnostica GmbH, Hamburg, Germany) and by a Konelab 60i Clinical Chemistry Analyzer (Thermo Electron Co, Finland).

4.3.3   Data Analysis

4.3.3.1 Definition of Obstructive Coronary Artery Disease

In Study II, significant CAD was defined as greater than 70% coronary stenosis in ICA or an FFR less than 0.8. In Study III, obstructive CAD was defined as a tight coronary lesion (>90%) or a reduced FFR less than 0.8. Coronary arteries with intermediate stenosis (30-90%) without FFR measurements were excluded from the study to confirm the hemodynamic significance of coronary lesions in the study. In Study IV, hemodynamically significant CAD was defined as greater than 75% anatomical coronary artery stenosis in ICA and in the case of intermediate stenosis (40-75%) a FFR less than 0.8 or a myocardial perfusion defect matching coronary lesion.

4.3.3.2   CTA and CCS Analysis

In Study I, coronary calcification was quantified by CCS as described by Agatston et al. (Agatston et al. 1990) using commercially available software (SmartScore, GE Healthcare). Total CCS was the combination of the CCS obtained from the left main, left anterior descending, left circumflex and right coronary artery. In Study II, the standard 17-segment American Heart Association model for coronary artery anatomy was used for CTA image analysis (Austen et al. 1975). Vessels were analyzed with an ADW 4.4 Work station (General Electric, Piscataway, NJ). The presence of intramural courses of the coronary artery were evaluated from multiplanar reconstruction images (Study II). Bridging segments were divided into superficial (1-2mm) or deep (>2mm) intramural courses. The relation between intramural courses and epicardial coronary plaques were described as proximal, at intramural segment, or distal to intramural segment. Coronary atherosclerosis in Study II was also further characterized for properties of the vulnerable plaque as previously described (Motoyama et al. 2009).

4.3.3.3 PET Analysis

The values of MBF are expressed in milliliters/minute/gram of heart muscle (mL/g/min) in all studies (I-IV). In Study IV, hyperemic MBF was further categorized as mildly reduced (2.0 – 2.5 mL/g/min) or severely reduced (< 2.0 mL/g/min). In Study III, absolute MBF was also corrected for rate pressure product to account for changes in resting flow caused by heart workload. CFR is defined as the ratio between resting flow and flow during vasodilator stress. Images were analyzed with Carimas software (Nesterov et al. 2010). In study III, Cardiac Vuer software was used in the VU University Medical Center and Uppsala University Hospital. Based on our recent observations, stress myocardial blood flow < 2.5 mL/g/min was considered as abnormal (Kajander et al. 2010). In Study I, visual analysis of the PET data did not reveal any regional differences in the distribution of MBF. Therefore, the average flow of global left ventricular myocardium was used and no regional analysis was done. In all studies arterial input function was extracted directly from the dynamic PET data and a single tissue compartment model with correction for perfusable tissue fraction was used to generate parametric MBF images. Information from anatomical imaging modalities (CTA and ICA) was used to match coronary artery regions to MBF (Study II-IV).

4.3.3.4 PET/CT Hybrid Imaging

In Study II and IV hybrid imaging was used to match MBF to coronary artery lesions and anatomy. In both studies standard polar plots and parametric volume of the heart were produced, thus allowing image fusion with ADW 4.4 software (CardiIQFusion). In Study II, PET/CT hybrid images were used to match coronary artery segments affected by myocardial bridging to the corresponding myocardial flow areas. Myocardial regions chosen for flow analysis were distal to the myocardial bridges. The myocardial areas of other coronary branches with obstructive CAD were avoided as much as possible to minimize their confounding effect on MBF.

4.3.3.5 Stress Echocardiography

In studies I and IV, wall motion was analyzed simultaneously by at least two experienced echocardiographers blinded to the results of the other diagnostic investigations. Wall motion was studied in all apical and short axis views at all stages of the test using a standard 16 segment model (Pellikka et al. 2007; Sicari et al. 2008). Both online and off-line analyses were used for visual wall motion analysis and wall motion score was calculated as previously described (Pellikka et al. 2007; Sicari et al. 2008). Any new wall motion abnormality induced by exercise or dobutamine infusion was considered as a positive result for ischemia.

4.3.3.6 Deformation Imaging

Quantitation of deformation by two-dimensional speckle tracking was used in study IV. Strain analyses were done with commercially available software (EchoPack PC version 10, GE healthcare, Horten, Norway) by an experienced analyzer blinded to the other diagnostic results of the patient. The endocardial borders were traced manually at the end-systolic frame in three standard apical views. The computer software then automatically tracked myocardial deformation and rejected poorly tracked segments. Poorly tracked segments were manually readjusted and myocardial segments rejected by both the software and the analyzer were excluded from the study. If more than two myocardial regions were excluded from one coronary artery area the vessel was excluded from the study. Speckle tracking strain was analyzed in four different time points: at rest, at dobutamine dose of 20 µg/Kg/min, peak stress and at recovery (1 minute after stress).

Strain is a measure of regional myocardial deformation and calculated as (L-L0)/L0 where *L* is the length of the object after deformation, and *L*0 is the baseline length of the object. In our study we measured peak systolic longitudinal strain. Strain rate is the rate of myocardial deformation and expressed as seconds[-1]. We measured peak systolic longitudinal strain rate. Post-systolic strain is defined as peak systolic strain subtracted from peak strain. In our study we used a post-systolic strain index (PSI) which is defined as the

ratio between post-systolic strain and peak strain. Computer software automatically approximated the end of systole and this was also confirmed by the visual assessment of aortic valve closure from the apical long axis view. Strain, strain rate and PSI were measured in all of the 16 regions of the left ventricle. Mean values were calculated for the whole left ventricle to form global speckle tracking variables and for myocardial regions supplied by major coronary arteries (LAD, LCX or RCA) to form regional speckle tracking variables. In the presence of obstructive coronary stenosis, the myocardial risk area was defined according to the stenosis location in anatomic imaging modalities (ICA and CTA). In the case of a left main coronary artery stenosis, the coronary lesion was considered to affect both LAD and LCX regions.

4.4.4 Statistical Methods

4.4.4.1 Study I

Continuous variables are presented as mean and standard deviation. Normally distributed variables were compared with Student's T-test and non-paired variables with the non-parametric Mann–Whitney U test. Multivariate logistic regression analysis was used to study the relationship between CFR and the risk factors of CAD. As ageing is known to be related to CCS, age at the time of calcium scan was included in the model as a variable and all other variables were normalized for age at the time of baseline PET study. Assuming a mean CFR of 4.1 ± 1.3, a study group of 77 individuals is enough to detect a 6% difference in CFR with a power of 90% and a confidence level of less than 0.05. Two-tailed P-values of less than 0.05 were considered statistically significant. Statistical analyses were done with SPSS statistical software (SPSS, Inc., Chicago, IL, USA).

4.4.4.2 Study II

Mean and standard deviation were calculated for variables. Normally distributed variables were studied

using the non-paired T-test and other variables with the use of non-parametric Mann–Whitney U test. Nominal data was analyzed using Chi-square test. In the case of multiple measurements from a single patient, a paired T-test and Wilcoxon signed rank test were used. McNemars test was used for paired non-parametric comparisons. Two-tailed P-values of 0.05 were considered statistically significant. Statistical analyses were done with SPSS (SPSS, Inc., Chicago, IL, USA).

4.4.4.3 Study III

Continuous variables are presented as a mean and standard deviation, while categorical variables are expressed as numbers. Continuous and normally distributed variables were studied using the non-paired T-test. A receiver-operator characteristic curve (ROC) analysis and the Youden index were used to study PET perfusion cutoff values. A comparison of ROC curves was done as described by deLong et al. (DeLong et al. 1988). The association between MBF, CFR and CAD risk factors were studied using univariate and multivariable linear regression analysis. A linear mixed-effects model with per patient random effects was used to account for the multiple coronary artery flow measurements from a single patient. Sensitivity, specificity, negative predictive value, positive predictive value, and accuracy on a per-patient and per-vessel basis were calculated for PET perfusion. Differences in diagnostic accuracy were studied using Chi-square or McNemar tests. A p-value less than 0.05 was considered statistically significant. Statistical analyses were performed with IBM SPSS Statistics software version 20 (IBM SPSS Statistics, IBM Corporation, Armonk, New York) and MedCalc software 12.7.4.0 (MedCalc Software, Mariakerke, Belgium).

4.4.4.4 Study IV

Continuous variables are presented as mean and standard deviation. Normally distributed variables were studied with a paired or non-paired T-test when appropriate. Non-parametric variables were compared with a Wilcoxon signed-rank test or Mann–Whitney U test. Two tailed p-values of less than 0.05 were considered statistically significant. ROC curves were used to compare the diagnostic performance of strain variables

and visual wall motion analysis as described by deLong et al. (DeLong et al. 1988). Differences in diagnostic accuracy were studied using McNemar's test. Coefficient of variation and Bland-Altman analyzes were used to test repeatability of deformation imaging during DSE. Statistical analyses were done using SPSS statistical software (SPSS inc., Chicago, IL, USA).

5.   RESULTS

5.1   Coronary Flow Reserve and Coronary Calcification (Study I)

5.1.1 Baseline Characteristics

The final study group consisted of 77 men who were healthy, non-smoking, lean and normotensive. All individuals underwent baseline PET perfusion with ^{15}O-water at baseline and CCS measurement with CT at follow-up. Mean age was 36 ± 4 years at the time of the baseline PET studies. None of the individuals had symptoms or medications of CAD at baseline. The average MBF at rest, during vasodilator induced hyperemia and the average CFR were 0.79 ± 0.2 mL/g/min, 3.3 ± 1.2 mL/g/min and 4.1 ± 1.3, respectively. There were 22 individuals with reduced MBF of less than 2.5 mL/g/min after dipyridamole or adenosine stress and 6 individuals with decreased CFR of less than 2.5. There was no association between common risk factors of CAD and CFR. Age, lipids, body mass index, fasting glucose, systolic and diastolic blood pressure were all comparable in patients with CFR lower or higher than median (4.0). Left ventricular mass was also comparable in individuals with CFR < 4.0 (183 ± 24 g, n=15) and ≥ 4.0 (194 ± 33 g, n=13).

5.1.2 Follow-Up Characteristics

The follow-up studies were done 11 ± 1 years after the baseline PET perfusion imaging. In the follow-up laboratory measurements there was a significant increase of total cholesterol (5.3 ± 1.0 vs. 5.6 ± 1.0 mmol/L, p=0.02), triglycerides (1.2 ± 0.7 vs. 1.8 ± 1.1 mmol/L, p<0.001), HDL (1.5 ± 0.5 vs. 1.6 ± 0.5 mmol/L, p<0.01), fasting glucose (5.1 ± 0.5 vs. 5.9 ± 1.3 mmol/L, p<0.001) and systolic and diastolic blood pressure (124 ± 13 vs. 131 ± 15, p<0.001 and 70 ± 10 vs. 82 ± 10 mmHg, p<0.001, respectively). There was statistically significant decrease in LDL (3.4 ± 0.9 vs. 3.2 ± 0.9 mmol/L, p=0.03).

At the time of follow-up, none of the individuals had symptoms of ischemic heart disease but 16 individuals were being treated for hypertension (n=8), hypercholesterolemia (n=10) or diabetes (n=2). A subgroup of patients (n=28) who underwent exercise echocardiography had no evidence of inducible ischemia. During the follow-up period seven individuals had started smoking. The prevalence of coronary calcification (CCS > 0) was 39% at the mean age of 46 ± 4 years. The average CCS was 25 ± 66 in the whole study group and 65 ± 93 in individuals with calcification.

5.1.2 Predictors of Coronary Calcification

Baseline MBF at rest and during vasodilator stress was comparable in individuals with and without coronary calcification at the follow-up CT scan (0.8 ± 0.2 vs. 0.8 ± 0.2, p=0.79 and 3.3 ± 1.2 vs. 3.3 ± 1.2 mL/g/min, p=0.99, respectively). Furthermore, baseline CFR was comparable in both groups (4.2 ± 1.4 vs. 4.0 ± 1.2, p=0.44). Similarly, the calcium score was not elevated in individuals with decreased hyperemic MBF (< 2.5 mL/g/min, n=22) (23 ± 61 vs. 26 ± 68, P=0.79). In addition, univariate and multivariable analyses showed no association between CFR, systolic blood pressure, total cholesterol, body mass index at the baseline and CCS at follow-up (p always > 0.05). Conventional CAD risk factors at follow-up including: blood pressure, lipids, plasma glucose and body mass index were also comparable in individuals with and without coronary calcification. However, systolic and diastolic blood pressure measured at follow-up were significantly higher in the presence of coronary calcification (128 ± 11 vs. 137 ± 18, p=0.04 and 78 ± 11 vs. 86 ± 12 mmHg, p=0.01, respectively).

5.2   Myocardial Bridging and Myocardial Blood Flow (Study II)

5.2.1   *General*

Myocardial bridging as an intramural course of coronary artery was more frequent in men than in women (29 vs. 5, $p < 0.001$). There was no association between the presence of a myocardial bridge and conventional CAD risk factors. An intramural course was detected in 34% of patients by CTA in 48 different coronary segments and 50% of these were classified as deep intramural courses (> 2 mm of overlying myocardium). Most of the intramural courses were located in the LAD and its diagonal branches (n = 18), in LCX and its marginal branches (n = 15) or in the intermediate coronary artery (n = 12). Intramural courses in the RCA were rare (n = 3). Systolic compression was found by ICA in 14 of the 48 (29%) coronary artery segments with an intramural course on CTA. All systolic compressions were less than 50% on quantitative ICA analysis. Of these 14 segments with systolic compression, 5 were located in the LAD and its diagonal branches, 5 in the LCX and obtuse marginal branches and 4 in an intermediate coronary artery. There was no observed systolic compression in RCA.

There was no difference in the presence of angina pectoris or positive exercise ECG finding in patients with and without an intramural course of coronary artery (59 vs. 52%, $p = 0.47$ and 87 vs. 79%, $p = 0.32$) or in patients with and without systolic compression of the coronary artery (75 vs. 51%, $p = 0.11$ and 84 vs. 85%, $p = 0.95$). The results remained comparable in patients with and without an intramural course after individuals with obstructive CAD were excluded (61 vs. 42%, $p = 0.17$ and 68 vs. 80%, $p = 0.30$, respectively). There was also no difference in the frequency of angina pectoris and positive exercise ECG in patients with and without systolic compression after exclusion of patients with significant CAD (44 vs. 83%, $p = 0.06$ and 78 vs. 71%, $p = 0.72$). After a median follow-up of five years, a total of three patients had died (all non-cardiac causes), one patient had an event of unstable angina pectoris, one had a myocardial infarction and one patient underwent elective coronary artery bypass surgery. These events were equally

distributed in patients with and without myocardial bridging (3 vs 2).

5.2.2 Myocardial Bridging and Myocardial Blood Flow

Hyperemic MBF distal to segments with an intramural course were comparable to remote myocardial control regions of the same patients (2.8 ± 1.1 vs. 2.9 ± 1.0 mL/g/min, p = 0.55). MBF distal to a superficial and deep intramural course were also comparable (3.0 ± 0.9 vs. 2.8 ± 1.2 mL/g/min, p = 0.47). There were no differences in regional MBF in myocardial segments with an intramural course and matched control myocardial regions of the control patients. In univariate analysis corrected for multiple comparisons, there was no statistically significant association between resting or hyperemic MBF and the presence of superficial or deep intramural course of the coronary artery (p > 0.05). There were no significant differences in resting or hyperemic MBF in the myocardial regions supplied by intramural courses with or without systolic compression on ICA (1.0 ± 0.2 vs. 1.0 ± 0.2, p = 0.68 and 3.0 ± 0.9 vs. 2.7 ± 1.0 mL/g/min, p = 0.43, respectively). On univariate analysis, systolic compression was not associated with decreased resting or hyperemic MBF (p always > 0.05). We analyzed further the subgroup of patients with an intramural coronary artery (n = 12) and an abnormally reduced MBF (<2.5 mL/g/min). The reduction of MBF was explained by an obstructive CAD (> 70% stenosis or FFR < 0.8) in most of the cases (10 of the 12 patients). In the remaining two patients the etiology of reduced MBF remained unexplained.

5.2.3 Myocardial Bridging and Coronary Atherosclerosis

Atherosclerotic changes could be observed in the majority of patients (79%) in 186 of the total of 300 coronary arteries. There was no significant difference in the presence and average number of atherosclerotic plaques in patients with or without an intramural course of coronary artery (73% vs. 60%, p = 0.14 and 2.0 ± 1.7 vs 1.5 ± 1.6, p = 0.06). However, coronary plaques were more frequently located proximal to (n=20, 71 %) than at (n = 2, 7%) or distal to the segment with an intramural course (n = 6, 21%). Average CCS and total number of calcified plaques was not elevated in coronary arteries with an intramural course (172 ± 279

vs. 120 ± 263, p = 0.21 and 0.6 ± 1.0 vs 0.6 ± 1.0, p = 0.46). The average number of partially calcified and non-calcified coronary plaques were also comparable (1.1 ± 1.3 vs. 0.7 ± 1.1, p = 0.06 and 0.3 ± 0.6 vs. 0.2 ± 0.5, p = 0.38). There was no difference between a superficial or deep myocardial bridge in the average number of atherosclerotic plaques, CCS or the presence of obstructive CAD (2.2 ± 1.9 vs. 1.9 ± 1.6, p = 0.64; 298 ± 374 vs. 75 ± 109, p = 0.07 and 29% vs. 30%, p = 0.94). There was also no difference in the presence of vulnerable plaque features in atherosclerotic lesions located proximal to an intramural course and in vessels with no bridging (non-calcified plaque, remodeling and spotty calcification).

The presence of systolic compression on ICA was not associated with an elevated CCS (121 ± 140 vs. 127 ± 270, p = 0.38) or the number of atherosclerotic plaques when compared to control coronary arteries (2.2 ± 1.7 vs. 1.5 ± 1.6, p = 0.18). Moreover, there was no association between systolic compression and the number of calcified, partially calcified and non-calcified plaques on CTA (0.9 ± 1.1 vs. 0.6 ± 0.9, p = 0.17; 1.2 ± 1.2 vs. 0.8 ± 1.1, p = 0.18 and 0.2 ± 0.4 vs. 0.2 ± 0.5, p = 0.64, respectively).

5.3 Diagnostic Value of ^{15}O-Water PET Perfusion (Study III)

5.3.1 General

The prevalence of nonobstructive atherosclerosis and obstructive CAD in patients fulfilling the enrollment criteria of the study were 59% in 165 patients and 41% in 116 patients, respectively. In total 689 (70%) coronary arteries contained a nonobstructive coronary plaque while an obstructive lesion was present in 174 (17%) of the coronary arteries. A total of 127 (13%) of the analyzed coronary arteries were excluded from the study due to the absence of a FFR measurement to evaluate the hemodynamic significance of the intermediate severity coronary plaque. There were no significant differences in the hemodynamic parameters (systolic and diastolic blood pressure or rate-pressure product) at rest or during adenosine induced hyperemia in patients with and without obstructive CAD. However, peak heart rate was slightly lower in patients with significant CAD (83 ± 14 vs. 78 ± 12, p = 0.01).

5.3.2   Obstructive Coronary Artery Disease and Myocardial Blood Flow

Global MBF was 1.0 ± 0.3 mL/g/min at rest, 2.9 ± 1.1 mL/g/min at vasodilator induced hyperemia with a CFR of 3.1 ± 1.1. The average regional myocardial flow was 1.0 ± 0.3 mL/g/min at rest, 2.9 ± 1.1 mL/g/min at adenosine stress and with a CFR of 3.1 ± 1.2, respectively. Resting flow and hyperemic MBF were significantly lower in areas supplied by an obstructed (FFR < 0.8) coronary vessel (0.9 ± 0.2 vs. 1.0 ± 0.3 mL/g/min, p < 0.001 and 1.7 ± 0.7 vs. 3.3 ± 1.0 mL/g/min, p < 0.001). CFR and CFR_{corr} corrected for baseline hemodynamics (rate-pressure product) were both lower in the coronary artery areas with obstructive CAD (2.6 ± 0.9 vs. 3.4 ± 1.1, p < 0.001 and 2.0 ± 0.9 vs. 2.6 ± 0.9, p < 0.001). Discordancy between resting MBF, hyperemic MBF and CFR with ICA measured FFR was observed in 16 %, 20 % and 21 % of the coronary arteries. In univariate analyses, age (p < 0.01), female gender (p < 0.001), type two diabetes (p = 0.01), hypertension (p = 0.02) and FFR < 0.8 (p < 0.001) were all associated with reduced hyperemic MBF. In multivariable analyses, age, gender, hypertension, a positive family history of CAD and FFR were independent predictors of hyperemic MBF.

5.3.3   Diagnostic Value of $[^{15}O]$ H_2O PET perfusion

In regional analyses for the detection of obstructive lesions, the area under curve for resting MBF, hyperemic MBF, CFR and CFR_{corr} were 0.60 (95% confidence interval (CI) 0.55;0.60), 0.90 (CI 0.88;0.93), 0.85 (CI 0.82;0.89) and 0.85 (CI 0.82;0.89), respectively. The diagnostic performance of hyperemic MBF was significantly better compared to resting MBF, CFR and CFR_{corr} (p always < 0.001). The diagnostic value of CFR and CFR_{corr} proved to be comparable on both a regional (p = 0.88) and a global (p = 0.95) basis.

The optimal cutoff value in the prediction of obstructive CAD (FFR < 0.8) for regional MBF during vasodilator stress was 2.3 mL/g/min and 2.5 for CFR. The optimal cutoff of MBF 2.3 mL/g/min remained with the use of different FFR thresholds (FFR 0.65, 0.70 and 0.75) in statistical analyses. Using these cutoff values, the diagnostic accuracy of regional and global hyperemic MBF were similar (85 % and 86 %),

whereas regional and global CFR had an accuracy of 81% and 78%. Global hyperemic MBF and CFR had similar sensitivity (89 % and 86 %) but MBF outperformed global CFR in both specificity (84 % vs. 72 %, p < 0.01) and accuracy (86 % vs. 78 %, p < 0.01). Regional hyperemic MBF had both greater specificity (85 % vs. 82 %, p = 0.05) and sensitivity (87 % vs. 80 %, p = 0.01) for obstructive CAD than CFR and thus superior accuracy (85 % vs. 81 %, p < 0.01). The diagnostic accuracy of quantitative PET perfusion was significantly higher in female patients in both regional and global flow analyses (82 % vs. 92%, p = 0.02).

## 5.4 Speckle Tracking in Stress Echocardiography (Study IV)

5.4.1 General

The final study group consisted of 50 patients (26 males) aged 63 ± 7 years. There were no signs of previous myocardial infarcts or structural heart disease in echocardiography. Ejection fraction was normal in all patients at rest (68 ± 5.2 %) and during peak dobutamine stress (77 ± 7 %). Obstructive CAD was defined as > 75 % stenosis or in the case of intermediate coronary stenosis (40-75 %) with either a FFR < 0.8 or a matching perfusion defect in the PET perfusion study. Obstructive CAD was present in 22 of 50 (44%) the patients and in 36 of 150 (24%) the coronary arteries.

5.4.2 Reproducibility of Speckle Tracking

Interobserver coefficient of variation for global peak systolic strain and strain rate were 6% and 3% at rest, 6% and 4% at the dobutamine dose of 20 μg/Kg/min, 5% and 3% at peak stress, and 8% and 5% at immediate recovery (1 min after peak stress). Intraobserver CVs for strain and strain rate were 6% and 5% at rest, 6% and 6% at the dobutamine dose of 20 μg/Kg/min, 9% and 9% at peak stress, and 7% and 6% at immediate recovery. Thus, the assessment of reproducibility of strain and strain rate revealed good repeatability at rest and during dobutamine stress. For PSI interobserver and intraobserver the CVs were 24% and 18% at rest, 19% and 18% at the dobutamine dose of 20 ug/Kg/min, 43% and 13% at peak stress, and 14% and 20% at immediate recovery. The variation of PSI was highest at peak stress. The clinical significance of PSI variation was further studied using Bland-Altman analyses (Figure 1).

Figure 1. Reproducibility of speckle tracking measured post-systolic strain during dobutamine stress echocardiography
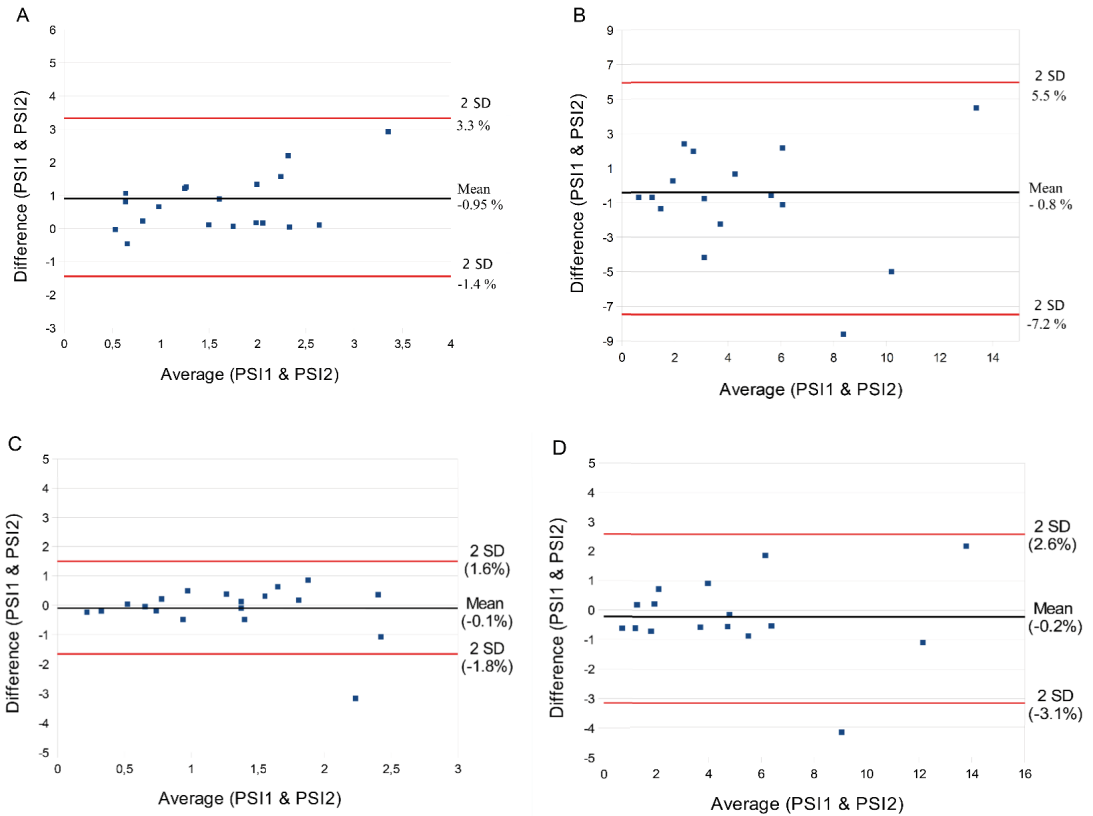
Bland-Altman analyses for the reproducibility of post-systolic strain index during dobutamine stress echocardiography. Intraobserver variability at rest (A) and at peak dobutamine stress (B). Interobserver variability at rest (C) and at peak dobutamine stress (D). PSI = Post-systolic strain; SD = Standard deviation.

5.4.3   *Global Strain, Strain Rate and Post-systolic Strain*

The differences in global peak systolic strain, strain rate and PSI at rest and during dobutamine stress in patients with and without obstructive CAD are shown in table 5. Global peak systolic strain remained relatively stable during dobutamine stress as compared to rest. In contrast, global strain rate increased significantly when measured at the dobutamine dose of 20 µg/Kg/min, peak stress and recovery. Interestingly, PSI was the highest at the recovery phase after stress in patients with obstructive CAD.

Table 5. Global strain variables in patients with (n=22) and without (n=28) coronary artery disease (CAD) during dobutamine stress.

Variable	No CAD	P-value (vs. rest)	CAD	P-value (vs. rest)	P-value (vs. No CAD)
Strain (%)					
Rest	-19.0 ± 2.5	-	-18.3 ± 2.5	-	0.34
20 ug/Kg/min	-21.0 ± 2.3	< 0.001	-20.0 ± 2.8	0.004	0.21
Peak stress	-18.9 ± 2.8	0.61	-17.9 ± 4.0	0.56	0.25
Recovery	-19.8 ± 2.1	0.04	-17.2 ± 4.0	0.12	0.01
Strain rate (% / s)					
Rest	-1.1 ± 0.2	-	-1.0 ± 0.2	-	0.08
20 ug/Kg/min	-1.7 ± 0.3	< 0.001	-1.6 ± 0.3	< 0.001	0.40
Peak stress	-2.2 ± 0.4	< 0.001	-2.1 ± 0.4	< 0.001	0.22
Recovery	-1.9 ± 0.3	< 0.001	-1.6 ± 0.4	< 0.001	0.02
PSI (%)					
Rest	2.8 ± 2.5	-	4.1 ± 2.7	-	0.03
20 ug/Kg/min	3.4 ± 2.4	0.22	6.4 ± 5.1	0.13	0.01
Peak stress	4.3 ± 3.9	0.07	6.3 ± 3.8	0.03	0.04
Recovery	3.0 ± 1.8	0.30	7.7 ± 5.7	0.01	< 0.001

Data are presented as mean ± SD. CAD = coronary artery disease, PSI = post-systolic strain index.

The relationship between the presence of multivessel CAD and extensive ischemia (> 2 segments) were studied in the tertiles of strain, strain rate and global PSI as depicted in Table 6, 7 and 8. Multivessel disease and extensive myocardial ischemia (> 2 myocardial segment) by PET perfusion were significantly more common in patients with a global PSI in the highest tertile at rest, the dobutamine dose of 20 µg/Kg/min and early recovery phase than in those with a PSI in the lowest tertile. Furthermore, multivessel disease and extensive myocardial ischemia were significantly more common in patients with a strain rate in the highest tertile at peak dobutamine stress and strain in the highest tertile at the early recovery phase.

Table 6. Global strain according to tertiles and the presence of severe coronary artery disease

Strain baseline	1st > 20.0 %	2nd 20.0–17.8 %	3th < 17.8 %	P-value (1st vs. 2nd)	P-value (1st vs. 3th)	P-value (2nd vs. 3th)
Multivessel CAD	4 (25%)	1 (6%)	5 (29%)	0.14	0.78	0.09
> 10% ischemia	5 (31%)	2 (13%)	8 (47%)	0.32	0.35	0.07
Strain 20 ug/Kg/min	**1st > 22.1 %**	**2nd 22.1-19.4 %**	**3th < 19.4 %**	**P-value (1st vs. 2nd)**	**P-value (1st vs. 3th)**	**P-value (2nd vs. 3th)**
Multivessel CAD	2 (13%)	3 (18%)	5 (29%)	0.68	0.24	0.42
> 10% ischemia	3 (19%)	4 (24%)	8 (47%)	0.60	0.04*	0.14
Strain Peak stress	**1st > 20.0 %**	**2nd 20.0-17.5 %**	**3th < 17.5 %**	**P-value (1st vs. 2nd)**	**P-value (1st vs. 3th)**	**P-value (2nd vs. 3th)**
Multivessel CAD	3 (19%)	2 (13%)	5 (29%)	0.63	0.48	0.24
> 10% ischemia	3 (20%)	3 (20%)	9 (60%)	1.0	0.03*	0.03*
Strain Recovery	**1st > 20.0 %**	**2nd 20.0-17.3 %**	**3th < 17.3 %**	**P-value (1st vs. 2nd)**	**P-value (1st vs. 3th)**	**P-value (2nd vs. 3th)**
Multivessel CAD	1 (6%)	3 (18%)	6 (35%)	0.32	0.04*	0.24
> 10% ischemia	1 (7%)	4 (25%)	10 (67%)	0.17	0.001***	0.02*

Data are presented as numbers and percentages. * $p < 0.05$, ** $p < 0.01$, *** $p < 0.001$. CAD= Coronary artery disease; PET= Positron emission tomography

Table 7. Global strain rate according to tertiles and the presence of severe coronary artery disease

SR baseline	1st ≥1.11 s^{-1}	2nd 1.10-1.02 s^{-1}	3th <1.02 s^{-1}	P-value (1st vs. 2nd)	P-value (1st vs. 3th)	P-value (2nd vs. 3th)
Multivessel CAD	3 (18%)	3 (18%)	4 (25%)	1.0	0.61	0.61
> 10% ischemia	4 (24%)	6 (38%)	5 (38%)	0.38	0.38	0.96
SR 20 ug/Kg/min	**1st >1.82 s^{-1}**	**2nd 1.82-1.63 s^{-1}**	**3th <1.63 s^{-1}**	**P-value (1st vs. 2nd)**	**P-value (1st vs. 3th)**	**P-value (2nd vs. 3th)**
Multivessel CAD	1 (6%)	4 (24%)	5 (29%)	0.17	0.09	0.70
> 10% ischemia	3 (20%)	6 (38%)	6 (40%)	0.28	0.23	0.89
SR Peak stress	**1st >2.30 s^{-1}**	**2nd 2.30-2.00 s^{-1}**	**3th <2.00 s^{-1}**	**P-value (1st vs. 2nd)**	**P-value (1st vs. 3th)**	**P-value (2nd vs. 3th)**
Multivessel CAD	2 (12%)	3 (19%)	5 (33%)	0.58	0.17	0.41
> 10% ischemia	3 (18%)	5 (31%)	7 (54%)	0.31	0.04*	0.27
SR Recovery	**1st >2.05 s^{-1}**	**2nd 2.05-1.65 s^{-1}**	**3th <1.65 s^{-1}**	**P-value (1st vs. 2nd)**	**P-value (1st vs. 3th)**	**P-value (2nd vs. 3th)**
Multivessel CAD	2 (12%)	2 (13%)	6 (35%)	0.95	0.11	0.13
> 10% ischemia	5 (29%)	3 (23%)	7 (44%)	0.70	0.39	0.24

Data are presented as numbers and percentages. * $p < 0.05$, ** $p < 0.01$, *** $p < 0.001$. CAD= Coronary artery disease; PET= Positron emission tomography; SR= Strain Rate

Table 8. Global post-systolic strain index (PSI) according to tertiles and the presence of severe coronary artery disease

PSI baseline	1st < 2.1%	2nd 2.1-3.3%	3th > 3.3%	P-value (1st vs. 2nd)	P-value (1st vs. 3th)	P-value (2nd vs. 3th)
Multivessel CAD	0	4 (50%)	6 (71%)	0.03*	<0.01**	0.52
> 10% ischemia	1 (7%)	4 (27%)	10 (59%)	0.16	<0.01**	0.07
PSI 20 ug/Kg/min	**1st < 2.6%**	**2nd 2.6-5.0%**	**3th > 5.0%**	**P-value (1st vs. 2nd)**	**P-value (1st vs. 3th)**	**P-value (2nd vs. 3th)**
Multivessel CAD	0	4 (24%)	6 (35%)	0.04*	0.01*	0.52
> 10% ischemia	1 (7%)	6 (38%)	8 (50%)	0.050	0.01*	0.48
PSI Peak stress	**1st < 3.0%**	**2nd 3.0-6.2%**	**3th > 6.3%**	**P-value (1st vs. 2nd)**	**P-value (1st vs. 3th)**	**P-value (2nd vs. 3th)**
Multivessel CAD	2 (13%)	3 (18%)	5 (29%)	0.68	0.24	0.42
> 10% ischemia	2 (13%)	6 (40%)	7 (44%)	0.10	0.06	0.83
PSI Recovery	**1st < 2.7**	**2nd 2.7-4.9**	**3th >4.9**	**P-value (1st vs. 2nd)**	**P-value (1st vs. 3th)**	**P-value (2nd vs. 3th)**
Multivessel CAD	0	2 (12%)	8 (47%)	0.16	<0.01*	0.02*
> 10% ischemia	1 (7%)	3 (20%)	11 (69%)	0.28	<0.001***	0.01*

Data are presented as numbers and percentages. * $p < 0.05$, ** $p < 0.01$, *** $p < 0.001$. CAD= Coronary artery disease; PET= Positron emission tomography and PSI= Post-systolic strain index.

5.4.4 Regional peak strain, strain rate and post-systolic strain

Differences in regional peak systolic strain, strain rate and PSI in patients with and without obstructive CAD are shown in Figure 2. Peak systolic strain was decreased in the myocardial regions supplied by obstructed compared nonobstructed coronary artery at early recovery ($p < 0.001$). However, regional strain rate was comparable between non-ischemic and ischemic regions at rest, the dobutamine dose of 20 µg/Kg/min, peak dobutamine stress and early recovery. Regional PSI was significantly elevated in the ischemic regions at rest ($p=0.01$), the dobutamine dose of 20 µg/Kg/min ($p=0.03$), peak stress ($p=0.02$) and at early recovery ($p<0.001$).

The impact of depth of ischemia to myocardial deformation were further studied. Normal MBF was defined as a flow greater than 2.5 mL/g/min, mild ischemia as 2.0-2.5 mL/g/min and severe ischemia as a flow less than 2.0 mL/g/min. Compared to normal myocardial areas, myocardial strain was significantly decreased in areas with severe ischemia at the dobutamine dose of 20 µg/Kg/min and at early recovery (-21.0 ± 3.9 vs. -19.0 ± 4.2 %, $p < 0.05$ and -19.5 ± 4.1 vs. -16.6 ± 4.7 %, $p < 0.01$, respectively). In addition, PSI was

significantly elevated in severely ischemic regions at early recovery (4.2 ± 9.4 vs. 9.3 ± 9.5 %, p = 0.03).

Thus, both decreased peak systolic strain and PSI were associated with severe ischemia during early

recovery.

Figure 2. Regional strain, strain rate (SR) and post-systolic strain index (PSI) in patients with and without obstructive coronary artery disease.
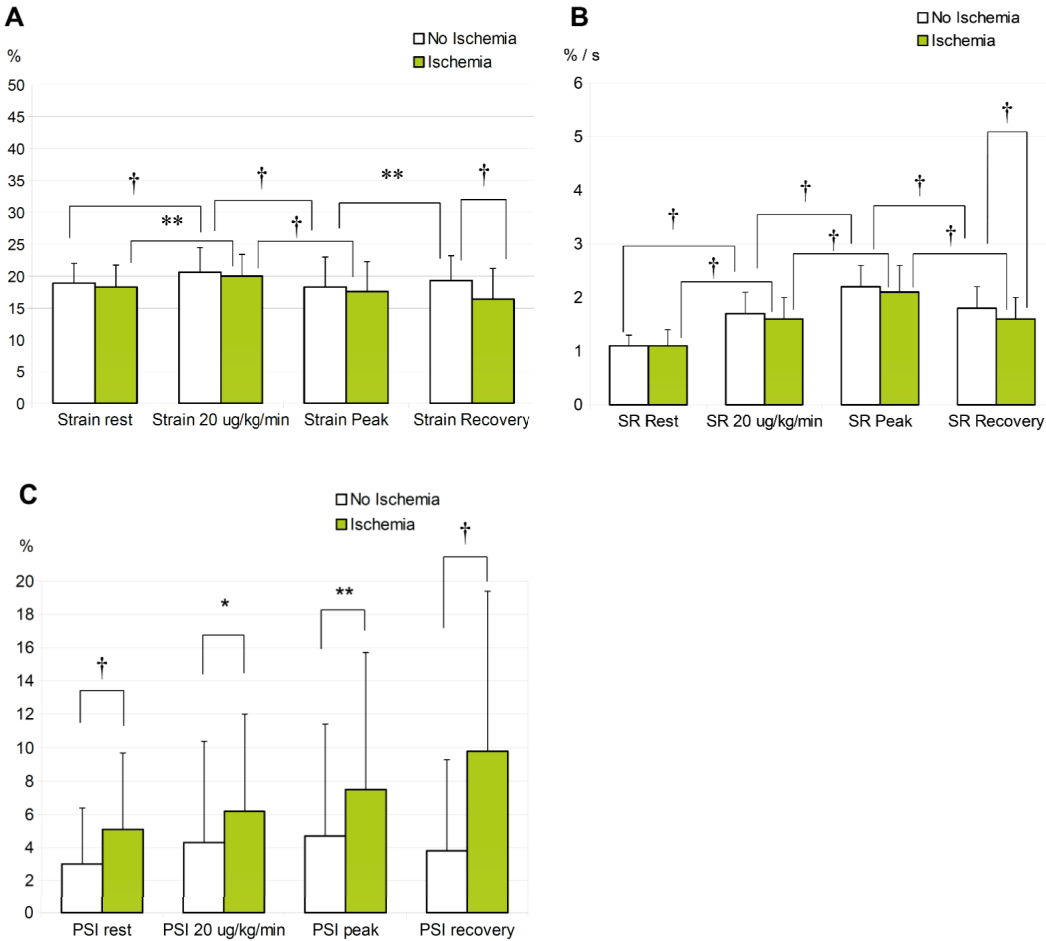
Differences in regional speckle tracking variables in myocardial areas with and without significant coronary artery disease, and increase or decrease of A) peak systolic strain, B) strain rate (SR) and D) Postsystolic strain index (PSI) during dobutamine stress echocardiography at different dobutamine doses. Significant corononary artery disease is defined as > 75% stenosis in invasive coronary angiography. In intermediate stenoses of 40-75%, hemodynamic significance was confirmed by reduced fractional flow reserve (<0.8) or abnormal myocardial positron emission tomography perfusion. * p < 0.05, ** p < 0.01 and † p < 0.001.

5.4.5   Diagnostic Value of Speckle Tracking

Subjective visual wall motion analysis resulted in a sensitivity and specificity of 59% and 86% with an accuracy of 74% for the detection of obstructive CAD on per patient basis. Due to the effort to localize ischemia, comparisons between different techniques were done on vessel basis. The diagnostic accuracies of peak systolic strain, strain rate and PSI at different dobutamine doses are shown in Table 9. Of the speckle tracking variables, a PSI greater than 6.2% at early recovery performed best for the detection of obstructive CAD with a sensitivity, specificity and accuracy of 60%, 79% and 74%, respectively. It was also comparable to visual wall motion analysis. In contrast, the accuracies of strain and strain rate were inferior to subjective wall motion analysis.

Table 9. Diagnostic accuracy of speckle tracking echocardiography for regional ischemia during dobutamine stress compared to wall motion analysis

Variable	Cutoff	Sensitivity	Specificity	PPV	NPV	Accuracy	P-value vs WM
WM	Positive	44	91	62	84	80	-
Rest							
Strain (%)	-18.6	54	55	29	81	56	<0.001
Strain rate (% / s)	-1.00	49	62	29	80	59	<0.001
PSI (%)	3.7	54	72	38	84	68	<0.001
20ug/Kg/min							
Strain (%)	-19.8	50	61	29	79	58	<0.001
Strain rate (% / s)	-1.6	50	61	29	80	59	<0.001
PSI (%)	6.6	52	81	46	84	74	0.11
Peak stress							
Strain (%)	-18.1	61	56	31	82	57	<0.001
Strain rate (% / s)	-2.0	55	65	34	82	63	<0.001
PSI (%)	4.1	56	65	33	82	63	<0.001
Recovery							
Strain (%)	-18.4	72	65	39	88	66	0.01
Strain rate (% / s)	-1.6	60	66	36	84	65	<0.001
PSI (%)	6.2	60	79	47	86	74	0.16

Data are presented as percentages. NPV = negative predictive value; PPV = positive predictive value; PSI = post-systolic strain index; predicting value; WM = wall motion analysis

6.   DISCUSSION

6.1   Coronary Flow Reserve and Coronary Calcification

In study I we assessed the predictive value of CFR by ^{15}O-water perfusion PET for coronary calcification over 10 years of follow-up in healthy young males. To avoid the confounding effect of conventional coronary risk factors to coronary artery calcification, the individuals selected for current study were normotensive, non-smoking, non-diabetic and lean. Previously, alterations of coronary endothelial function have been demonstrated to precede atherosclerotic changes in experimental and clinical studies (Raitakari et al. 2001; Tamaki et al. 2010; Schindler et al. 2010). In a previous cross-sectional study Wang et al. demonstrated that coronary vasodilator function measured by CFR was inversely associated to the presence and severity of coronary calcification in a population of 222 asymptomatic individuals (Wang et al. 2006) In contrast, Pirich et al. found no association between CCS and CFR in a study of 22 asymptomatic individuals with a positive family history of premature CAD (Pirich et al. 2004). Curillova et al. documented a statistically significant but weak relationship between CCS and CFR in patients studied for suspected obstructive CAD (Curillova et al. 2009). Based on these recent findings, we hypothesized that coronary microvascular function measured as CFR by PET perfusion would predict the development of coronary atherosclerosis. Our current study is the first longitudinal study to evaluate the independent predictive value of CFR and the long-term development of coronary atherosclerosis more than 10 years later. Interestingly, in contrast to the majority of previous studies, our results suggest that in young asymptomatic males with low likelihood of obstructive CAD, microvascular dysfunction is not a strong predictor of future coronary artery calcification.

There are several potential reasons for the lack of association between CFR and future coronary calcification in our study. Although it has been previously suggested that microvascular and endothelial function are the key events that precede the development of coronary atherosclerosis, the relationship between the anatomical and physiological features of atherosclerosis might not be straightforward and they might

actually reflect different aspects of pathophysiology (Pirich et al. 2004; Yan et al. 2005; Andersson et al. 2011). CCS is a well-established marker for atherosclerosis (Agatston et al. 1990; Hecht 2015). However, it does not provide information about the phenotype of atherosclerotic plaques and might actually detect stable calcified coronary lesions. In a recent study, statin medication was found to increase coronary calcification as a possible mechanism for plaque stabilization (Puri et al. 2015). Since microvascular dysfunction and epicardial atherosclerosis share multiple risk factors, it is of great importance to study their relationship in healthy individuals without confounding effects such as hypertension, obesity, diabetes and smoking. As a result, the likelihood of CAD and microvascular dysfunction were small in this population. When compared with the previous cross-sectional studies, our study group was much younger and had less coronary calcifications.

The fact that our study group was selected might explain the lack of association between the common risk factors of CAD and the presence of coronary calcification. The presence of risk factors of CAD at baseline were comparable in patients with and without coronary calcification at the time of follow-up. However, systolic and diastolic blood pressure at the follow-up were elevated in patients with coronary calcification. The possibility that significant changes in lifestyle might have confounded the association between baseline risk factors of CAD and coronary calcification at follow-up cannot be excluded. There was also a number of individuals who had started the use of cardiovascular medication during follow-up. Especially the initiation of statin medication might be a confounding factor (Puri et al. 2015). Possible bias due to a relatively large number of individuals who did not participate to the follow-up study cannot be excluded. Obstructive epicardial stenosis could influence the relationship between MBF and CCS. Invasive coronary angiography was not done in the current study as it was clinically unjustified in individuals with low pretest probability of CAD. In addition, regional myocardial perfusion was homogenous in all individuals and the subgroup of individuals who underwent stress echocardiography had no findings suggesting inducible ischemia. Due to logistic reasons only a subgroup of patients with coronary calcification underwent stress echocardiography at follow-up. Unfortunately, a CCS scan was not available at baseline and thus the change in calcification

cannot be measured. In previous studies, increasing coronary calcification in serial scanning has shown incremental prognostic value (Raggi et al. 2004; Budoff et al. 2013). Measurement of PET perfusion at follow-up might have also provided additional information but would have also increased the radiation dose.

6.2   Myocardial Bridging and Myocardial Blood Flow

Myocardial bridging is an anatomic variation of coronary anatomy in which a band of myocardium overlies a segment of coronary artery. Contraction of the myocardium at the bridging segment can cause dynamic coronary stenosis during cardiac systole. Although myocardial bridging has been thought of as a relatively benign congenital variation of coronary artery anatomy, some previous clinical studies have associated it with chest pain, ischemia, left ventricular dysfunction, arrhythmia and even sudden cardiac death (Bruschke et al. 2013; Alegria et al. 2005). In Study II, the association between MBF and dynamic stenosis of myocardial bridging was evaluated with the use of multimodality imaging. Myocardial bridging was evaluated by both an anatomical definition as intramural course (CTA) and a functional definition as the systolic compression of coronary artery (ICA). MBF was quantified in absolute terms by [^{15}O] H$_2$O PET perfusion. In addition, the relationship between myocardial bridging and coronary atherosclerosis was comprehensively evaluated by CTA. To our knowledge, we are the first to describe the effects of myocardial bridging defined as both an intramural course of a coronary artery and as systolic compression to absolute MBF. The strength of our patient population is that it represents symptomatic patients with an intermediate probability of CAD, those who are generally considered as candidates for cardiac imaging in clinical medicine. In other studies patients have been highly selected based on systolic compression by ICA.

An intramural coronary artery was a common CTA finding in our study group (34 %) while only a third of these intramural segments had observable systolic compression on ICA study. The frequency of systolic compression in bridging segments was similar to previous studies (21-46 %) (Leschka et al. 2008; Kim et al. 2011; Kim et al. 2014). None of the bridging segments had severe systolic compression (>50%). This

suggests that the presence of severe coronary compression previously associated with myocardial ischemia is a rare finding. Our results are similar to previous clinical studies demonstrating an excellent cardiovascular prognosis with myocardial bridging (Juillière et al. 1995; Rubinstein et al. 2013). In our study, absolute MBF during adenosine stress was not influenced by myocardial bridging. Furthermore, there was no association between increased atherosclerotic burden and bridging. However, as in previous studies, coronary plaques were predominantly localized proximal to the coronary segments with myocardial bridge. The coronary atherosclerosis proximal to myocardial bridges were further characterized for high risk features. The presence of CTA findings associated with plaque vulnerability were found to be comparable with other coronary arteries. Therefore, according to our findings myocardial bridging was not associated with accelerated atherosclerotic disease.

Our findings of unaffected myocardial perfusion in the presence of coronary artery bridging are in contrast to the majority of previous publications. Based on our findings and on previous studies, a threshold of greater than 50-75% of systolic compression seems to be required for the induction of myocardial ischemia (Ahmad et al. 1981; Vallejo et al. 2005; Gawor et al. 2011). However, as segments with a myocardial bridge are frequently associated with proximal atherosclerotic plaques the threshold might be lower in patients with CAD. Although in our study all systolic compressions were less than 50%, systolic compression is a dynamic stenosis that is not always seen on ICA without a provocation test (Escaned et al. 2003; Hazenberg et al. 2008). Furthermore, it is possible that the degree of systolic compression has variability. Previous studies have focused on highly selected patient populations with detected systolic compression on ICA study. Our study group was less selected and unlike most of the previous studies was not limited to mid LAD. A considerable amount of segments with myocardial bridging was found in other branches of the coronary tree.

In Study II adenosine was used as a stressor for PET perfusion. As a vasodilator it differs from exercise

stress but is comparable to dipyridamole used in some of the previous studies. Elevated heart rate in exercise and dobutamine stress affect the relative length between systole and diastole and thus they might be more effective in inducing perfusion abnormalities caused by the systolic compression of myocardial bridges. However, exercise and dipyridamole SPECT have been previously validated for imaging of myocardial bridging and found comparable (Vallejo et al. 2005). We cannot exclude the possibility that beta-blockers used prior to the CTA scan in our hybrid imaging protocol affected the MBF by alleviating systolic compression. However, we have previously demonstrated that beta-blockers received before the CTA scan had no effect on MBF in our imaging protocol (Joutsiniemi et al. 2014). It can be also be argued that adenosine can increase coronary susceptibility to systolic compression by microvascular vasodilation. Myocardial bridges were commonly associated with proximal atherosclerotic plaques, which is a confounding factor in our study. We acknowledge the possibility of a type two statistical error due to the small number of patients with myocardial bridging without CAD. The current study was underpowered to study the effect of myocardial bridging on cardiovascular prognosis.

6.3   Diagnostic Value of [^{15}O] H$_2$O PET Perfusion

In Study III, the diagnostic value of ^{15}O-water perfusion PET for obstructive CAD was investigated. The study was a collaborative study to standardize and establish accurate thresholds for quantitative [^{15}O] H$_2$O PET perfusion in three imaging centers (Turku, Amsterdam and Uppsala). Currently, there is a global interest in utilizing noninvasive PET imaging for the diagnosis of CAD and large multicenter trials are needed. Defining the optimal threshold for myocardial ischemia is the fundamental issue in quantitative cardiac PET. Furthermore, collaborative studies facilitate patient management and the exchange of patient data for future imaging trials. There are previous cardiac PET imaging studies which have reported good diagnostic accuracy with ^{15}O-water. However, these single-center studies often lack the use of a functional gold standard for ithe dentification of CAD induced ischemia. In addition, they are hampered by the inherent limitations of a single-center study setting. In the present study both ICA and FFR were used to determine the hemodynamic severity of coronary stenoses in a clinical cohort of patients studied for the suspicion for

symptomatic CAD. Since the anatomic degree of coronary stenosis is a poor predictor of the presence of myocardial ischemia a strict anatomic definition for flow-limiting stenosis was used (>90%) and FFR measurements were favored. The symptomatic patients of Study III also represent well the individuals that are usually the target of diagnostic cardiac imaging in a clinical setting.

In addition to absolute hyperemic MBF, CFR and CFR_{corr} adjusted for baseline, hemodynamics were evaluated. The optimal threshold to detect CAD induced ischemia were 2.3 mL/g/min for hyperemic MBF and 2.5 mL/g/min for CFR. Correction of CFR for baseline hemodynamics with rate-pressure product did not add significantly to the diagnostic value. Hyperemic MBF provided an accuracy of 86 % in the detection of flow-limiting coronary stenoses and was superior compared to the accuracy of CFR (78 %). Age and gender were both significant independent predictors for the diagnostic accuracy of the quantitative PET study. Currently, there is a lack of uniformity in the previously described absolute flow value thresholds for myocardial ischemia (Kajander et al. 2010; Danad et al. 2013). This variability might be explained by the use of different radiotracers with different kinetic properties and imaging protocols. Also, the study populations of previous single-center studies may differ significantly. However, a general cutoff value for obstructive CAD is important in order to facilitate the greater use of cardiac PET in clinical medicine. This variation of optimal cutoff values in different studies also underlines the importance of our study which had a robust functional gold standard for ischemia. Detected optimal cutoff values were in line with the previous study by Kajander et al. (2.5 mL/g/min for both stress MBF and CFR) who also used ^{15}O-water in patients with intermediate pretest probability for obstructive CAD (Kajander et al. 2010). However, Danad et al. have previously observed that a considerably lower flow value of 1.9 mL/g/min had the best accuracy (Danad et al. 2013). This might be explained by the methodological differences. Interestingly, in the study by Kajander et al. there was routine use of FFR in invasive angiographies. Similarly to our study, better diagnostic value of hyperemic MBF compared to CFR has been previously described (Haijiri et al. 2009; Danad et al. 2013; Joutsiniemi et al. 2014). Diminished hyperemic MBF might result in normal CFR depending on resting flow value. This dependency on resting flow might explain the diagnostic superiority

of hyperemic MBF. Our observation paves way to stress-only PET imaging protocols which could reduce per patient radiation dose and improve the workflow of the imaging department through decreased scan time. However, the incremental prognostic value of CFR has been previously observed (Herzog et al. 2009).

There was a high diagnostic performance with the use of [^{15}O] H$_2$O PET perfusion for flow-limiting CAD and only 13 (5%) obstructive coronary stenoses were missed by quantitative PET. The high accuracy of the current study is in agreement of the previous single-center studies (Kajander et al. 2010; Danad et al. 2013). Although normal myocardial perfusion rules out CAD with good negative predictive value (96% per vessel and 92% per patient), a decreased flow does not always imply to epicardial coronary obstruction. In the present study there was a discrepancy between invasive FFR and hyperemic MBF in 16% of the measurements. This is in line with previous observations (Meuwissen et al. 2001; Johnson et al. 2012). However, since FFR and CFR reflect different aspects of the pathophysiology of coronary arteries their information should be viewed as incremental instead of conflicting. While FFR is a lesion specific marker of decreased pressure, CFR is a combined measurement of both epicardial and microvascular function. Thus, decreased MBF in the presence of normal FFR can be due to a microvascular disease. A limitation in Study III is that FFR was only measured in the case of intermediate stenoses (30-90 %). This decision was based on a previous observation that subtotal coronary lesions are virtually always hemodynamically significant (96%) (Tonino et al. 2010). Visual assessment of perfusion images was not done as the quantitative assessment of perfusion has been shown to provide better diagnostic accuracy (Kajander et al. 2011; Fiechter et al. 2012). Although intracoronary administration of adenosine is the reference standard in invasive FFR, intravenous adenosine was also used. There was no diagnostically significant difference in FFR in patients with intracoronary and intravenous adenosine. Although the matching of coronary anatomy (ICA) to MBF areas was done carefully, some misclassification may have occurred. We cannot exclude the effect of different imaging centers to MBF values. However, great care was used to standardize image analysis. Our results with [^{15}O] H$_2$O PET might not be applied directly to other PET perfusion tracers or study populations.

6.4 Diagnostic Value of Speckle Tracking Stress Echocardiography

The diagnostic accuracy of stress echocardiography for obstructive CAD has been established in multiple studies (Sicari et al. 2008). However, considerable expertise is required to achieve the published levels of accuracy with the visual assessment of myocardial wall motion. Quantitative echocardiographic analysis of myocardial deformation by strain imaging may aid in the detection of wall motion abnormalities induced by myocardial ischemia. Previous studies have indicated the potential diagnostic value of speckle tracking strain and strain rate in the detection of obstructive CAD (Voigt et al. 2003; Voigt et al. 2004; Bjork Ingul et al. 2007). In addition, post-systolic strain has also been suggested as a marker for myocardial ischemia (Asanuma and Nakatani 2015). However, there is a need for further studies for the evaluation of the clinical value of post-systolic strain during quantitative two-dimensional (2D) speckle tracking DSE. In Study IV, the clinical value of 2D speckle tracking strain, strain rate and post-systolic strain were prospectively studied for the detection of myocardial ischemia during DSE. The study group consisted of symptomatic patients with an intermediate pretest probability for CAD. The main finding in Study IV was that the evaluation of strain and post-systolic strain can detect hemodynamically significant CAD during the early recovery phase of dobutamine stress as well as provide information about the depth and extent of myocardial ischemia. Quantitative [^{15}O] H$_2$O PET perfusion was used to evaluate the presence, depth and extent of inducible ischemia. Post-systolic strain measured as PSI provided similar diagnostic accuracy than expert visual analysis of myocardial deformation. The repeatability of speckle tracking was good at rest, the dobutamine dose of 20 µg/Kg/min and during recovery. Strain variables were more variable during peak dobutamine stress.

The results of Study IV are in line with the previous clinical and experimental studies that indicate that post-systolic strain is a useful marker for myocardial ischemia (Voight et al. 2003; Voigt et al. 2004; Asanuma and Nakatani 2015). In these studies the accuracy of post-systolic strain have been similar to visual wall motion analysis (Voight et al. 2003; Voigt et al. 2004). However, in another DSE study, PSI measured by speckle tracking had a lower diagnostic accuracy than other strain variables (Ingul et al. 2007). This is potentially

explained by the relatively low temporal resolution of speckle tracking that can miss subtle post-systolic deformation at high heart rates. This is supported by our results of higher PSI variability at peak dobutamine stress. The accuracy for the detection of CAD and severe ischemia were highest at the early recovery phase and comparable to expert visual analysis. Furthermore, PSI performed better than strain and strain rate. Interestingly, in previous observations PSI has been shown to persist after stress (Asanuma and Nakatani 2015). Imaging after dobutamine stress or exercise might provide a more optimal time point for imaging considering the frame rate requirements of speckle tracking technology. In addition, the post-systolic strain of normal myocardium has been shown to decrease while the post-systolic strain in the ischemic myocardium stays elevated after stress (Asanuma and Nakatani 2015). As a novel finding in Study IV, high PSI was associated with deep and extensive myocardial ischemia and could provide guidance in the treatment of CAD.

Global peak systolic strain and strain rate demonstrated similar response patterns to dobutamine stress as in previous studies (Voigt et al. 2004; Bjork Ingul et al. 2007; Mor-Avi et al. 2011). The normal physiologic pattern of myocardial deformation during stress is an initial increase of peak strain while it later remains un-changed and might even decrease as diastolic filling decreases at elevated heart rates. However, strain rate typically increases linearly during increasing stress (Mor-Avi et al. 2011). Decreased global peak longitudi-nal strain and strain rate during DSE have been promising markers for the diagnosis of obstructive CAD and have been shown to provide incremental diagnostic value in combination with the visual analysis of wall motion (Ng et al. 2009; Mor-Avi et al. 2011). Global strain and strain rate have been observed to be lower in patients with a multivessel disease (Yu et al. 2013). As in the previous studies, we observed lower global strain and strain rate in patients with obstructive CAD after DSE at the early recovery phase even though most of the patients had a single-vessel disease. Interestingly, global PSI was elevated in patients with ob-structive CAD at rest and all DSE phases. Global PSI was highest in patients with a multivessel disease or a large area of myocardial ischemia.

Regional peak systolic strain and strain rate have been shown to be able to detect and locate CAD induced ischemia during DSE with similar accuracy to visual analysis (Ingul et al. 2007; Hanekom et al. 2007; Mor-Avi et al. 2011). In Study IV, while regional strain and strain rate were sensitive to obstructive CAD their accuracy was limited by poor specificity. The reason for the lower diagnostic accuracy of 2D strain and strain rate to visual wall motion analysis compared to some of the previous studies is unclear. However, similar results have been observed in some previous clinical studies (Voigt et al 2003, Celutkiene et al. 2012). Postero-lateral location of coronary stenoses or differences in image acquisition protocols are possible reasons. Surprisingly, global strain rate was significantly decreased at early recovery while regional strain rate was comparable in patients with and without obstructive CAD. This is probably due to the termination of the stress test at lower dobutamine doses in patients with symptomatic CAD and could explain the lower average strain rate also in the non-ischemic parts of the myocardium. As in previous validation studies, strain and strain rate were repeatable during DSE (Yamada et al. 2014). In contrast, the reproducibility of conventional stress echocardiography has previously been moderate even among imaging specialists (Hoffmann et al. 1996; Hoffmann 2002). Thus, speckle tracking might increase the confidence of interpretation particularly in less experienced echocardiographers.

Compared to earlier studies, a clear limitation in Study IV is the lower overall sensitivity (59%) of DSE for obstructive CAD, even though we utilized the standard protocol and visual analyzes were done by echocardiographers with more than 20 years of experience with stress echocardiography. However, similar sensitivity and accuracy of DSE have been observed in a recent multicenter trial (Neglia et al. 2015). The sensitivity of DSE is probably affected by the large number of patients with single vessel CAD and stenoses in distal or small coronary branches. Compared to PET perfusion used as a functional gold standard, an inherent limitation of stress echocardiography is that wall motion abnormalities appear later in the ischemic cascade than flow abnormalities which may translate into a lower sensitivity. It is possible that the optimization of speckle tracking images during DSE could have affected the image quality of the conventional echocardiographic reading. However, the primary goal of Study IV was to compare the

accuracy and feasibility of different strain variables rather than to establish the absolute accuracy of conventional DSE, which needs to be studied in a larger study setting. The number of patients with obstructive CAD was relatively low in our study. However, the study group of symptomatic patients with intermediate pretest probability of CAD represent the real target population for noninvasive cardiac imaging. The cutoff values of the ROC analyses were applied to the same patient population they were derived from and should be further studied in a separate study. There was no echocardiographic signs of cardiac diseases other than CAD and therefore the results in Study IV might not apply to patients with different cardiac conditions.

6.5.   Future Research Perspectives of Quantitative Cardiac Imaging

6.5.1   Quantitative Anatomical Imaging of CAD

The optimal selection of different cardiac imaging modalities for the diagnosis and risk stratification of CAD is still debated. The optimal combination of anatomical and functional multimodality imaging is also currently unknown. In a recent large imaging study, functional evaluation compared to CTA imaging of CAD was found to have a similar effect on patient outcome (Douglas et al. 2015). On the other hand, the optimal management of atherosclerosis based on CTA is currently unclear. CTA has great clinical potential in selecting the correct patients for preventive treatment of atherosclerosis and the clinical value of individualized CTA guided cardiovascular therapy should be evaluated in future studies. (Hecht 2015; Nasir et al. 2015; Thomas et al. 2015). For example, in a previous study almost half of the patients eligible for statin medication based on the current clinical criteria had no coronary atherosclerosis on CTA study (Nasir et al. 2015). The application of modern imaging and reconstruction techniques increase the accuracy and reduce the radiation dose of CCS scan even further (Hecht 2015). However, these methods need further clinical validation. Multiple different features of nonobstructive atherosclerosis have been associated with increased cardiac risk. Thus, a comprehensive quantitative atherosclerosis risk score integrating

atherosclerotic burden, location of coronary lesions and specific subtypes of individual plaques could potentially improve risk stratification of nonobstructive atherosclerosis (De Graaf 2014; Mushtaq et al. 2015). The prognostic value of such a comprehensive risk score should be validated in a large patient population in the future.

Magnetic resonance angiography is technically challenging owing to the small size, tortuosity, complex anatomy and motion of coronary arteries (Kohsaka and Makaryus 2008). Further technical progress is needed to adapt the MRI imaging of coronary arteries to clinical cardiology. However, characterization of atherosclerotic palaques by MRI has great potential for finding vulnerable plaques and predicting future cardiac events (Kohsaka and Makaryus 2008; Matsumoto et al. 2015). Since MRI technology is radiation free, serial imaging of coronary plaques could be utilized to measure the progression of atherosclerotic lesions or the effect of pharmacological interventions (Noguchi et al. 2015).

6.5.2 Quantitative Functional Imaging of CAD

The diagnostic value of quantitative imaging of both MBF and myocardial deformation has been demonstrated in multiple previous studies (Mor-Avi et al. 2011; Knuuti et al. 2009; Saraste 2012). Nevertheless, larger clinical trials for the optimization of imaging protocols and for more accurate cutoff values are needed. The prognostic significance of quantitative functional imaging has also been shown (Mor-Avi et al. 2011; Acampa et al. 2015). However, there is a pausity of studies assessing the clinical impact of quantitative functional imaging in guiding medical treatment and revascularizations. Reduced CFR was not associated with increased future coronary calcification in Study I. True incidence, prognostic impact and optimal clinical management of microvascular dysfunction should be evaluated in larger studies. In Study IV, post-systolic strain provided a good diagnostic value for obstructive CAD. It also correctly risk stratified patients with a large ischemic area or multivessel disease. Interestingly, the greatest diagnostic accuracy for PSI was achieved after dobutamine stress. This is in line with previous observations where

post-systolic stress has been shown to persist long after stress (Asanuma and Nakatani 2015). Thus, speckle tracking echocardiography could have great potential, for example after exercise ECG in the diagnosis and risk stratification of obstructive CAD. The lower heart rate after stress could prove to be more optimal for the frame rate requirements of speckle tracking- technology. However, the diagnostic accuracy of cutoff values obtained in Study IV for strain, strain rate and PSI should be evaluated in another larger study population. Quantitative functional imaging by noninvasive FFR using CT perfusion has shown great promise in initial imaging studies and its diagnostic and prognostic value should be further assessed in a large-scale clinical trial (Min et al. 2015). There has also been considerable technical development in older well-established cardiac imaging modalities. The diagnostic impact of different radiotracers, imaging protocols, advancements in technology and techniques reducing radiation doses need to be evaluated in future studies against conventional imaging methods (Underwood et al. 2014; Hecht 2015). The optimal integration of quantitative anatomical and functional imaging in hybrid imaging is currently unknown. The possible incremental prognostic value of hybrid imaging in the risk stratification of CAD should be also evaluated in a future study.

6.5.3   *Myocardial Bridging*

In Study II, myocardial bridging was not associated with abnormally low myocardial blood flow. This is probably explained by the fact that severe systolic compression (>50-75%) is a rare phenomenon in an unselected study population. True incidence and the functional significance of severe systolic compression (>50-70%) should be evaluated in future clinical studies. In addition, the diagnostic value of other imaging modalities such as MRI and stress echocardiography for the functional assessment of myocardial bridging should be studied. The potential difference in the diagnostic value of a vasodilator and dobutamine stress on patients with myocardial bridging should be evaluated. Furthermore, clinical consensus for the optimal management and assessment of myocardial bridging is needed.

7.   CONCLUSIONS

The major findings and conclusions of the studies presented in this thesis are:

I   Coronary reactivity to vasodilator-induced hyperemia as assessed by [^{15}O] H_2O perfusion PET was not predictive of the presence or amount of coronary calcification after a 11 year follow-up in asymptomatic men with low likelihood of coronary artery disease.

II   Myocardial bridging seen as intramural course on CTA is a common finding, but only 29% of these segments have visible systolic compression. Severe systolic compression (> 50%) is a rare phenomenon. Myocardial bridges are not associated with abnormal myocardial blood flow during vasodilator stress as assessed by [^{15}O] H_2O perfusion PET. Myocardial bridging is not linked with increased atherosclerotic burden or vulnerable plaques. However, atherosclerotic plaques are predominantly located proximal to segments with myocardial bridges.

III   The current study was the first collaborative study to assess the diagnostic value of quantitative [^{15}O] H_2O perfusion PET. The optimal thresholds for the detection of flow-limiting coronary stenosis for hyperemic myocardial blood flow was 2.3 mL/g/min and 2.5 for coronary flow reserve. Hyperemic myocardial blood flow was accurate and superior to coronary flow reserve in the diagnosis of obstructive coronary artery disease. These results imply that stress-only protocols are sufficient for the diagnosis of ischemia in clinical PET protocols.

IV   Two-dimensional speckle tracking is feasible during dobutamine stress echocardiography. Post-systolic strain at the early recovery phase provides similar accuracy to visual wall motion analysis for obstructive coronary artery disease. Both strain and post-systolic strain provide information on the depth and extent of myocardial ischemia as assessed by [^{15}O] H_2O perfusion PET. Post-systolic strain during and after stress may be useful for guiding decisions on coronary revascularization.

8.   ACKNOWLEDGEMENTS

Turku, November 2015

Valtteri Uusitalo

References:

1. Abidov A, Germano G, Hachamovitch R, Slomka P, Berman DS. Gated SPECT in assessment of regional and global left ventricular function: an update. J Nucl Cardiol. 2013;20:1118-43.

2. Abrams J. Role of endothelial dysfunction in coronary artery disease. Am J Cardiol. 1997;79:2-9.

3. Acampa W, Gaemperli O, Gimelli A, Knaapen P, Schindler TH, Verberne HJ, Zellweger MJ; Document Reviewers. Role of risk stratification by SPECT, PET, and hybrid imaging in guiding management of stable patients with ischaemic heart disease: expert panel of the EANM cardiovascular committee and EACVI. Eur Heart J Cardiovasc Imaging. 2015 Apr 22.

4. Agatston AS, Janowitz WR, Hildner FJ, Zusmer NR, Viamonte M Jr, Detrano R. Quantification of coronary artery calcium using ultrafast computed tomography. J Am Coll Cardiol 1990;15:827–32

5. Aggarwal NR, Drozdova A, Wells Askew J 3rd, Kemp BJ, Chareonthaitawee P. Feasibility and diagnostic accuracy of exercise treadmill nitrogen-13 ammonia PET myocardial perfusion imaging of obese patients. J Nucl Cardiol. 2015 Mar 17.

6. Ahmad M, Merry SL, Haibach H. Evidence of impaired myocardial perfusion and abnormal left ventricular function during exercise in patients with isolated systolic narrowing of the left anterior descending coronary artery. Am J Cardiol. 1981;48:832-6.

7. Al Jaroudi W, Iskandrian AE. Regadenoson: a new myocardial stress agent. J Am Coll Cardiol. 2009;54:1123-30.

8. Al Sayari S, Kopp S, Bremerich J. Stress cardiac MR imaging: the role of stress functional assessment and perfusion imaging in the evaluation of ischemic heart disease. Radiol Clin North Am. 2015;53:355-67.

9. Alegria JR, Herrmann J, Holmes DR Jr, Lerman A, Rihal CS. Myocardial bridging. Eur Heart J. 2005;26:1159-68.

10. Alluri K, Joshi PH, Henry TS, Blumenthal RS, Nasir K, Blaha MJ. Scoring of coronary artery calcium scans: history, assumptions, current limitations, and future directions. Atherosclerosis. 2015 Mar;239(1):109-17.

11. Ambrose JA, Fuster V. The risk of coronary occlusion is not proportional to the prior severity of coronary stenoses. Heart. 1998;79:3-4.

12. Anderson TJ, Charbonneau F, Title LM, Buithieu J, Rose MS, Conradson H, Hildebrand K, Fung M, Verma S, Lonn EM. Microvascular function predicts cardiovascular events in primary prevention: long-term results from the Firefighters and Their Endothelium (FATE) study. Circulation 2011;123:163–9.

13. Androulakis A, Aznaouridis KA, Aggeli CJ, Roussakis GN, Michaelides AP, Kartalis AN, Stougiannos PN, Dilaveris PE, Misovoulos PI, Stefanadis CI, Kallikazaros IE. Transient ST-segment depression during paroxysms of atrial fibrillation in otherwise normal individuals: relation with underlying coronary artery disease. J Am Coll Cardiol 2007;50:1909–1911.

14. Arbab-Zadeh A, Miller JM, Rochitte CE, Dewey M, Niinuma H, Gottlieb I, Paul N, Clouse ME, Shapiro EP, Hoe J, Lardo AC, Bush DE, de Roos A, Cox C, Brinker J, Lima JA. Diagnostic accuracy of computed tomography coronary angiography according to pre-test probability of coronary artery disease and severity of coronary arterial calcification. The CORE-64 (Coronary Artery Evaluation Using 64-Row Multidetector Computed Tomography Angiography) International Multicenter Study. J Am Coll Cardiol. 2012;59:379-87

15. Asanuma T, Nakatani S. Myocardial ischaemia and post-systolic shortening. Heart. 2015;101:509-516

16. Austen WG, Edwards JE, Frye RL, Gensini GG, Gott VL, Griffith LS, McGoon DC, Murphy ML, Roe BB. A reporting system on patients evaluated for coronary artery disease. Report of the Ad Hoc Committee for Grading of Coronary Artery Disease, Council on Cardiovascular Surgery, American Heart Association. Circulation. 1975;51:5-40.

17. Bartenstein P, Schober O, Hasfeld M, Schäfers M, Matheja P, Breithardt G. Thallium-201 single photon emission tomography of myocardium: additional information in reinjection studies is dependent on collateral circulation. Eur J Nucl Med. 1992;19:790-5.

18. Bateman TM, Heller GV, McGhie AI, Friedman JD, Case JA, Bryngelson JR, Hertenstein GK, Moutray KL, Reid K, Cullom SJ. Diagnostic accuracy of rest/stress ECG-gated Rb-82 myocardial perfusion PET: comparison with ECG-gated Tc-99m sestamibi SPECT. J Nucl Cardiol. 2006;13:24-33.

19. Bax JJ, Wijns W. Fluorodeoxyglucose imaging to assess myocardial viability: PET, SPECT or gamma camera coincidence imaging? J Nucl Med. 1999;40:1893-5.

20. Beanlands RS, Chow BJ, Dick A, Friedrich MG, Gulenchyn KY, Kiess M, Leong-Poi H, Miller RM, Nichol G, Freeman M, Bogaty P, Honos G, Hudon G, Wisenberg G, Van Berkom J, Williams K, Yoshinaga K, Graham J; Canadian Cardiovascular Society; Canadian Association of Radiologists; Canadian Association of Nuclear Medicine; Canadian Nuclear Cardiology Society; Canadian Society of Cardiac Magnetic Resonance. CCS/CAR/CANM/CNCS/CanSCMR joint position statement on advanced noninvasive cardiac imaging using positron emission tomography, magnetic resonance imaging and multidetector computed tomographic angiography in the diagnosis and evaluation of ischemic heart disease--executive summary. Can J Cardiol. 2007;23:107-19.

21. Becker A, Becker C. CT imaging of myocardial perfusion: possibilities and perspectives. J Nucl Cardiol. 2013;20:289-96.

22. Bergmann SR, Fox KA, Rand AL, McElvany KD, Welch MJ, Markham J, Sobel BE. Quantification of regional myocardial blood flow in vivo with H215O. Circulation 1984;70:724-33.

23. Berman DS, Maddahi J, Tamarappoo BK, Czernin J, Taillefer R, Udelson JE, Gibson CM, Devine M, Lazewatsky J, Bhat G, Washburn D. Phase II safety and clinical comparison with single-photon emission computed tomography myocardial perfusion imaging for detection of coronary artery disease: flurpiridaz F 18 positron emission tomography. J Am Coll Cardiol. 2013;61:469-77.

24. Bernhardt P, Walcher T, Rottbauer W, Wöhrle J. Quantification of myocardial perfusion reserve at 1.5 and 3.0 Tesla: a comparison to fractional flow reserve. Int J Cardiovasc Imaging. 2012;28:2049-56.

25. Beyer T, Townsend DW, Brun T, Kinahan PE, Charron M, Roddy R, Jerin J, Young J, Byars L, Nutt R. A combined PET/CT scanner for clinical oncology. J Nucl Med. 2000;41:1369-79.

26. Bittencourt MS, Hulten E, Ghoshhajra B, O'Leary D, Christman MP, Montana P, Truong QA, Steigner M, Murthy VL, Rybicki FJ, Nasir K, Gowdak LH, Hainer J, Brady TJ, Di Carli MF, Hoffmann U, Abbara S, Blankstein R. Prognostic value of nonobstructive and obstructive coronary artery disease detected by coronary computed tomography angiography to identify cardiovascular events. Circ Cardiovasc Imaging. 2014;7:282-91.

27. Bjork Ingul C, Rozis E, Slordahl SA, Marwick TH. Incremental value of strain rate imaging to wall motion analysis for prediction of outcome in patients undergoing dobutamine stress echocardiography. Circulation. 2007;115:1252-9.

28. Blaha M, Budoff MJ, Shaw LJ, Khosa F, Rumberger JA, Berman D, Callister T, Raggi P, Blumenthal RS, Nasir K. Absence of coronary artery calcification and all-cause mortality. JACC Cardiovasc Imaging. 2009;2:692-700.

29. Blankenhorn DH, Stern D. Calcification of the coronary arteries. Am J Roentgenol Radium Ther Nucl Med. 1959;81:772-7.

30. Blankstein R, Shturman LD, Rogers IS, Rocha-Filho JA, Okada DR, Sarwar A, Soni AV, Bezerra H, Ghoshhajra BB, Petranovic M, Loureiro R, Feuchtner G, Gewirtz H, Hoffmann U, Mamuya WS, Brady TJ, Cury RC. Adenosine-induced stress myocardial perfusion imaging using dual-source cardiac computed tomography. J Am Coll Cardiol. 2009;54:1072-84.

31. Bol A, Melin JA, Vanoverschelde JL, Baudhuin T, Vogelaers D, De Pauw M, Michel C, Luxen A, Labar D, Cogneau M. Direct comparison of [13 N] ammonia and [15O]water estimates of perfusion with quantification of regional myocardial blood flow by microspheres. *Circulation* 1993;87:512-25.

32. Bruschke AV, Veltman CE, de Graaf MA, Vliegen HW. Myocardial bridging: what have we learned in the past and will new diagnostic modalities provide new insights? Neth Heart J. 2013;2:6-13.

33. Budoff MJ, Dowe D, Jollis JG, Gitter M, Sutherland J, Halamert E, Scherer M, Bellinger R, Martin A, Benton R, Delago A, Min JK. Diagnostic performance of 64-multidetector row coronary computed tomographic angiography for evaluation of coronary artery stenosis in individuals without known coronary artery disease: results from the prospective multicenter ACCURACY (Assessment by Coronary Computed Tomographic Angiography of Individuals Undergoing Invasive Coronary Angiography) trial. J Am Coll Cardiol. 2008;52:1724-32.

34. Budoff MJ, Young R, Lopez VA, et al. Progression of coronary calcium and incident coronary heart disease events: MESA (Multi-Ethnic Study of Atherosclerosis). J Am Coll Cardiol 2013;61:1231–9

35. Califf RM, Mark DB, Harrell FE Jr, Hlatky MA, Lee KL, Rosati RA, Pryor DB. Importance of clinical measures of ischemia in the prognosis of patients with documented coronary artery disease. J Am Coll Cardiol. 1988;11:20-6.

36. Camici PG, Crea F. Coronary microvascular dysfunction. N Engl J Med. 2007;356:830-40.

37. Cannon RO III, Quyyumi AA, Schenke WH, Fananapazir L, Tucker EE, Gaughan AM, Gracely RH, Cattau EL Jr, Epstein SE. Abnormal cardiac sensitivity in patients with chest pain and normal coronary arteries. J Am Coll Cardiol. 1990;16:1359–1366.

38. Carlos ME, Smart SC, Wynsen JC, Sagar KB. Dobutamine stress echocardiography for risk stratification after myocardial infarction. Circulation. 1997;95:1402-10.

39. Castelli WP, Garrison RJ, Wilson PW, Abbott RD, Kalousdian S, Kannel WB. Incidence of coronary heart disease and lipoprotein cholesterol levels. The Framingham Study. JAMA. 1986;256:2835-8.

40. Catalano O, Moro G, Perotti M, Frascaroli M, Ceresa M, Antonaci S, Baiardi P, Napolitano C, Baldi M, Priori SG. Late gadolinium enhancement by cardiovascular magnetic resonance is complementary to left ventricle ejection fraction in predicting prognosis of patients with stable coronary artery disease. J Cardiovasc Magn Reson. 2012;14:29.

41. Chen CC, Chen CC, Hsieh IC, Liu YC, Liu CY, Chan T, Wen MS, Wan YL. The effect of calcium score on the diagnostic accuracy of coronary computed tomography angiography. Int J Cardiovasc Imaging. 2011;27 Suppl 1:37-42.

42. Cheng AS, Pegg TJ, Karamitsos TD, Searle N, Jerosch-Herold M, Choudhury RP, Banning AP, Neubauer S, Robson MD, Selvanayagam JB. Cardiovascular magnetic resonance perfusion imaging at 3-tesla

for the detection of coronary artery disease: a comparison with 1.5-tesla. J Am Coll Cardiol. 2007;49:2440-9.

43. Christie J, Sheldahl LM, Tristani FE, Sagar KB, Ptacin MJ, Wann S. Determination of stroke volume and cardiac output during exercise: comparison of two-dimensional and Doppler echocardiography, Fick oximetry, and thermodilution. Circulation. 1987;76:539-47.

44. Chuah SC, Pellikka PA, Roger VL, McCully RB, Seward JB. Role of dobutamine stress echocardiography in predicting outcome in 860 patients with known or suspected coronary artery disease. Circulation. 1998;97:1474-80.

45. Celutkiene J, Zakarkaite D, Skorniakov V, Zvironaite V, Grabauskiene V, Burca J, Ciparyte L, Laucevicius A. Quantitative approach using multiple single parameters versus visual assessment in dobutamine stress echocardiography. Cardiovasc Ultrasound. 2012;10:31.

46. Cerqueira MD, Verani MS, Schwaiger M, Heo J, Iskandrian AS. Safety profile of adenosine stress perfusion imaging: results from the Adenoscan Multicenter Trial Registry. J Am Coll Cardiol. 1994;23:384-9.

47. Cohen JL, Ottenweller JE, George AK, Duvvuri S. Comparison of dobutamine and exercise echocardiography for detecting coronary artery disease. Am J Cardiol. 1993;72:1226-31.

48. Curillova Z, Yaman BF, Dorbala S, Kwong RY, Sitek A, El Fakhri G, Anagnostopoulos C, Di Carli MF. Quantitative relationship between coronary calcium content and coronary flow reserve as assessed by integrated PET/CT imaging. Eur J Nucl Med Mol Imaging 2009;36:1603–10.

49. Daly C, Norrie J, Murdoch DL, Ford I, Dargie HJ, Fox K; TIBET (Total Ischaemic Burden European Trial) study group. The value of routine non-invasive tests to predict clinical outcome in stable angina. Eur Heart J. 2003;24:532-40.

50. Danad I, Raijmakers PG, Appelman YE, Harms HJ, de Haan S, van den Oever ML, Heymans MW, Tulevski II, van Kuijk C, Hoekstra OS, Lammertsma AA, Lubberink M, van Rossum AC, Knaapen P. Hybrid imaging using quantitative H215O PET and CT-based coronary angiography for the detection of coronary artery disease. J Nucl Med. 2013;54:55-63.

51. Danesh J, Wheeler JG, Hirschfield GM, Eda S, Eiriksdottir G, Rumley A, Lowe GD, Pepys MB, Gudnason V. C-reactive protein and other circulating markers of inflammation in the prediction of coronary heart disease. N Engl J Med. 2004;350:1387-97.

52. de Graaf MA, Broersen A, Ahmed W, Kitslaar PH, Dijkstra J, Kroft LJ, Delgado V, Bax JJ, Reiber JH, Scholte AJ. Feasibility of an automated quantitative computed tomography angiography-derived risk score for risk stratification of patients with suspected coronary

artery disease. Am J Cardiol. 2014;113:1947-55.

53. De Graaf MA, Broersen A, Kitslaar PH, Roos CJ, Dijkstra J, Lelieveldt BP, Jukema JW, Schalij MJ, Delgado V, Bax JJ, Reiber JH, Scholte AJ. Automatic quantification and characterization of coronary atherosclerosis with computed tomography coronary angiography: cross-correlation with intravascular ultrasound virtual histology. Int J Cardiovasc Imaging. 2013;29:1177-90.

54. DeLong ER, DeLong DM, Clarke-Pearson DL. Comparing the areas under two or more correlated receiver operating characteristic curves: a nonparametric approach. Biometrics 1988;44: 837–45.

55. Deedwania PC, Carbajal EV. Silent ischemia during daily life is an independent predictor of mortality in stable angina. Circulation. 1990;81:748-56.

56. Deng SB, Jing XD, Wang J, Huang C, Xia S, Du JL, Liu YJ, She Q. Diagnostic performance of noninvasive fractional flow reserve derived from coronary computed tomography angiography in coronary artery disease: A systematic review and meta-analysis. Int J Cardiol. 2015;184:703-9.

57. Detrano R, Guerci AD, Carr JJ, Bild DE, Burke G, Folsom AR, Liu K, Shea S, Szklo M, Bluemke DA, O'Leary DH, Tracy R, Watson K, Wong ND, Kronmal RA. Coronary calcium as a predictor of coronary events in four racial or ethnic groups. N Engl J Med. 2008;358:1336-45.

58. Detrano R, Hsiai T, Wang S, Puentes G, Fallavollita J, Shields P, Stanford W, Wolfkiel C, Georgiou D, Budoff M, Reed J. Prognostic value of coronary calcification and angiographic stenoses in patients undergoing coronary angiography. J Am Coll Cardiol. 1996;27:285-90.

59. Detry JM. The pathophysiology of myocardial ischaemia. Eur Heart J. 1996;17 Suppl G:48-52.

60. Di Angelantonio E, Chowdhury R, Sarwar N, Aspelund T, Danesh J, Gudnason V. Chronic kidney disease and risk of major cardiovascular disease and non-vascular mortality: prospective population based cohortstudy. BMJ 2010;341:c4986.

61. Diamond GA, Forrester JS. Analysis of probability as an aid in the clinical diagnosis of coronary-artery disease. N Engl J Med. 1979;300:1350-8.

62. Dorbala S, Di Carli MF. Cardiac PET perfusion: prognosis, risk stratification, and clinical management. Semin Nucl Med. 2014;44:344-57.

63. Dorbala S, Di Carli MF, Beanlands RS, Merhige ME, Williams BA, Veledar E, Chow BJ, Min JK, Pencina MJ, Berman DS, Shaw LJ. Prognostic value of stress myocardial perfusion positron emission tomography: results from a multicenter observational registry. J Am

Coll Cardiol. 2013;61:176-84.

64. Einstein AJ. Radiation risk from coronary artery disease imaging: how do different diagnostic tests compare? Heart. 2008;94:1519-21.

65. Elhendy A, Bax JJ, Poldermans D: Dobutamine stress myocardial perfusion imaging in coronary artery disease, J Nucl Med 43:1634–1646, 2002.

66. Emond M, Mock MB, Davis KB, Fisher LD, Holmes DR Jr, Chaitman BR, Kaiser GC, Alderman E, Killip T 3rd. Long-term survival of medically treated patients in the Coronary Artery Surgery Study (CASS) Registry. Circulation. 1994;90:2645-57.

67. Erbel R, Möhlenkamp S, Moebus S, Schmermund A, Lehmann N, Stang A, Dragano N, Grönemeyer D, Seibel R, Kälsch H, Bröcker-Preuss M, Mann K, Siegrist J, Jöckel KH; Heinz Nixdorf Recall Study Investigative Group. Coronary risk stratification, discrimination, and reclassification improvement based on quantification of subclinical coronary atherosclerosis: the Heinz Nixdorf Recall study. J Am Coll Cardiol. 2010;56:1397-406.

68. Escaned J, Cortés J, Flores A, Goicolea J, Alfonso F, Hernández R, Fernández-Ortiz A, Sabaté M, Bañuelos C, Macaya C. Importance of diastolic fractional flow reserve and dobutamine challenge in physiologic assessment of myocardial bridging. J Am Coll Cardiol. 2003;42:226-33.

69. Feigl EO. Coronary physiology. Physiol Rev. 1983;63:1-205.

70. Fiechter M, Ghadri JR, Gebhard C, Fuchs TA, Pazhenkottil AP, Nkoulou RN,Herzog BA, Wyss CA, Gaemperli O, Kaufmann PA. Diagnostic value of 13N-ammonia myocardial perfusion PET: added value of myocardial flow reserve. J Nucl Med. 2012;53:1230-4.

71. Fischer JJ, Samady H, McPherson JA, Sarembock IJ, Powers ER, Gimple LW, Ragosta M. Comparison between visual assessment and quantitative angiography versus fractional flow reserve for native coronary narrowings of moderate severity. Am J Cardiol. 2002;90:210-5.

72. Fihn SD, Gardin JM, Abrams J, Berra K, Blankenship JC, Dallas AP, Douglas PS, Foody JM, Gerber TC, Hinderliter AL, King SB 3rd, Kligfield PD, Krumholz HM, Kwong RY, Lim MJ, Linderbaum JA, Mack MJ, Munger MA, Prager RL, Sabik JF, Shaw LJ, Sikkema JD, Smith CR Jr, Smith SC Jr, Spertus JA, Williams SV; American College of Cardiology Foundation. 2012 ACCF/AHA/ACP/AATS/PCNA/SCAI/STS Guideline for the diagnosis and management of patients with stable ischemic heart disease: a report of the American College of Cardiology Foundation/American Heart Association Task Force on Practice Guidelines, and the American College of Physicians, American Association for Thoracic Surgery, Preventive Cardiovascular Nurses Association, Society for Cardiovascular Angiography and Interventions, and Society of Thoracic Surgeons. J Am Coll Cardiol.

2012;60:e44-e164.

73. Finn AV, Nakano M, Narula J, Kolodgie FD, Virmani R. Concept of vulnerable/unstable plaque. Arterioscler Thromb Vasc Biol 2010;30:1282–92.

74. Fischer C, Hulten E, Belur P, Smith R, Voros S, Villines TC. Coronary CT angiography versus intravascular ultrasound for estimation of coronary stenosis and atherosclerotic plaque burden: a meta-analysis. J Cardiovasc Comput Tomogr.2013;7:256-66

75. Gawor R, Kuśmierek J, Płachcińska A, Bieńkiewicz M, Drożdż J, Piotrowski G, Chiżyński K. Myocardial perfusion GSPECT imaging in patients with myocardial bridging. J Nucl Cardiol. 2011;18:1059-65.

76. Ge J, Jeremias A, Rupp A, Abels M, Baumgart D, Liu F, Haude M, Görge G, von Birgelen C, Sack S, Erbel R. New signs characteristic of myocardial bridging demonstrated by intracoronary ultrasound and Doppler. Eur Heart J. 1999;20:1707-16.

77. Geleijnse ML, Fioretti PM, Roelandt JR. Methodology, feasibility, safety and diagnostic accuracy of dobutamine stress echocardiography. J Am Coll Cardiol.1997;30:595-606.

78. Genders TS, Steyerberg EW, Alkadhi H, Leschka S, Desbiolles L, Nieman K, Galema TW, Meijboom WB, Mollet NR, de Feyter PJ, Cademartiri F, Maffei E, Dewey M, Zimmermann E, Laule M, Pugliese F, Barbagallo R, Sinitsyn V, Bogaert J, Goetschalckx K, Schoepf UJ, Rowe GW, Schuijf JD, Bax JJ, de Graaf FR, Knuuti J, Kajander S, van Mieghem CA, Meijs MF, Cramer MJ, Gopalan D, Feuchtner G, Friedrich G, Krestin GP, Hunink MG; CAD Consortium. A clinical prediction rule for the diagnosis of coronary artery disease: validation, updating, and extension. Eur Heart J. 2011;32:1316-30.

79. Gould KL, Lipscomb K, Hamilton GW. Physiologic basis for assessing critical coronary stenosis. Instantaneous flow response and regional distribution during coronary hyperemia as measures of coronary flow reserve. Am J Cardiol. 1974;33:87-94.

80. Gould KL, Nakagawa Y, Nakagawa K, Sdringola S, Hess MJ, Haynie M, Parker N, Mullani N, Kirkeeide R. Frequency and clinical implications of fluid dynamically significant diffuse coronary artery disease manifest as graded, longitudinal, base-to-apex myocardial perfusion abnormalities by noninvasive positron emission tomography. Circulation. 2000;101:1931-9.

81. Greenland P, Bonow RO, Brundage BH, Budoff MJ, Eisenberg MJ, Grundy SM, Lauer MS, Post WS, Raggi P, Redberg RF, Rodgers GP, Shaw LJ, Taylor AJ, Weintraub WS; American College of Cardiology Foundation Clinical Expert Consensus Task Force (ACCF/AHA Writing Committee to Update the 2000 Expert Consensus Document on Electron Beam Computed Tomography); Society of Atherosclerosis Imaging and Prevention; Society of Cardiovascular Computed Tomography. ACCF/AHA 2007 clinical expert consensus

document on coronary artery calcium scoring by computed tomography in global cardiovascular risk assessment and in evaluation of patients with chest pain: a report of the American College of Cardiology Foundation Clinical Expert Consensus Task Force (ACCF/AHA Writing Committee to Update the 2000 Expert Consensus Document on Electron Beam Computed Tomography) developed in collaboration with the Society of Atherosclerosis Imaging and Prevention and the Society of Cardiovascular Computed Tomography. J Am Coll Cardiol. 2007;49:378-402.

82. Greenwood JP, Maredia N, Younger JF, Brown JM, Nixon J, Everett CC, Bijsterveld P, Ridgway JP, Radjenovic A, Dickinson CJ, Ball SG, Plein S. Cardiovascular magnetic resonance and single-photon emission computed tomography for diagnosis of coronary heart disease (CE-MARC): a prospective trial. Lancet. 2012;379:453-60.

83. Gupta S, Rohatgi A, Ayers CR, Willis BL, Haskell WL, Khera A, Drazner MH, de Lemos JA, Berry JD. Cardiorespiratory fitness and classification of risk of cardiovascular disease mortality. Circulation. 2011;123:1377-83.

84. Gutstein A, Wolak A, Lee C, Dey D, Ohba M, Suzuki Y, Cheng V, Gransar H, Suzuki S, Friedman J, Thomson LE, Hayes S, Pimentel R, Paz W, Slomka P, Berman DS. Predicting success of prospective and retrospective gating with dual-source coronary computed tomography angiography: development of selection criteria and initial experience. J Cardiovasc Comput Tomogr. 2008;2:81-90.

85. Hachamovitch R, Hayes SW, Friedman JD, Cohen I, Berman DS. Comparison of the short-term survival benefit associated with revascularization compared with medical therapy in patients with no prior coronary artery disease undergoing stress myocardial perfusion single photon emission computed tomography. Circulation. 2003;107:2900-7.

86. Hack SN, Eichling JO, Bergmann SR, Welch MJ. Sobel BE. External quantification of myocardial perfusion by exponential infusion of positron-emitting radionuclides. J Clin Invest 1980;66:918.

87. Hajjiri MM, Leavitt MB, Zheng H, Spooner AE, Fischman AJ, Gewirtz H. Comparison of positron emission tomography measurement of adenosine stimulated absolute myocardial blood flow versus relative myocardial tracer content for physiological assessment of coronary artery stenosis severity and location. J Am Coll Cardiol Img 2009;2:751–8.

88. Hamm CW, Bassand JP, Agewall S, Bax J, Boersma E, Bueno H, Caso P, Dudek D, Gielen S, Huber K, Ohman M, Petrie MC, Sonntag F, Uva MS, Storey RF, Wijns W, Zahger D; ESC Committee for Practice Guidelines. ESC Guidelines for the management of acute coronary syndromes in patients presenting without persistent ST-segment elevation: The Task Force for the management of acute coronary syndromes (ACS) in patients presenting without persistent ST-segment elevation of the European Society of Cardiology (ESC). Eur Heart J. 2011;32:2999-3054.

89. Hanekom L, Cho GY, Leano R, Jeffriess L, Marwick TH. Comparison of two-dimensional speckle and tissue Doppler strain measurement during dobutamine stress echocardiography: an angiographic correlation. Eur Heart J 2007;28:1765-72

90. Hansson GK, Libby P. The immune response in atherosclerosis: a double-edged sword. Nat Rev Immunol. 2006;6:508-19.

91. Hazenberg AJ, Jessurun GA, Tio RA. Mechanisms involved in symptomatic myocardial bridging: Value of sequential testing for endothelial function, flow reserve measurements and dobutamine stress angiography. Neth Heart J. 2008;16:10-5

92. Hecht HS. Coronary Artery Calcium Scanning: Past, Present, and Future. JACC Cardiovasc Imaging. 2015;8:579-596.

93. Heller GV, Calnon D, Dorbala S. Recent advances in cardiac PET and PET/CT myocardial perfusion imaging. J Nucl Cardiol. 2009;16:962-9.

94. Henzlova MJ, Cerqueira MD, Mahmarian JJ, Yao SS; Quality Assurance Committee of the American Society of Nuclear Cardiology. Stress protocols and tracers. J Nucl Cardiol. 2006;13:e80-90.

95. Herzog BA, Husmann L, Valenta I, Gaemperli O, Siegrist PT, Tay FM, Burkhard N, Wyss CA, Kaufmann PA. Long-term prognostic value of 13N-ammonia myocardial perfusion positron emission tomography added value of coronary flow reserve. J AmColl Cardiol. 2009;54:150-6.

96. Hilgendorf I, Swirski FK, Robbins CS. Monocyte fate in atherosclerosis. Arterioscler Thromb Vasc Biol. 2015;35:272-9.

97. Hoffmann R, Lethen H, Marwick T, Arnese M, Fioretti P, Pingitore A, Picano E, Buck T, Erbel R, Flachskampf FA, Hanrath P. Analysis of interinstitutional observer agreement in interpretation of dobutamine stress echocardiograms. J Am Coll Cardiol. 1996;27:330-6.

98. Hoffmann R, Marwick TH, Poldermans D, Lethen H, Ciani R, van der Meer P, Tries HP, Gianfagna P, Fioretti P, Bax JJ, Katz MA, Erbel R, Hanrath P. Refinements in stress echocardiographic techniques improve inter-institutional agreement in interpretation of dobutamine stress echocardiograms. Eur Heart J. 2002;23:821-9.

99. Ingelsson E, Sullivan LM, Fox CS, Murabito JM, Benjamin EJ, Polak JF, Meigs JB, Keyes MJ, O'Donnell CJ, Wang TJ, D'Agostino RB, Wolf PA, Vasan RS. Burden and prognostic importance of subclinical cardiovascular disease in overweight and obese individuals. Circulation. 2007;116:375-84.

100. Ingul CB, Stoylen A, Slordahl SA, Wiseth R, Burgess M, Marwick TH. Automated analysis of myocardial deformation at dobutamine stress echocardiography: an angiographic validation. J Am Coll Cardiol. 2007;49:1651-9

101. Iskandrian AE, Bateman TM, Belardinelli L, Blackburn B, Cerqueira MD, Hendel RC, Lieu H, Mahmarian JJ, Olmsted A, Underwood SR, Vitola J, Wang W; ADVANCE MPI Investigators. Adenosine versus regadenoson comparative evaluation in myocardial perfusion imaging: results of the ADVANCE phase 3 multicenter international trial. J Nucl Cardiol. 2007;14:645-58.

102. Jaarsma C, Leiner T, Bekkers SC, Crijns HJ, Wildberger JE, Nagel E, Nelemans PJ, Schalla S. Diagnostic performance of noninvasive myocardial perfusion imaging using single-photon emission computed tomography, cardiac magnetic resonance, and positron emission tomography imaging for the detection of obstructive coronary artery disease: a meta-analysis. J Am Coll Cardiol. 2012;59:1719-28.

103. Jagathesan R, Barnes E, Rosen SD, Foale RA, Camici PG. Comparison of myocardial blood flow and coronary flow reserve during dobutamine and adenosine stress: Implications for pharmacologic stress testing in coronary artery disease. J Nucl Cardiol. 2006;13:324-32.

104. Jahnke C, Nagel E, Gebker R, Kokocinski T, Kelle S, Manka R, Fleck E, Paetsch I. Prognostic value of cardiac magnetic resonance stress tests: adenosine stress perfusion and dobutamine stress wall motion imaging. Circulation. 2007;115:1769-76.

105. Johnson NP, Kirkeeide RL, Gould KL. Is discordance of coronary flow reserve and fractional flow reserve due to methodology or clinically relevant coronary pathophysiology? JACC Cardiovasc Imaging. 2012;5:193-202.

106. Johnson RC, Leopold JA, Loscalzo J. Vascular calcification: pathobiological mechanisms and clinical implications. Circ Res. 2006;99:1044-59.

107. Joutsiniemi E, Saraste A, Pietilä M, Mäki M, Kajander S, Ukkonen H, Airaksinen J, Knuuti J. Absolute flow or myocardial flow reserve for the detection of significant coronary artery disease? Eur Heart J Cardiovasc Imaging. 2014;15:659-65.

108. Juilliére Y, Berder V, Suty-Selton C, Buffet P, Danchin N, Cherrier F. Isolated myocardial bridges with angiographic milking of the left anterior descending coronary artery: a long-term follow-up study. Am Heart J. 1995;129:663-5.

109. Kajander S, Joutsiniemi E, Saraste M, Pietilä M, Ukkonen H, Saraste A, Sipilä HT, Teräs M, Mäki M, Airaksinen J, Hartiala J, Knuuti J. Cardiac positron emission tomography/computed tomography imaging accurately detects anatomically and functionally significant coronary artery disease. Circulation. 2010;122:603-13.

110. Kajander SA, Joutsiniemi E, Saraste M, Pietilä M, Ukkonen H, Saraste A, Sipilä HT, Teräs M, Mäki M, Airaksinen J, Hartiala J, Knuuti J. Clinical value of absolute quantification of myocardial perfusion with (15)O-water in coronary artery disease. Circ Cardiovasc Imaging. 2011;4:678-84.

111. Kajander S, Ukkonen H, Sipilä H, Teräs M, Knuuti J. Low radiation dose imaging of myocardial perfusion and coronary angiography with a hybrid PET/CT scanner. Clin Physiol Funct Imaging. 2009;29:81-8.

112. Kalam K, Otahal P, Marwick TH. Prognostic implications of global LV dysfunction: a systematic review and meta-analysis of global longitudinal strain and ejection fraction. Heart. 2014;100:1673-80.

113. Kannel WB, McGee DL. Diabetes and cardiovascular disease. The Framingham study. JAMA. 1979;241:2035-8.

114. Kannel WB. Hazards, risks, and threats of heart disease from the early stages to symptomatic coronary heart disease and cardiac failure. Cardiovasc Drugs Ther. 1997;11 Suppl 1:199-212.

115. Kaski JC, Rosano GMC, Collins P, Nihoyannopoulos P, Maseri A, Poole-Wilson PA. Cardiac syndrome X: clinical characteristics and left ventricular function: long-term follow-up study. J Am Coll Cardiol. 1995;25:807–814.

116. Kawawa Y, Ishikawa Y, Gomi T, Nagamoto M, Terada H, Ishii T, Kohda E. Detection of myocardial bridge and evaluation of its anatomical properties by coronary multislice spiral computed tomography. Eur J Radiol. 2007;61:130-8.

117. Kim C, Kwok YS, Heagerty P, Redberg R. Pharmacologic stress testing for coronary disease diagnosis: A meta-analysis. Am Heart J. 2001;142:934-44.

118. Kim PJ, Hur G, Kim SY, Namgung J, Hong SW, Kim YH, Lee WR. Frequency of myocardial bridges and dynamic compression of epicardial coronary arteries: a comparison between computed tomography and invasive coronary angiography. Circulation. 2009;119:1408-16.

119. Kim SS, Ko SM, Song MG, Hwang HG. Systolic luminal narrowing and morphologic characteristics of myocardial bridging of the mid-left anterior descending coronary artery by dual-source computed tomography. Int J Cardiovasc Imaging. 2011;27 Suppl 1:73-83

120. Klocke FJ. Coronary blood flow in man. Prog Cardiovasc Dis. 1976;19:117-66.

121. Knabb RM, Fox KA, Sobel BE, Bergmann SR. Characterization of the functional significance of subcritical coronary stenoses with H(2)15O and positron-emission tomography. Circulation 1985;71:1271-8.

122. Knuuti J, Kajander S, Mäki M, Ukkonen H. Quantification of myocardial blood flow will reform the detection of CAD. J Nucl Cardiol. 2009;16:497-506.

123. Konen E, Goitein O, Sternik L, Eshet Y, Shemesh J, Di Segni E. The prevalence and anatomical patterns of intramuscular coronary arteries: a coronary computed tomography angiographic study. J Am Coll Cardiol. 2007;49:587-93.

124. Korosoglou G, Lossnitzer D, Schellberg D, Lewien A, Wochele A, Schaeufele T, Neizel M, Steen H, Giannitsis E, Katus HA, Osman NF. Strain-encoded cardiac MRI as an adjunct for dobutamine stress testing: incremental value to conventional wall motion analysis. Circ Cardiovasc Imaging. 2009;2:132-40.

125. Kohsaka S, Makaryus AN. Coronary Angiography Using Noninvasive Imaging Techniques of Cardiac CT and MRI. Curr Cardiol Rev. 2008;4:323-30.

126. Kramer JR, Kitazume H, Proudfit WL, Sones FM Jr. Clinical significance of isolated coronary bridges: benign and frequent condition involving the left anterior descending artery. Am Heart J. 1982;103:283-8.

127. Krivokapich J, Huang SC, Phelps ME, MacDonald NS, Shine KI. Dependence of 13NH3 myocardial extraction and clearance on flow and metabolism. Am J Physiol. 1982;242:H536-42. PubMed PMID: 7065268.

128. Krivokapich J, Smith GT, Huang SC, Hoffman EJ, Ratib O, Phelps ME, Schelbert HR. 13N ammonia myocardial imaging at rest and with exercise in normal volunteers. Quantification of absolute myocardial perfusion with dynamic positron emission tomography. Circulation. 1989;80:1328-37.

129. Kwok Y, Kim C, Grady D, Segal M, Redberg R. Meta-analysis of exercise testing to detect coronary artery disease in women. Am J Cardiol. 1999;83:660-6.

130. Laaksonen MS, Kalliokoski KK, Luotolahti M, Kemppainen J, Teräs M, Kyröläinen H, Nuutila P, Knuuti J. Myocardial perfusion during exercise in endurance-trained and untrained humans. Am J Physiol Regul Integr Comp Physiol. 2007;293:R837-43.

131. Laine H, Raitakari OT, Niinikoski H, Pitka¨nen OP, Iida H, Viikari J, Nuutila P, Knuuti J. Early impairment of coronary flow reserve in young men with borderline hypertension. J Am Coll Cardiol 1998;32:147–53.

132. Lamendola P, Lanza GA, Spinelli A, Sgueglia GA, Di Monaco A, Barone L, Sestito A, Crea F. Long-term prognosis of patients with cardiac syndrome X. Int J Cardiol. 2010; 140: 197–199.

133. Lanza GA. Cardiac syndrome X: a critical overview and future per-spectives. Heart. 2007;93:159–166.

134. Lanza GA, Crea F. Primary coronary microvascular dysfunction: clinical presentation, pathophysiology, and management. Circulation. 2010;121:2317-25.

135. Lauer MS. How will exercise capacity gain enough respect? Circulation. 2011;123:1364-6

136. Lauer MS, Pothier CE, Magid DJ, Smith SS, Kattan MW. An externally validated model for predicting long-term survival after exercise treadmill testing in patients with suspected coronary artery disease and a normal electrocardiogram.Ann Intern Med. 2007;147:821-8.

137. Leschka S, Koepfli P, Husmann L, Plass A, Vachenauer R, Gaemperli O, Schepis T, Genoni M, Marincek B, Eberli FR, Kaufmann PA, Alkadhi H. Myocardial bridging: depiction rate and morphology at CT coronary angiography--comparison with conventional coronary angiography. Radiology. 2008;246:754-62.

138. Levy D, Garrison RJ, Savage DD, Kannel WB, Castelli WP. Prognostic implications of echocardiographically determined left ventricular mass in the Framingham Heart Study. N Engl J Med. 1990;322:1561-6.

139. Libby P, Aikawa M, Schönbeck U. Cholesterol and atherosclerosis. Biochim Biophys Acta. 2000;1529:299-309.

140. Libby P, Theroux P. Pathophysiology of coronary artery disease. Circulation. 2005;111:3481-8

141. Lipinski MJ, McVey CM, Berger JS, Kramer CM, Salerno M. Prognostic value of stress cardiac magnetic resonance imaging in patients with known or suspected coronary artery disease: a systematic review and meta-analysis. J Am Coll Cardiol. 2013;62:826-38.

142. Lockie T, Ishida M, Perera D, Chiribiri A, De Silva K, Kozerke S, Marber M, Nagel E, Rezavi R, Redwood S, Plein S. High-resolution magnetic resonance myocardial perfusion imaging at 3.0-Tesla to detect hemodynamically significant coronary stenoses as determined by fractional flow reserve. J Am Coll Cardiol. 2011;57:70-5.

143. Loimaala A, Groundstroem K, Pasanen M, Vuori I I. Overall and Seg-mental Agreement of Stress Echocardiography. Echocardiography. 1999;16:531-538.

144. Lopez AD, Mathers CD, Ezzati M, Jamison DT, Murray CJ. Global and regional burden of disease and risk factors, 2001: systematic analysis of population health data. Lancet. 2006;367:1747-57.

145. Macwar RR, Williams BA, Shirani J. Prognostic value of adenosine cardiac magnetic resonance imaging in patients presenting with chest pain. Am J Cardiol. 2013;112:46-50.

146. Mancia G, Manolis AJ, McMurray J, Pajak A, Parkhomenko A, Rallidis L, Rigo F, Rocha E, Ruilope LM, van der Velde E, Vanuzzo D, Viigimaa M, Volpe M, Wiklund O,Wolpert C. European Guide-lines on cardiovascular disease prevention in clinical practice (version 2012): The Fifth Joint Task Force of the European Society of Cardiol-ogy and Other Societies on Cardiovascular Disease Prevention in Clinical Practice. Eur Heart J 2012;33:1635–1701.

147. Manka R, Wissmann L, Gebker R, Jogiya R, Motwani M, Frick M, Reinartz S, Schnackenburg B, Niemann M, Gotschy A, Kuhl C, Nagel

E, Fleck E, Marx N, Luescher TF, Plein S, Kozerke S. Multicenter evaluation of dynamic three-dimensional magnetic resonance myocardial perfusion imaging for the detection of coronary artery disease defined by fractional flow reserve. Circ Cardiovasc Imaging. 2015;8.

148. Margolis JR, Chen JT, Kong Y, Peter RH, Behar VS, Kisslo JA. The diagnostic and prognostic significance of coronary artery calcification. A report of 800 cases. Radiology. 1980;137:609-16.

149. Mark DB, Shaw L, Harrell FE Jr, Hlatky MA, Lee KL, Bengtson JR, McCants CB, Califf RM, Pryor DB. Prognostic value of a treadmill exercise score in outpatients with suspected coronary artery disease. N Engl J Med. 1991;325:849-53.

150. Matsumoto K, Ehara S, Hasegawa T, Sakaguchi M, Otsuka K, Yoshikawa J, Shimada K. Localization of Coronary High-Intensity Signals on T1-Weighted MR Imaging: Relation to Plaque Morphology and Clinical Severity of Angina Pectoris. JACC Cardiovasc Imaging. 2015;8:1143-52.

151. Marwick TH. Measurement of strain and strain rate by echocardiography: ready for prime time? J Am Coll Cardiol. 2006;47:1313-27

152. Marwick TH. Stress echocardiography. Heart. 2003;89:113-8

153. Marwick TH, Case C, Sawada S, Vasey C, Thomas JD. Prediction of outcomes in hypertensive patients with suspected coronary disease. Hypertension. 2002;39:1113-8.

154. Maurovich-Horvat P, Ferencik M, Voros S, Merkely B, Hoffmann U. Comprehensive plaque assessment by coronary CT angiography. Nat Rev Cardiol. 2014;11:390-402.

155. Mc Ardle BA, Dowsley TF, deKemp RA, Wells GA, Beanlands RS. Does rubidium-82 PET have superior accuracy to SPECT perfusion imaging for the diagnosis of obstructive coronary disease?: A systematic review and meta-analysis. J Am Coll Cardiol. 2012;60:1828-37.

156. Meijboom WB, Meijs MF, Schuijf JD, Cramer MJ, Mollet NR, van Mieghem CA, Nieman K, van Werkhoven JM, Pundziute G, Weustink AC, de Vos AM, Pugliese F, Rensing B, Jukema JW, Bax JJ, Prokop M, Doevendans PA, Hunink MG, Krestin GP, de Feyter PJ. Diagnostic accuracy of 64-slice computed tomography coronary angiography: a prospective, multicenter, multivendor study. J Am Coll Cardiol. 2008;52:2135-44.

157. Meijboom WB, Van Mieghem CA, van Pelt N, Weustink A, Pugliese F, Mollet NR, Boersma E, Regar E, van Geuns RJ, de Jaegere PJ, Serruys PW, Krestin GP, de Feyter PJ. Comprehensive assessment of coronary artery stenoses: computed tomography coronary angiography versus conventional coronary angiography and correlation with fractional flow reserve in patients with stable angina.

J Am Coll Cardiol. 2008;52:636-43.

158. Meimoun P, Tribouilloy C. Non-invasive assessment of coronary flow and coronary flow reserve by transthoracic Doppler echocardiography: a magic tool for the real world. Eur J Echocardiogr. 2008;9:449-57.

159. Meuwissen M, Chamuleau SA, Siebes M, Schotborgh CE, Koch KT, de Winter RJ, Bax M, de Jong A, Spaan JA, Piek JJ. Role of variability in microvascular resistance on fractional flow reserve and coronary blood flow velocity reserve in intermediate coronary lesions. Circulation. 2001;103:184-7.

160. Miller DD: Pharmacologic stressors in coronary artery disease. *In* Dilsizian V, Narula J, Braunwald E (eds): Atlas of Nuclear Cardiology. 3rd ed. Philadelphia, Current Medicine, 2009, pp 61-78.

161. Miller TD, Roger VL, Hodge DO, Gibbons RJ. A simple clinical score accurately predicts outcome in a community-based population undergoing stress testing. Am J Med. 2005;118:866-72.

162. Min JK, Dunning A, Lin FY, Achenbach S, Al-Mallah M, Budoff MJ, Cademartiri F, Callister TQ, Chang HJ, Cheng V, Chinnaiyan K, Chow BJ, Delago A, Hadamitzky M, Hausleiter J, Kaufmann P, Maffei E, Raff G, Shaw LJ, Villines T, Berman DS; CONFIRM Investigators. Age- and sex-related differences in all-cause mortality risk based on coronary computed tomography angiography findings results from the International Multicenter CONFIRM (Coronary CT Angiography Evaluation for Clinical Outcomes: An International Multicenter Registry) of 23,854 patients without known coronary artery disease. J Am Coll Cardiol. 2011;58:849-60.

163. Min JK, Taylor CA, Achenbach S, Koo BK, Leipsic J, Nørgaard BL, Pijls NJ, De Bruyne B. Noninvasive Fractional Flow Reserve Derived From Coronary CT Angiography: Clinical Data and Scientific Principles. JACC Cardiovasc Imaging. 2015;8:1209-22.

164. Montalescot G, Sechtem U, Achenbach S, Andreotti F, Arden C, Budaj A, Bugiardini R, Crea F, Cuisset T, Di Mario C, Ferreira JR, Gersh BJ, Gitt AK, Hulot JS, Marx N, Opie LH, Pfisterer M, Prescott E, Ruschitzka F, Sabaté M, Senior R, Taggart DP, van der Wall EE, Vrints CJ; ESC Committee for Practice Guidelines, Zamorano JL, Achenbach S, Baumgartner H, Bax JJ, Bueno H, Dean V, Deaton C, Erol C, Fagard R, Ferrari R, Hasdai D, Hoes AW, Kirchhof P, Knuuti J, Kolh P, Lancellotti P, Linhart A, Nihoyannopoulos P, Piepoli MF, Ponikowski P, Sirnes PA, Tamargo JL, Tendera M, Torbicki A, Wijns W, Windecker S; Document Reviewers, Knuuti J, Valgimigli M, Bueno H, Claeys MJ, Donner-Banzhoff N, Erol C, Frank H, Funck-Brentano C, Gaemperli O, Gonzalez-Juanatey JR, Hamilos M, Hasdai D, Husted S, James SK, Kervinen K, Kolh P, Kristensen SD, Lancellotti P, Maggioni AP, Piepoli MF, Pries AR, Romeo F, Rydén L, Simoons ML, Sirnes PA, Steg PG, Timmis A, Wijns W, Windecker S, Yildirir A, Zamorano JL. 2013 ESC guidelines on the management of stable coronary artery disease: the Task Force on the management of stable coronary artery disease of the European Society of Cardiology.

Eur Heart J. 201;34:2949-3003.

165. McCully RB, Roger VL, Mahoney DW, Burger KN, Click RL, Seward JB, Pellikka PA. Outcome after abnormal exercise echocardiography for patients with good exercise capacity: prognostic importance of the extent and severity of exercise-related left ventricular dysfunction. J Am Coll Cardiol. 2002;39:1345-52.

166. Moore KJ, Tabas I. Macrophages in the pathogenesis of atherosclerosis. Cell. 2011;145:341-55.

167. Mor-Avi V, Lang RM, Badano LP, Belohlavek M, Cardim NM, Derumeaux G et al. Current and evolving echocardiographic techniques for the quantitative evaluation of cardiac mechanics: ASE/EAE consensus statement on methodology and indications endorsed by the Japanese Society of Echocardiography. J Am Soc Echocardiogr. 2011;24:277-313

168. Morise AP, Diamond GA. Comparison of the sensitivity and specificity of exercise electrocardiography in biased and unbiased populations of men and women. Am Heart J. 1995;130:741-7

169. Motoyama S, Sarai M, Harigaya H, Anno H, Inoue K, Hara T, Naruse H, Ishii J, Hishida H, Wong ND, Virmani R, Kondo T, Ozaki Y, Narula J. Computed tomographic angiography characteristics of atherosclerotic plaques subsequently resulting in acute coronary syndrome. J Am Coll Cardiol. 2009;54:49-57.

170. Mozaffarian D, Benjamin EJ, Go AS, Arnett DK, Blaha MJ, Cushman M, de Ferranti S, Després JP, Fullerton HJ, Howard VJ, Huffman MD, Judd SE, Kissela BM, Lackland DT, Lichtman JH, Lisabeth LD, Liu S, Mackey RH, Matchar DB, McGuire DK, Mohler ER 3rd, Moy CS, Muntner P, Mussolino ME, Nasir K, Neumar RW, Nichol G, Palaniappan L, Pandey DK, Reeves MJ, Rodriguez CJ, Sorlie PD, Stein J, Towfighi A,

171. Myers RH, Kiely DK, Cupples LA, Kannel WB. Parental history is an independent risk factor for coronary artery disease: the Framingham Study. Am Heart J. 1990;120:963-9.

172. Murthy VL, Naya M, Foster CR, Gaber M, Hainer J, Klein J, Dorbala S, Blankstein R, Di Carli MF. Association between coronary vascular dysfunction and cardiac mortality in patients with and without diabetes mellitus. Circulation. 2012;126:1858-68.

173. Mushtaq S, De Araujo Gonçalves P, Garcia-Garcia HM, Pontone G, Bartorelli AL, Bertella E, Campos CM, Pepi M, Serruys PW, Andreini D. Long-term prognostic effect of coronary atherosclerotic burden: validation of the computed tomography-Leaman score. Circ Cardiovasc Imaging. 2015;8:e002332.

174. Muzik O, Beanlands RS, Hutchins GD, Mangner TJ, Nguyen N, Schwaiger M. Validation of nitrogen-13-ammonia tracer kinetic model for quantification of myocardial blood flow using PET. J Nucl

Med. 1993;34:83-91.

175. Muzik O, Duvernoy C, Beanlands RS, Sawada S, Dayanikli F, Wolfe ER Jr, Schwaiger M. Assessment of diagnostic performance of quantitative flow measurements in normal subjects and patients with angiographically documented coronary artery disease by means of nitrogen-13 ammonia and positron emission tomography. J Am Coll Cardiol. 1998;31:534-40.

176. Myers J, Prakash M, Froelicher V, Do D, Partington S, Atwood JE. Exercise capacity and mortality among men referred for exercise testing. N Engl J Med. 2002;346:793-801.

177. Möhlenkamp S, Hort W, Ge J, Erbel R. Update on myocardial bridging. Circulation. 2002;106:2616-22.

178. Narula J, Garg P, Achenbach S, Motoyama S, Virmani R, Strauss HW. Arithmetic of vulnerable plaques for noninvasive imaging. Nat Clin Pract Cardiovasc Med. 2008;5 Suppl 2:S2-10.

179. Nasir K, Bittencourt MS, Blaha MJ, Blankstein R, Agatson AS, Rivera JJ, Miemdema MD, Sibley CT, Shaw LJ, Blumenthal RS, Budoff MJ, Krumholz HM. Implications of Coronary Artery Calcium Testing Among Statin Candidates According to American College of Cardiology/American Heart Association Cholesterol Management Guidelines: MESA (Multi-Ethnic Study of Atherosclerosis). J Am Coll Cardiol. 2015;66:1657-68.

180. Neglia D, Rovai D, Caselli C, Pietila M, Teresinska A, Aguadé-Bruix S et al. Detection of significant coronary artery disease by noninvasive anatomical and functional imaging. Circ Cardiovasc Imaging. 2015;8(3).

181. Nekolla SG, Saraste A. Novel F-18-labeled PET myocardial perfusion tracers: bench to bedside. Curr Cardiol Rep. 2011;13:145-50.

182. Nesterov SV, Han C, Mäki M, Kajander S, Naum AG, Helenius H, Lisinen I, Ukkonen H, Pietilä M, Joutsiniemi E, Knuuti J. Myocardial perfusion quantitation with 15O-labelled water PET: high reproducibility of the new cardiac analysis software (Carimas). Eur J Nucl Med Mol Imaging. 2009;36:1594-602.

183. Noguchi T, Tanaka A, Kawasaki T, Goto Y, Morita Y, Asaumi Y, Nakao K, Fujiwara R, Nishimura K, Miyamoto Y, Ishihara M, Ogawa H, Koga N, Narula J, Yasuda S. Effect of Intensive Statin Therapy on Coronary High-Intensity Plaques Detected byNoncontrast T1-Weighted Imaging: The AQUAMARINE Pilot Study. J Am Coll Cardiol. 2015;66:245-56.

184. Olmos LI, Dakik H, Gordon R, Dunn JK, Verani MS, Quiñones MA, Zoghbi WA. Long-term prognostic value of exercise echocardiography compared with exercise 201Tl, ECG, and clinical variables in

patients evaluated for coronary artery disease. Circulation. 1998;98:2679-86.

185. Otsuka K, Fukuda S, Tanaka A, Nakanishi K, Taguchi H, Yoshikawa J, Shimada K, Yoshiyama M. Napkin-ring sign on coronary CT angiography for the prediction of acute coronary syndrome. JACC Cardiovasc Imaging. 2013;6:448-57.

186. Ostrom MP, Gopal A, Ahmadi N, Nasir K, Yang E, Kakadiaris I, Flores F, Mao SS, Budoff MJ. Mortality Incidence and the severity of coronary atherosclerosis assessed by computed tomography angiography. J Am Coll Cardiol. 2008;52:1335-43.

187. Park HB, Heo R, ó Hartaigh B, Cho I, Gransar H, Nakazato R, Leipsic J, Mancini GB, Koo BK, Otake H, Budoff MJ, Berman DS, Erglis A, Chang HJ, Min JK. Atherosclerotic plaque characteristics by CT angiography identify coronary lesions that cause ischemia: a direct comparison to fractional flow reserve. JACC Cardiovasc Imaging. 2015;8:1-10.

188. Parrinello R, Sestito A, Di Franco A, Russo G, Villano A, Figliozzi S, Nerla R, Tarzia P, Stazi A, Lanza GA, Crea F. Peripheral arterial function and coronary microvascular function in patients with variant angina. Cardiology. 2014;129:20-4

189. Pazhenkottil AP, Nkoulou RN, Ghadri JR, Herzog BA, Buechel RR, Küest SM, Wolfrum M, Fiechter M, Husmann L, Gaemperli O, Kaufmann PA. Prognostic value of cardiac hybrid imaging integrating single-photon emission computed tomography with coronary computed tomography angiography. Eur Heart J. 2011;32:1465-71.

190. Perk J, De Backer G, Gohlke H, Graham I, Reiner Z, Verschuren M, Albus C, Benlian P, Boysen G, Cifkova R, Deaton C, Ebrahim S, Fisher M, Germano G, Hobbs R, Hoes A, Karadeniz S, Mezzani A, Prescott E, Ryden L, Scherer M, Syvanne M, Scholte Op Reimer WJ, Vrints C, Wood D, Zamorano JL, Zannad F, Cooney MT, Bax J, Baumgartner H, Ceconi C, Dean V, Fagard R, Funck-Brentano C, Hasdai D, Kirchhof P, Knuuti J, Kolh P, McDonagh T, Moulin C, Popescu BA, Sechtem U, Sirnes PA, Tendera M, Torbicki A, Vahanian A, Windecker S, Aboyans V, Ezquerra EA, Baigent C, Brotons C, Burell G, Ceriello A, De Sutter J, Deckers J, Del Prato S, Diener HC, Fitzsimons D, Fras Z, Hambrecht R, Jankowski P, Keil U, Kirby M, Larsen ML,

191. Pellikka PA, Nagueh SF, Elhendy AA, Kuehl CA, Sawada SG; American Society of Echocardiography. American Society of Echocardiography recommendations for performance, interpretation, and application of stress echocardiography. J Am Soc Echocardiogr. 2007;20:1021-41

192. Pennell DJ, Sechtem UP, Higgins CB, et al. Clinical indications for cardiovascular magnetic resonance (CMR): Consensus Panel report. Eur Heart J. 2004;25:1940–65

193. Picano E, Bedetti G, Varga A, Cseh E. The comparable diagnostic accuracies of dobutamine-stress and dipyridamole-stress echocardiographies: a meta-analysis.Coron Artery Dis. 2000;11:151-9.

194. Pijls NH, De Bruyne B, Peels K, Van Der Voort PH, Bonnier HJ, Bartunek J Koolen JJ, Koolen JJ. Measurement of fractional flow reserve to assess the functional severity of coronary-artery stenoses. N Engl J Med. 1996;334:1703-8.

195. Pijls NH, Fearon WF, Tonino PA, Siebert U, Ikeno F, Bornschein B, van't Veer M, Klauss V, Manoharan G, Engstrøm T, Oldroyd KG, Ver Lee PN, MacCarthy PA, De Bruyne B; FAME Study Investigators. Fractional flow reserve versus angiography for guiding percutaneous coronary intervention in patients with multivessel coronary artery disease: 2-year follow-up of the FAME (Fractional Flow Reserve Versus Angiography for Multivessel Evaluation) study. J Am Coll Cardiol. 2010;56:177-84.

196. Pirich C, Leber A, Knez A, Bengel FM, Nekolla SG, Haberl R, Schwaiger M. Relation of coronary vasoreactivity and coronary calcification in asymptomatic subjects with a family history of premature coronary artery disease. Eur J Nucl Med Mol Imaging 2004;31:663–70.

197. Pingitore A, Picano E, Varga A, Gigli G, Cortigiani L, Previtali M, Minardi G, Colosso MQ, Lowenstein J, Mathias W Jr, Landi P. Prognostic value of pharmacological stress echocardiography in patients with known or suspected coronary artery disease: a prospective, large-scale, multicenter, head-to-head comparison between dipyridamole and dobutamine test. Echo-Persantine International Cooperative (EPIC) and Echo-Dobutamine International Cooperative (EDIC) Study Groups. J Am Coll Cardiol. 1999;34:1769-77.

198. Plana JC, Mikati IA, Dokainish H, Lakkis N, Abukhalil J, Davis R, Hetzell BC, Zoghbi WA. A randomized cross-over study for evaluation of the effect of image optimization with contrast on the diagnostic accuracy of dobutamine echocardiography in coronary artery disease The OPTIMIZE Trial. JACC Cardiovasc Imaging. 2008;1:145-52.

199. Planer D, Mehran R, Ohman EM, White HD, Newman JD, Xu K, Stone GW. Prognosis of patients with non-ST-segment-elevation myocardial infarction and nonobstructive coronary artery disease: propensity-matched analysis from the acute catheterization and urgent intervention triage strategy trial. Circ Cardiovasc Interv. 2014;7:285-93.

200. Poldermans D, Arnese M, Fioretti PM, Salustri A, Boersma E, Thomson IR, Roelandt JR, van Urk H. Improved cardiac risk stratification in major vascular surgery with dobutamine-atropine stress echocardiography. J Am Coll Cardiol. 1995;26:648-53.

201. Precious B, Blanke P, Nørgaard BL, Min JK, Leipsic J. Fractional flow reserve modeled from resting coronary CT angiography: state of the science. AJR Am J Roentgenol. 2015;204:W243-8.

202. Raggi P, Callister TQ, Shaw LJ. Progression of coronary artery calcium and risk of first myocardial infarction in patients receiving cholesterol-lowering therapy. Arterioscler Thromb Vasc Biol 2004;24:1–7.

203. Raitakari OT, Toikka JO, Laine H, Ahotupa M, Iida H, Viikari JS, Hartiala J, Knuuti J. Reduced myocardial flow reserve relates to increased carotid intima-media thickness in healthy young men. Atherosclerosis 2001;156:469–75.

204. Rischpler C, Nekolla SG, Kunze KP, Schwaiger M. PET/MRI of the Heart. Semin Nucl Med. 2015;45:234-247.

205. Rocha-Filho JA, Blankstein R, Shturman LD, Bezerra HG, Okada DR, Rogers IS, Ghoshhajra B, Hoffmann U, Feuchtner G, Mamuya WS, Brady TJ, Cury RC. Incremental value of adenosine-induced stress myocardial perfusion imaging with dual-source CT at cardiac CT angiography. Radiology. 2010;254:410-9.

206. Roberts R. A genetic basis for coronary artery disease. Trends Cardiovasc Med. 2015;25:171-178.

207. Roobottom CA, Mitchell G, Morgan-Hughes G. Radiation-reduction strategies in cardiac computed tomographic angiography. Clin Radiol. 2010;65:859-67.

208. Rubinshtein R, Gaspar T, Lewis BS, Prasad A, Peled N, Halon DA. Long-term prognosis and outcome in patients with a chest pain syndrome and myocardial bridging: a 64-slice coronary computed tomography angiography study. Eur Heart J Cardiovasc Imaging. 2013;14:579-85.

209. Saraste A, Kajander S, Han C, Nesterov SV, Knuuti J. PET: Is myocardial flow quantification a clinical reality? J Nucl Cardiol. 2012;19:1044-59.

210. Sarwar A, Shaw LJ, Shapiro MD, Blankstein R, Hoffmann U, Cury RC, Abbara S, Brady TJ, Budoff MJ, Blumenthal RS, Nasir K. Diagnostic and prognostic value of absence of coronary artery calcification. JACC Cardiovasc Imaging. 2009;2:675-88.

211. Sato A, Terata K, Miura H, Toyama K, Loberiza FR Jr, Hatoum OA, Saito T, Sakuma I, Gutterman DD. Mechanism of vasodilation to adenosine in coronary arterioles from patients with heart disease. Am J Physiol Heart Circ Physiol. 2005;288:H1633-40.

212. Sawada S, Muzik O, Beanlands RS, Wolfe E, Hutchins GD, Schwaiger M. Interobserver and interstudy variability of myocardial blood flow and flow-reserve measurements with nitrogen 13 ammonia-labeled positron emission tomography. J Nucl Cardiol. 1995;2:413-22.

213. Schang SJ Jr, Pepine CJ. Transient asymptomatic S-T segment depression during daily activity. Am J Cardiol. 1977;39:396-402.

214. Schindler TH. Positron-Emitting Myocardial Blood Flow Tracers and Clinical Potential. Prog Cardiovasc Dis. 2015 Jan 27.

215. Schuetz GM, Zacharopoulou NM, Schlattmann P, Dewey M. Meta-analysis: noninvasive coronary angiography using computed tomography versus magnetic resonance imaging. Ann Intern Med. 2010;152:167-77.

216. Schindler TH, Schelbert HR, Quercioli A, Dilsizian V. Cardiac PET imaging for the detection and monitoring of coronary artery disease and microvascular health. JACC Cardiovasc Imaging. 2010;3:623-40.

217. Schwarz ER, Klues HG, vom Dahl J, Klein I, Krebs W, Hanrath P. Functional characteristics of myocardial bridging. A combined angiographic and intracoronary Doppler flow study. Eur Heart J. 1997;18:434-42.

218. Schwitter J, Wacker CM, Wilke N, Al-Saadi N, Sauer E, Huettle K, Schönberg SO, Luchner A, Strohm O, Ahlstrom H, Dill T, Hoebel N, Simor T; MR-IMPACT Investigators. MR-IMPACT II: Magnetic Resonance Imaging for Myocardial Perfusion Assessment in Coronary artery disease Trial: perfusion-cardiac magnetic resonance vs. single-photon emission computed tomography for the detection of coronary artery disease: a comparative multicentre, multivendor trial. Eur Heart J. 2013;34:775-81.

219. Seol SH, Lindner JR. A primer on the methods and applications for contrast echocardiography in clinical imaging. J Cardiovasc Ultrasound. 2014;22:101-10.

220. Shaw LJ, Berman DS, Maron DJ, Mancini GB, Hayes SW, Hartigan PM, Weintraub WS, O'Rourke RA, Dada M, Spertus JA, Chaitman BR, Friedman J, Slomka P, Heller GV, Germano G, Gosselin G, Berger P, Kostuk WJ, Schwartz RG, Knudtson M, Veledar E, Bates ER, McCallister B, Teo KK, Boden WE; COURAGE Investigators. Optimal medical therapy with or without percutaneous coronary intervention to reduce ischemic burden: results from the Clinical Outcomes Utilizing Revascularization and Aggressive Drug Evaluation (COURAGE) trial nuclear substudy. Circulation. 2008;117:1283-91.

221. Shmilovich H, Cheng VY, Tamarappoo BK, Dey D, Nakazato R, Gransar H, Thomson LE, Hayes SW, Friedman JD, Germano G, Slomka PJ, Berman DS. Vulnerable plaque features on coronary CT angiography as markers of inducible regional myocardial hypoperfusion from severe coronary artery stenoses. Atherosclerosis. 2011;219:588-95.

222. Sicari R, Nihoyannopoulos P, Evangelista A, Kasprzak J, Lancellotti P, Poldermans D, Voigt JU, Zamorano JL; European Association of Echocardiography. Stress echocardiography expert consensus statement: European Association of Echocardiography (EAE) (a registered branch of the ESC). Eur J Echocardiogr. 2008;9:415-37.

223. Steg PG, James SK, Atar D, Badano LP, Blömstrom-Lundqvist C, Borger MA, Di Mario C, Dickstein K, Ducrocq G, Fernandez-Aviles

F, Gershlick AH, Giannuzzi P, Halvorsen S, Huber K, Juni P, Kastrati A, Knuuti J, Lenzen MJ, Mahaffey KW, Valgimigli M, van't Hof A, Widimsky P, Zahger D. ESC Guidelines for the management of acute myocardial infarction in patients presenting with ST-segment elevation. Eur Heart J. 2012;33:2569-619.

224. Stein JH, Korcarz CE, Hurst RT, Lonn E, Kendall CB, Mohler ER, Najjar SS, Rembold CM, Post WS, American Society of Echocardiography Carotid Intima-Media Thickness Task F. Use of carotid ultrasound to identify subclinical vascular disease and evaluate cardiovascular disease risk: a consensus statement from the American Society of Echocardiography Carotid Intima-Media Thickness Task Force. Endorsed by the Society for Vascular Medicine. J Am Soc Echocardiogr 2008;21:93–111.

225. Strong JP, Malcom GT, McMahan CA, Tracy RE, Newman WP 3rd, Herderick EE, Cornhill JF. Prevalence and extent of atherosclerosis in adolescents and young adults: implications for prevention from the Pathobiological Determinants of Atherosclerosis in Youth Study. JAMA. 1999;281:727-35.

226. Tadamura E, Iida H, Matsumoto K, Mamede M, Kubo S, Toyoda H, Shiozaki T, Mukai T, Magata Y, Konishi J. Comparison of myocardial blood flow during dobutamine-atropine infusion with that after dipyridamole administration in normal men. J Am Coll Cardiol. 2001;37:130-6.

227. Tamaki N, Yoshinaga K, Naya M. Coronary vasomotor function assessed by positron emission tomography. Eur J Nucl Med Mol Imaging. 2010;37:1213-24.

228. Taqueti VR, Hachamovitch R, Murthy VL, Naya M, Foster CR, Hainer J, Dorbala S, Blankstein R, Di Carli MF. Global coronary flow reserve is associated with adverse cardiovascular events independently of luminal angiographic severity and modifies the effect of early revascularization. Circulation. 2015;131:19-27.

229. Taylor AJ, Cerqueira M, Hodgson JM, Mark D, Min J, O'Gara P, Rubin GD; American College of Cardiology Foundation Appropriate Use Criteria Task Force; Society of Cardiovascular Computed Tomography; American College of Radiology; American Heart Association; American Society of Echocardiography; American Society of Nuclear Cardiology; North American Society for Cardiovascular Imaging; Society for Cardiovascular Angiography and Interventions; Society for Cardiovascular Magnetic Resonance. Appropriate Use Criteria for Cardiac Computed Tomography. A Report of the American College of Cardiology Foundation Appropriate Use Criteria Task Force, the Society of Cardiovascular Computed Tomography, the American College of Radiology, the American Heart Association, the American Society of Echocardiography, the American Society of Nuclear Cardiology, the North American Society for Cardiovascular Imaging, the Society for Cardiovascular Angiography and Interventions, and the Society for Cardiovascular Magnetic Resonance. J Cardiovasc Comput Tomogr. 2010;4:407.e1-33.

230. Thomas DM, Divakaran S, Villines TC, Nasir K, Shah NR, Slim AM, Blankstein R, Cheezum MK. Management of Coronary Artery Calcium and Coronary CTA Findings. Curr Cardiovasc Imaging Rep. 2015;8:18.

231. Thygesen K, Alpert JS, Jaffe AS, Simoons ML, Chaitman BR, White HD; Writing Group on the Joint Thygesen K, Alpert JS, White HD, Jaffe AS, Katus HA, Apple FS, Lindahl B, Morrow DA, Chaitman BA, Clemmensen PM, Johanson P, Hod H, Underwood R, Bax JJ, Bonow RO, Pinto F, Gibbons RJ, Fox KA, Atar D, Newby LK, Galvani M, Hamm CW, Uretsky BF, Steg PG, Wijns W, Bassand JP, Menasché P, Ravkilde J, Ohman EM, Antman EM, Wallentin LC, Armstrong PW, Simoons ML, Januzzi JL, Nieminen MS, Gheorghiade M, Filippatos G, Luepker RV, Fortmann SP, Rosamond WD, Levy D, Wood D, Smith SC, Hu D, Lopez-Sendon JL, Robertson RM, Weaver D, Tendera M, Bove AA, Parkhomenko AN, Vasilieva EJ, Mendis S; ESC Committee for Practice Guidelines (CPG). Third universal definition of myocardial infarction. Eur Heart J. 2012;33:2551-67.

232. Tonino PA, De Bruyne B, Pijls NH, Siebert U, Ikeno F, van' t Veer M, Klauss V, Manoharan G, Engstrøm T, Oldroyd KG, Ver Lee PN, MacCarthy PA, Fearon WF; FAME Study Investigators. Fractional flow reserve versus angiography for guiding percutaneous coronary intervention. N Engl J Med. 2009;360:213-24.

233. Tonino PA, Fearon WF, De Bruyne B, Oldroyd KG, Leesar MA, Ver Lee PN, Maccarthy PA, Van't Veer M, Pijls NH. Angiographic versus functional severity of coronary artery stenoses in the FAME study fractional flow reserve versus angiography in multivessel evaluation. J Am Coll Cardiol. 2010;55:2816-21.

234. Tsimikas S, Mallat Z, Talmud PJ, Kastelein JJ, Wareham NJ, Sandhu MS, Miller ER, Benessiano J, Tedgui A, Witztum JL, Khaw KT, Boekholdt SM. Oxidation-specific biomarkers, lipoprotein(a), and risk of fatal and nonfatal coronary events. J Am Coll Cardiol. 2010;56:946-55.

235. Turan TN, Virani SS, Willey JZ, Woo D, Yeh RW, Turner MB; American Heart Association Statistics Committee and Stroke Statistics Subcommittee. Heart disease and stroke statistics--2015 update: a report from the American Heart Association. Circulation. 2015;131:e29-322.

236. Underwood SR, de Bondt P, Flotats A, Marcasa C, Pinto F, Schaefer W, Verberne HJ. The current and future status of nuclear cardiology: a consensus report. Eur Heart J Cardiovasc Imaging. 2014;15:949-55.

237. Ural E, Bildirici U, Celikyurt U, Kilic T, Sahin T, Acar E, Kahraman G, Ural D. Long-term prognosis of non-interventionally followed patients with isolated myocardial bridge and severe systolic compression of the left anterior descending coronary artery. Clin Cardiol. 2009;32:454-7.

238. Uusitalo V, Saraste A, Kajander S, Luotolahti M, Wendelin-Saarenhovi M, Sundell J, Raitakari O, Knuuti J. The association between

coronary flow reserve and development of coronary calcifications: a follow-up study for 11 years in healthy young men. Eur Heart J Cardiovasc Imaging. 2013;14:812-8.

239. Vallejo E, Morales M, Sánchez I, Sánchez G, Alburez JC, Bialostozky D. Myocardial perfusion SPECT imaging in patients with myocardial bridging. J Nucl Cardiol. 2005;12:318-23.

240. van Velzen JE, de Graaf FR, de Graaf MA, Schuijf JD, Kroft LJ, de Roos A, Reiber JH, Bax JJ, Jukema JW, Boersma E, Schalij MJ, van der Wall EE. Comprehensive assessment of spotty calcifications on computed tomography angiography: comparison to plaque characteristics on intravascular ultrasound with radiofrequency backscatter analysis. J Nucl Cardiol. 2011;18:893-903.

241. Virmani R, Kolodgie FD, Burke AP, Farb A, Schwartz SM. Lessons from sudden coronary death: a comprehensive morphological classification scheme for atherosclerotic lesions. Arterioscler Thromb Vasc Biol. 2000;20:1262-75.

242. Voigt JU, Exner B, Schmiedehausen K, Huchzermeyer C, Reulbach U, Nixdorff U et al. Strain-rate imaging during dobutamine stress echocardiography provides objective evidence of inducible ischemia. Circulation. 2003;107:2120-6

243. Voigt JU, Nixdorff U, Bogdan R, Exner B, Schmiedehausen K, Platsch G, Kuwert T, Daniel WG, Flachskampf FA. Comparison of deformation imaging and velocity imaging for detecting regional inducible ischaemia during dobutamine stress echocardiography. Eur Heart J. 2004;25:1517-25.

244. Wahl A, Paetsch I, Gollesch A, Roethemeyer S, Foell D, Gebker R, Langreck H, Klein C, Fleck E, Nagel E. Safety and feasibility of high-dose dobutamine-atropine stress cardiovascular magnetic resonance for diagnosis of myocardial ischaemia: experience in 1000 consecutive cases. Eur Heart J. 2004;25:1230-6.

245. Wang L, Jerosch-Herold M, Jacobs DR Jr, Shahar E, Detrano R, Folsom AR. Coronary artery calcification and myocardial perfusion in asymptomatic adults: the MESA (Multi- Ethnic Study of Atherosclerosis). J Am Coll Cardiol 2006;48:1018–26.

246. Wilson PW, D'Agostino RB, Levy D, Belanger AM, Silbershatz H, Kannel WB. Prediction of coronary heart disease using risk factor categories. Circulation. 1998;97:1837-47.

247. Wirianta J, Mouden M, Ottervanger JP, Timmer JR, Juwana YB, de Boer MJ, Suryapranata H. Prevalence and predictors of bridging of coronary arteries in a large Indonesian population, as detected by 64-slice computed tomography scan. Neth Heart J. 2012;20:396-401.

248. Wolfe F, Freundlich B, Straus WL. Increase in cardiovascular and cerebrovascular disease prevalence in rheumatoid arthritis. J Rheumatol. 2003;30:36-40.

249. Yamada A, Luis SA, Sathianathan D, Khandheria BK, Cafaro J, Hamilton-Craig CR, Platts DG, Haseler L, Burstow D, Chan J. Reproducibility of regional and global longitudinal strains derived from two-dimensional speckle-tracking and Doppler tissue imaging between expert and novice readers during quantitative dobutamine stress echocardiography. J Am Soc Echocardiogr. 2014;27:880-7.

250. Yan RT, Anderson TJ, Charbonneau F, Title L, Verma S, Lonn E. Relationship between carotid artery intima-media thickness and brachial artery flow-mediated dilation in middle-aged healthy men. J Am Coll Cardiol 2005;45:1980–6.

251. Yoshinaga K, Chow BJ, Williams K, Chen L, deKemp RA, Garrard L, Lok-Tin Szeto A, Aung M, Davies RA, Ruddy TD, Beanlands RS. What is the prognostic value of myocardial perfusion imaging using rubidium-82 positron emission tomography? J *Am Coll Cardiol*. 2006;5;48:1029-39.

252. Yoshinaga K, Klein R, Tamaki N. Generator-produced rubidium-82 positron emission tomography myocardial perfusion imaging-From basic aspects to clinical applications. J Cardiol. 2010;55:163-73.

253. Yu Y, Villarraga HR, Saleh HK, Cha SS, Pellikka PA. Can ischemia and dyssynchrony be detected during early stages of dobutamine stress echocardiography by 2-dimensional speckle tracking echocardiography? Int J Cardiovasc Imaging. 2013;29:95-102

254. Zeiher AM, Drexler H, Wollschläger H, Just H. Endothelial dysfunction of the coronary microvasculature is associated with coronary blood flow regulation in patients with early atherosclerosis. Circulation. 1991;84:1984-92.